PRECAMBRIAN GEOLOGY OF THE COW CREEK ULTRAMAFIC COMPLEX, SAN MIGUEL COUNTY, NEW MEXICO

by

William F. Wyman

Submitted in Partial Fulfillment
of the Requirements for the Degree of
Master of Science in Geology

New Mexico Institute of Mining and Technology

Socorro, New Mexico

October, 1980

ABSTRACT

The Cow Creek ultramafic complex is composed of ultramafic rocks (55%), and amphibolites (45%) and includes minor amounts of mafic meta-sedimentary and volcaniclastic rocks. The complex is intruded by felsic plutonic bodies, including diorites and quartz-diorites. All of the granitic bodies are younger than the mafic-ultramafic rocks based on crosscutting relationships. The Precambrian rocks (with the exception of an unfoliated granite) have undergone at least one regional metamorphic event to the lower amphibolite facies and subsequent retrograde metamorphism to the greenschist facies.

The ultramafic rocks contain between 18 and 28 wt. per cent MgO, low TiO2 (< 0.50 wt. per cent), SiO2 (< 45 wt.per cent), Na2O and K2O both < 0.90 wt. per cent respectively, and have CaO/Al2O3 ratios of greater than 0.8. These rocks consistently plot within the pyroxenitic and peridotitic komatiite fields on chemical variation diagrams described in the literature. Trace metal ratios, selected quench textures, and rare earth patterns are all consistent with this interpretation.

The komatiitic rocks are interbedded with high-Mg tholeiites (now amphibolites) and minor mafic meta-sedimentary rocks. An extrusive origin for many of the komatiitic rocks is suggested by pillow-like structures, polyhedral jointing, relict flow banding, and chilled

margins. The chilled margins exhibit skeletal tremolite (after clinopyroxene) in a matrix of chlorite. The chlorite probably represents devitrified glassy material originally formed during quenching. Spinifex textures can not be confirmed, but are suggested by large (>6cm) radiating tremolite crystals in some rocks. The remaining ultramafic units are believed to be hypabyssal equivalents of the flows based primarily on whole rock geochemistry and the lack of extrusive textures.

The ultramafic rocks of Cow Creek are believed to be the first Proterozoic (1.7-1.8 b.y.) komatiites identified in the United States and only the second occurrence of such rocks described in North America. Based upon geochemical relations and geographic proximity, the komatiites appear to represent part of the basal stratigraphy of an extensive middle Proterozoic volcano-sedimentary terrane that is collectively called the Pecos greenstone belt.

TABLE OF CONTENTS

APPENDIXES

PLATES

FIGURES

TABLES

INTRODUCTION

Location

The study area is located approximately 15 miles due east of Sante Fe, on the south side of Elk Mountain in San Miguel County, New Mexico (Figure 1). The study area is composed of two separate field areas referred to as Area 1 (Lower Cow Creek) and Area 2 (Upper Cow Creek). The two study areas are approximately three miles apart along Cow Creek. Area 1 is located 8 miles northeast of the town of Pecos in the east central part of the U.S.G.S. Rosilla Peak 7.5 Minute Quadrangle. The U.S. Forest Service Service Cow Creek public campground is in the heart of the area. Area 2 is approximately 3 miles northeast of Area 1 in the north central part of the U.S.G.S. Honey Boy Ranch 7.5 Minute Quadrangle. Area 2 is bisected by Elk Creek and Sheep Creek which are tributaries to Cow Creek. Both study areas are reached by taking U.S. Forest Service Road no. 86, directly from the town of Pecos.

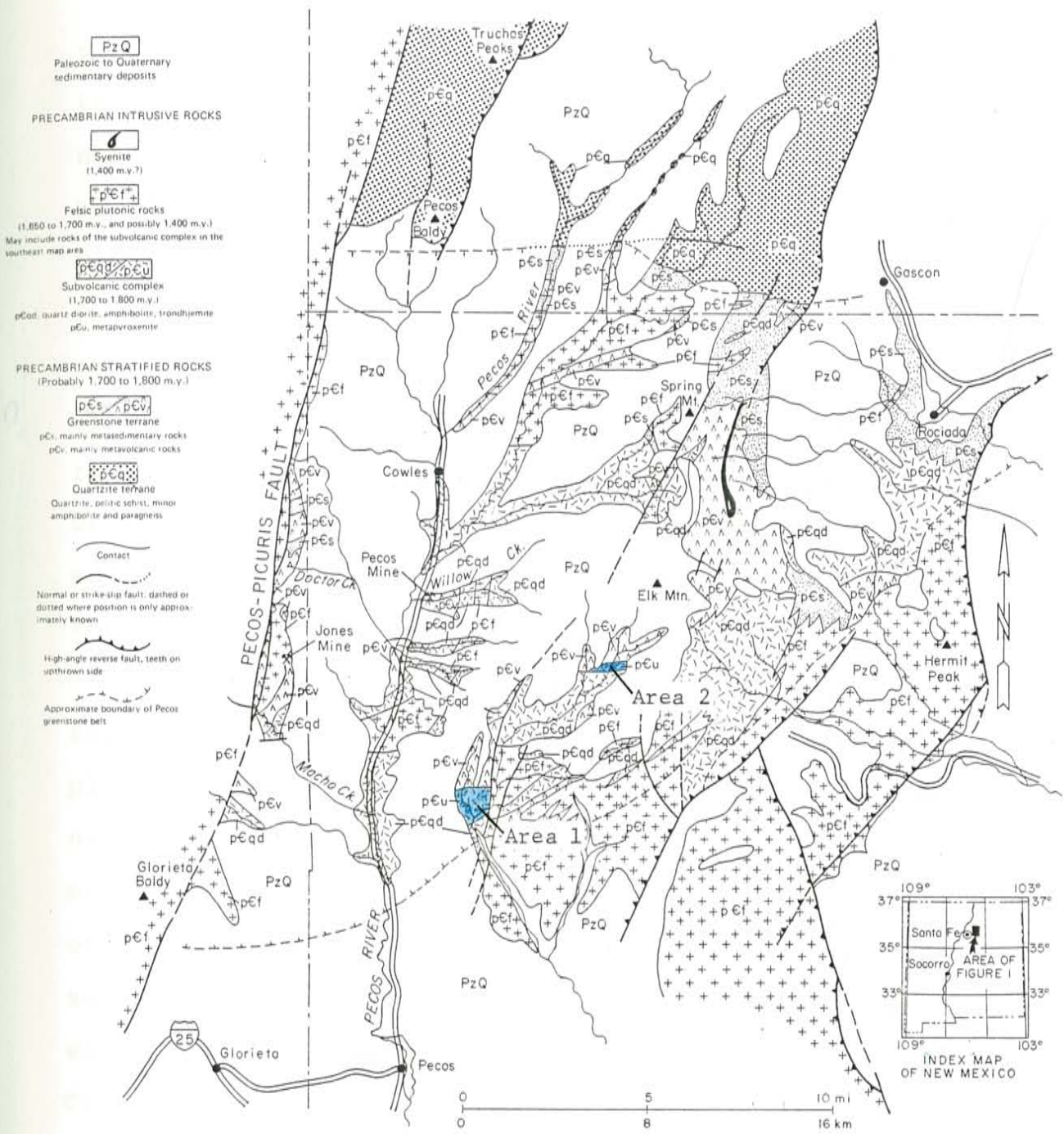

Figure 1. Location Map showing the Pecos greenstone belt and Cow Creek Areas 1 and 2.

Statement of the problem and Purpose

There are very few reported occurrences of Precambrian ultramafic rocks in New Mexico. They are mainly confined to the Pecos greenstone belt, and Precambrian rocks of the northern part of the state. Within the Pecos greenstone belt, (Figure 1) ultramafics are found in two places along Cow Creek, a tributary to the Pecos River, and in two small localities near Rociada, northeast of Elk Mountain. These rocks and associated amphibolites appear to be related spatially and possibly genetically to volcanic and plutonic rocks of the Pecos greenstone belt. Careful documentation of the petrology and chemistry of these rocks should shed much light on magma origin and genesis of early-Proterozoic rocks on northern New Mexico.

Ultramafic and mafic rocks are potential source rocks for economic concentrations of nickel, copper, chromium and platinum. Nickel-copper mineralization is found in one nearby prospect on the western flank of Barillas Peak, 15 miles due east of Pecos and approximately 10 miles southeast of Cow Creek. This prospect is associated with a large xenolith of amphibolite in the Embudo Granite. This study was prompted because of the geographic proximity of the Cow Creek ultramafics to mineralized prospects in the Pecos greenstone belt and Barillas peak, and because of gross textural and chemical similarities between the Cow Creek ultramafics and other ultramafic rocks found in greenstone belts worldwide.

The purpose of this project is to: 1) construct a detailed geologic map (scale 1:6000) of the two separate areas of exposed Precambrian ultramafic and mafic rocks in the Cow Creek drainage, 2) determine, using geochemical and field methods, whether or not the ultramafic rocks are intrusive or extrusive and their possible tectonic setting, 3) determine the relationship of the ultramafic rocks to the associated amphibolites and granites, and to other volcanic and sub-volcanic rocks of the Pecos greenstone belt, 4) assess the economic potential of the ultramafic and mafic rocks in the Cow Creek drainage.

Previous work

Until recently the Precambrian terrane of the Pecos River drainage received little detailed attention. Most older work was confined to speculation about the various granite rocks such as the "Embudo" granite (Montgomery, 1953; Miller and others, 1963; and Fullagar and Shiver, 1973). Peripheral work to the Pecos greenstone terrane has been done by Budding (1972), and Grambling (1979). Not until 1976 was detailed work undertaken by R. Moench of the U.S. Geological Survey and later by J.M. Robertson of the New Mexico Bureau of Mines (see Robertson and Moench, 1979). Dave Mathewson mapped Precambrian rocks south and southwest of Elk Mountain as part of his Ph.D thesis at the New Mexico Institute of Mining and Technology (in progress) and was the first to recognize the ultramafic rocks of Cow Creek. His mapping subsequently led to this study. Detailed work near the Pecos Mine was completed by Riesmeyer as part of his M.S. thesis at the University of New Mexico and later published by Riesmeyer and Robertson (1979).

Method of Investigation

Detailed mapping was done at a scale of 1:6000 on enlargements made from the U.S.G.S. Rosilla Peak and Honey Boy Ranch 7.5 minute quadrangles.

Eighty-two thin sections were analyzed to supplement and support field correlations and define petrographic characteristics. Rock names are taken mainly from Viljoen and Viljoen (1969), Irvine and Baragar (1971) and Barker et. al. (1976). Plagioclase compositions were determined by the Michel-Levy method as described in Kerr (1977).

Major element geochemistry (Si,Ti,Al,Fe,Mg,Ca,Na,K,Mn) was determined by conventional X-ray fluorescence methods (Jenkins, 1976; see APPENDIX A and B for details on sample preparation and error analysis). Trace metals (Ni,Co,Cr,Zn,Cu) and P2O5 were obtained by atomic absorption methods at the laboratory at the New Mexico Bureau of Mines and Mineral Resources (NMBMMR). Loss on ignition was also done at the NMBMMR lab. Four samples were analyzed for rare earth elements by neutron activation techniques described by Gordon et. al. (1968).

Acknowledgments

I gratefully acknowledge the many individuals who helped me during this study. Babe Martin, Daniel Kelly, and William Carter III allowed access to their private property. Tina Maggio was of great help in drafting figures and typing manuscript. Dale Armstrong provided criticism and several stimulating field discussions. Dr. D.I. Norman and Dr. K.C. Condie provided much critical review and help with the geochemistry and also served on my thesis committee.

A special thanks to Dr. James M. Robertson for serving as my thesis advisor and for his advice both in the field and office. CONOCO, Inc. of Albuquerque and the New Mexico Bureau of Mines and Mineral Resources provided financial support for this thesis.

GEOLOGIC SETTING

All recognized Precambrian rocks in the southwestern United States are Proterozoic in age. These rocks form three distinct NE-SW trending belts that range in age from 1.0 to 1.9 b.y. and decrease in age from northwest to southeast. The plutonic rocks of northern New Mexico and southern Colorado have been dated at 1.6-1.8 b.y. (Barker, et.al., 1974,1976; Fullagar and Shiver, 1973; and Long, 1974) and appear to be part of a 1.69-1.78 b.y. age belt that extends from central Arizona thru Illinois. These age provinces are thoroughly described by Van Schmus and Bickford (in press). Extensive exposures of Proterozoic volcanic and sedimentary rocks in southern Colorado and northern New Mexico appear to be older than the plutonic rocks based on crosscutting relations. These volcanic and sedimentary rocks are well exposed in the Tusas Mountains, Picuris Range, and Sangre de Cristo Mountains of northern New Mexico where they form extensive quartzite and greenstone terranes.

The Pecos greenstone belt of the southern Sangre de Cristo Mountains, as defined by Robertson and Moench (1979), is composed of a closely interrelated assemblage of metamorphosed subaqueous basalts and locally important felsic metavolcanic rocks, iron-formation, and metasedimentary rocks, some of volcanic provenance. The Pecos greenstone belt is bounded on the west by the

Pecos-Picuris fault which separates the greenstone terrane from a voluminous plutonic terrane composed primarily of intermediate to granitic rocks, which are collectively called the Embudo Granite (Fullagar and Shiver, 1973; Miller and others, 1963; and Montgomery, 1953). The Embudo Granite also displays intrusive contacts with many of the rocks in the southern part of the greenstone belt and thus forms both the western and southern boundaries. To the north, the greenstone terrane is bounded by an extensive quartzite terrane which has been described by Grambling (1979). There is still some question however, as to the relative ages of the quartzite terrane and the greenstone belt. In the northeast the greenstone terrane becomes mixed with arkosic metasandstones (now quartz-feldspar paragneiss) interbedded with aluminous quartz-mica schist, quartzite and thin layers of calc-silicate rock (Robertson and Moench, 1979). This predominantly sedimentary package is interbedded with amphibolites of the greenstone belt but becomes progressively more sedimentary toward the northeast and may represent a vertical transition between the Pecos greenstone and a younger quartzite terrane. An alternative explanation is that the transition represents lateral facies changes between the greenstone terrane and a coeval quartzite terrane (Robertson, J.M., personal communication). Part of the eastern boundary of the greenstone terrane is defined by several high-angle reverse faults which have thrust Precambrian rocks over Paleozoic strata, Baltz (1972, 1978) and Baltz and Bachman (1956).

Metamorphism in the Pecos greenstone belt is regional and varies from lower greenschist to amphibolite facies. Grade appears to increase from south to north.

The entire Precambrian terrane is unconformably overlain by Paleozoic limestones, sandstones and shales (see Miller and others, 1963).

Ultramafic Rocks in general

It is important at this point to briefly review the various types of ultramafic and associated rocks and their tectonic settings. Despite numerous difficulties in classifying the many varieties of ultramafic rocks, Naldrett and Cabri (1976), have proposed a comprehensive system based on tectonic environment. This system divides ultramafic rocks into two major groups, depending on whether or not the rocks were emplaced in an active orogenic or non-orogenic environment. "Orogenic", according to Naldrett and Cabri, applies to any area actively undergoing or about to become involved in mountain building, and includes areas under extension such as marginal-basins and continental rifts as well as compressional settings such as continental margins and island-arcs. Non-orogenic refers to stable cratonic areas. The classification is briefly summarized on the next page:

Table 1 (after Naldrett and Cabri (1976))

Classification of ultramafic and related mafic bodies

A. Bodies emplaced in active orogenic areas

1. Bodies contemporaneous with eugeosynclinal volcanism

(I) Tholeiitic Suite

(a) Picritic subtype.....occur as basal accumulations to differentiated sills and flows.

(b) Anorthositic Subtype ....anorthosite, anorthosite gabbro or gabbroic anorthosite.

(II) Komatiitic Suite.....occurs as simple flows, spinifex-capped flows, differentiated flows and differentiated sills. Composition varies from peridotite to basalt.

2. Alpine-Type Bodies.....emplaced in solid state during tectonism.

(I) Large obducted sheets

(II) Ophiolite complexes.....all younger than about 1.0 billion years. interpreted as being oceanic crust and upper mantle.

(III) Deformed ophiolite complexes and clastic blocks in melange terranes.

(IV) Possible diapirs

3. Alaskan-type complexes.....concentrically zoned, highly calcic clinopyroxene, no orthopyroxene.

B. Bodies emplaced in non-orogenic areas

4. Large stratiformly layered complexes.....overall compositions tend to be mafic but ultramafic zones are present.

5. Sills and sheets equivalent to flood basalts. occur near flood basalts and have high K_2O content.

6. Medium and small sized intrusions

7. Alkalic ultramafic rocks in ring complexes and kimberlite pipes.

PRECAMBRIAN GEOLOGY OF COW CREEK

Other Ultramafic rocks in New Mexico

Two small ultramafic bodies have been reported near Rociada northeast of Elk Mountain. The writer briefly examined one of the occurrences with Dale Armstrong of CONOCO, Inc. and determined that it may be similar to the ultramafic rocks of Cow Creek based on field relations and hand sample characteristics. The Rociada ultramafics are small in aerial extent (200m X 200m). They appear to be intruded on all sides by quartz-monzonite and may be large xenoliths floating in the granitic rock. However, before any conclusions can be drawn detailed mapping must first be completed and good geochemistry obtained. Other small ultramafic occurrences have been reported in the Tusas Mountains (Kent, 1980) and the Wheeler Peak area near Taos (Condie, 1979; Robertson, J.M., personal communication).

Cow Creek

Ultramafic rocks are exposed in two locations along Cow Creek and its tributary, Elk Creek (Plates 1 and 2). The Precambrian rocks of Area 1 (lower Cow Creek) are primarily ultramafics, amphibolites, and granites with lesser amounts of diorites and other rocks. Exposure is poor (Approx. 10 percent), although much better than in Area 2 (upper Cow Creek) in which outcrop is very poor (Approx. 2 percent). The Precambrian rocks of Area 2 are predominantly amphibolites, granites and felsic metavolcanics with less than 1 percent ultramafics by area. Outcrop in Area 2 is best along old logging roads and along the creek bottoms. Because of the lack of good outcrop and extremely limited amounts of ultramafics in Area 2, the majority of the following discussions dealing with the petrology and chemistry of the ultramafics and amphibolites in the Cow Creek area is based on the rocks of Area 1.

Cow Creek: Area 1

Ultramafic rocks

Ultramafic rocks make up about 30 percent of the Precambrian rocks in the area and about 55 percent of the Cow Creek mafic-ultramafic complex. They decrease in relative abundance from south to north giving way to a series of amphibolites which commonly display conformable contacts with the ultramafics. The ultramafic rocks are intruded on the south and east by a well-foliated tonalite-trondhjemite. The relationship of the ultramafics to country rocks on the northwest and west is obscured by Paleozoic rocks which unconformably overlie the Precambrian rocks in the area. A large fault, hereafter informally called the Cow Creek fault, cuts the ultramafic rocks on the northeast (PLATE 1), obscuring the original contacts with a granitic body in that area.

The best exposures of ultramafic rocks are along the west side of Cow Creek near the middle of the mapped area. The rocks have steeply dipping (45 degrees to vertical) contacts with the amphibolite units. A distinct metamorphic foliation is common which also dips steeply and typically strikes in a west to northwest direction. The ultramafics generally have a micaceous dark green, khaki, khaki green or brownish red appearance. Well-crystallized chlorite, often as large (>1 x 1 mm) green flakes, and tremolite are

ubiquitous and give these rocks a distinctive micaceous appearance. Outcrops are massive and structureless (Figure 2) except on very fresh or recently weathered surfaces. Some weathered surfaces exhibit elephant hide ("olifantklip", Figure 3) texture. This is caused by selective weathering of less resistant fracture filling, usually tremolite, from the more resistant ultramafic rock. Spheroidal weathering (Figure 4) is also seen.

Contacts with other rock units are obscured in most locations, although contacts with the amphibolite and the tonalite-trondhjemite are found in some places. Figure 5 shows a tonalite-trondhjemite contact with the ultramafic rocks. The contacts with the amphibolite units all appear to be sharp. Contact metamorphic effects between the tonalite-trondhjemite and the mafic and ultramafic rocks are characterized by sodium and potassium enrichment (see geochemical section).

Pillow-like structures (Figure 6) up to 1 meter across have fine-grained selvages up to 3 cm in thickness. Some of these pillow-like structures filled in the troughs formed by the tops of similar underlying structures (Figure 7). Due to metamorphic recrystallization, grain sizes and altered zones have been homogenized, but the contacts are still well preserved. The internal structure includes polygonal fracturing and an overall decussate texture. Fine-grained margins (Figure 8) made up of small lath-like crystals of tremolite after clinopyroxene, up to 9 mm in length, set in

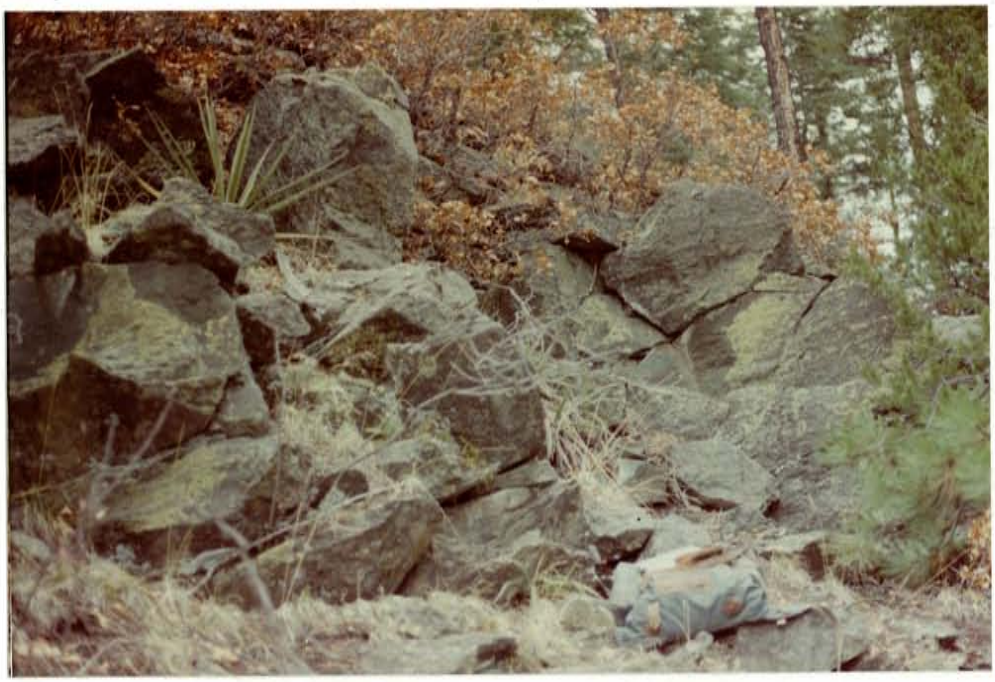

Figure 2. Typical outcrop of ultramafic rock in lower Cow Creek, Area 1.

Figure 3. "Olifantklip" or elephant hide texture within an ultramafic unit in lower Cow Creek, Area 1.

Figure 4. Spheroidal weathering in ultramafic rock from Area 1.

Figure 5. Tonalite-Trondhjemite contact with ultramafic unit in Area 1.

Figure 6. Pillow-like structures within the ultramafic units from Area 1.

Figure 7. Pillow-like structure (A) filling in the trough formed by the top of a similar underlying structure (B).

Figure 8. Fine-grained chlorite forming the margin of an ultramafic unit.

a matrix of chlorite (Figure 9) are also found. The chlorite probably represents devitrified glassy material. Fine-grained margins exhibit polyhedral jointing possibly formed by rapid cooling. Some also show well developed amygdules now filled with pale green microcrystalline quartz and tremolite. In one sample (Figures 10 and 10a) large radiating aggregates of tremolite up to 6 cm in length are seen. This would be expected if large clinopyroxene or orthopyroxene crystals were subjected to recrystallization during metamorphism. Relict cumulus textures are suggested in a few places by the presence of progressively finer layers of chlorite and tremolite from 1 to 4 cm in thickness (Figure 11).

Figure 12 is a photograph of a breccia made up of angular xenoliths of amphibolite in an ultramafic matrix. This suggests that at least some of the ultramafic rocks postdated (or were contemporaneous with) the deposition of the amphibolite protoliths.

Mineralogically the ultramafic rocks are chiefly composed of chlorite, hornblende, and tremolite in varying amounts. Lesser minerals include clinopyroxene, interstitial plagioclase, antigorite, magnetite and biotite, which combined may account for up to 15 per cent of the rock. Deformed polysynthetic twinning is seen in most plagioclase and in some hornblende. Relict phenocrysts of pyroxene are rare, but when seen they have been partially or totally replaced by hornblende, tremolite or chlorite.

2 mm

Figure 9. Photomicrograph of skeletal tremolite in a matrix of chlorite from within a fine-grained margin from an ultramafic unit, 10x, crossed-nicols.

Figure 10. Radiating tremolite in a hand specimen of ultramafic rock.

Figure 10a. Photomicrograph of radiating tremolite in ultramafic rock, 10x, plain light.

Figure 11. Photomicrograph of possible relict cumulus texture from within an ultramafic unit from Area 1, 10x, crossed-nicols.

Figure 12. Breccia made up of amphibolite fragements in a matrix of ultramafic material from lower Cow Creek, Area 1.

Biotite is seen forming as an alteration product of hornblende and chlorite (Figure 13). Chlorite mainly forms as an alteration product of hornblende and occurs as both coarse (>1 X 1 mm) and fine (<1 X 1 mm) aggragates forming the matrix of the ultramafic rocks (Figures 14 and 14a). Tremolite occurs as either an alteration product of pyroxenes or as skeletal crystals in a matrix of chlorite and hornblende (Figure 15). Grain boundaries are generally embayed and corroded evidencing alteration by hydrothermal processes. Trace minerals are clinozoisite, zoisite, epidote, carbonate, sphene, garnet and quartz. (See APPENDIX C for detailed petrographic descriptions.)

Most of the Cow Creek ultramafic rocks are strongly foliated resulting from alignment of chlorite flakes and tremolite blades. Porphyroclasts of chlorite and clinopyroxene are found up to 3 mm x 3 mm. Hornblende occurs as both crystalline and fibrous aggregates parallel to foliation.

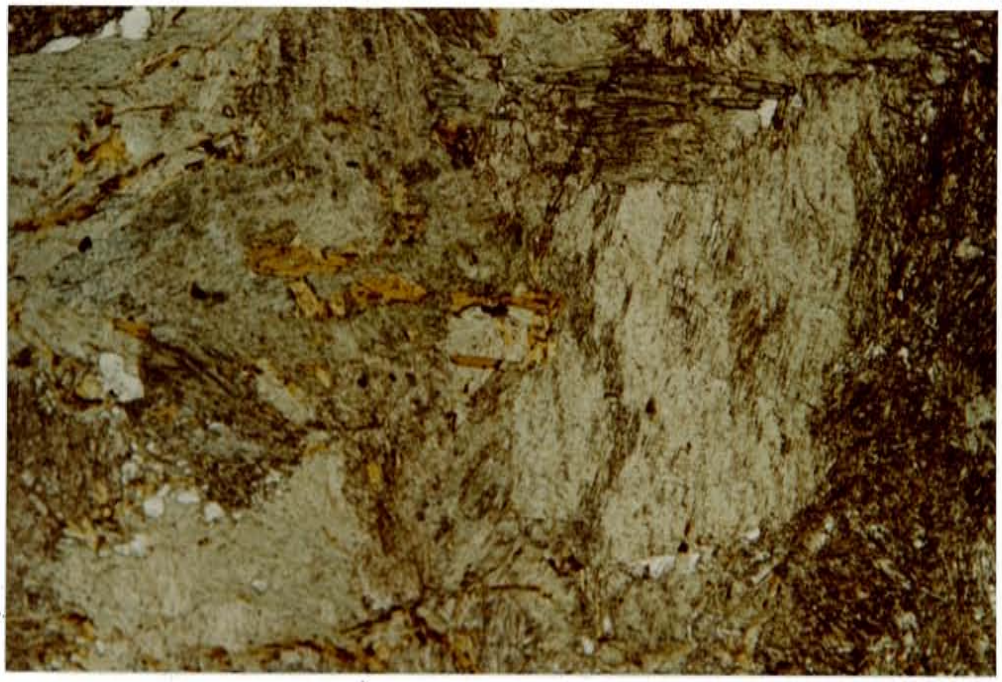

1 mm

Figure 13. Photomicrograph of biotite forming as an alteration product of hornblende and chlorite in the ultramafic rock, 25x, plain light.

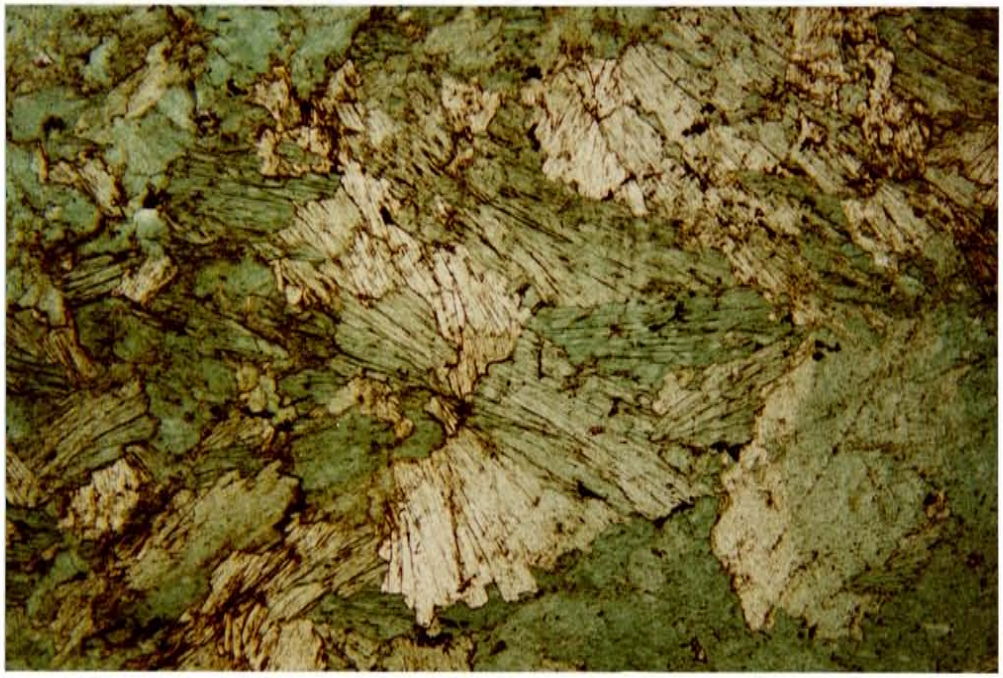

2 mm

Figure 14. Photomicrograph of coarse chlorite (>1 x 1 mm) forming as an alteration product of hornblende in ultramafic rock, 10x, plain light.

1 mm

Figure 14a. Photomicrograph of fine chlorite (<1 x 1 mm) in ultramafic rock, 25x, plain light.

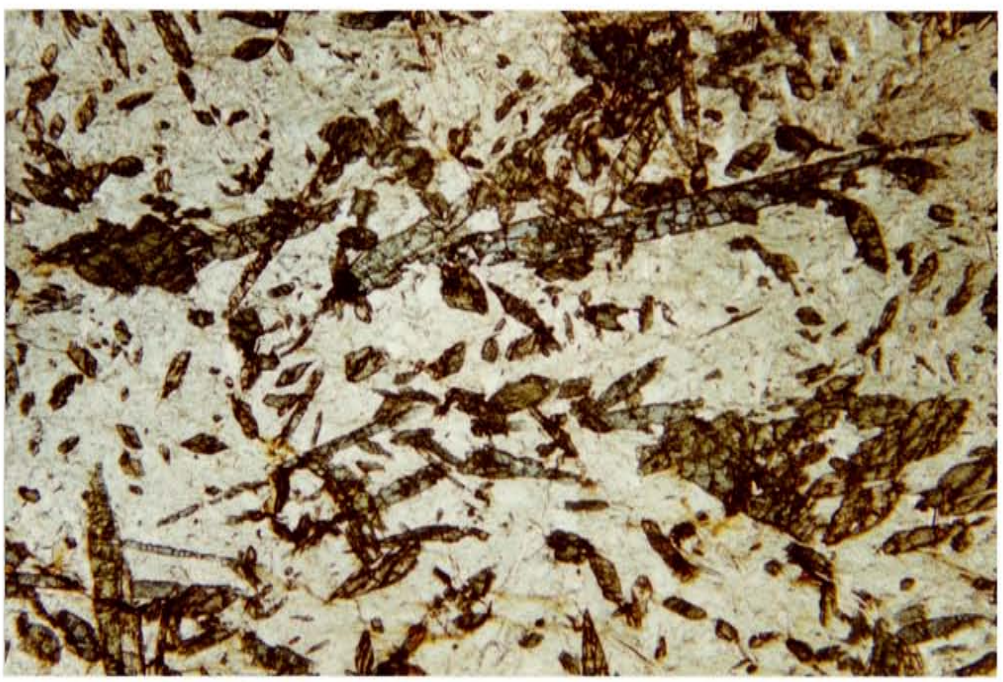

2 mm

Figure 15. Photomicrograph of skeletal tremolite in a matrix of hornblende and chlorite in the ultramafic rock, 10x, plain light.

Amphibolites

Amphibolite make up about 25 percent of the total area of Precambrian rocks and 45 percent of the mafic-ultramafic complex. They increase in relative abundance northward. Amphibolite occurs as both lensoidal bodies and large irregular masses (see Plate 1) and is generally found in sharp contact with the ultramafic rocks. Individual units of amphibolite range from 10 cm to many meters thick and generally have steeply dipping contacts. The amphibolites are black to dark green and either occur as thick (10's of meters) successions or as minor small (several meters) concordant units within the ultramafic rocks. A variety of petrographic textures are found including fine-grained (small but visible), aphanitic, ophitic and pegmatitic. Outcrops are massive and structureless although foliations are found. Near granitic contacts, amphibolites are migmatitic (Figure 16). Sodium and potassium enrichment caused by injection of small granitic stringers is common (see geochemical section). This is very pervasive in the northeast part of the study area near a foliated quartz-monzonite plug. Chloritization, epidotization and silicification are variably developed throughout the area but typically increase near the Cow Creek fault.

Two important variants of the amphibolite occur in the metavolcanic succession. The most abundant variant is a coarse-grained (> 2-3 mm) amphibolite (Figure 17) which is

Figure 16. Migmatitic amphibolite near a granitic contact in Cow Creek Area 1.

sometimes accompanied by a very coarse-grained pegmatitic phase (Figure 18). The least abundant is a very fine-grained (< 1 mm) amphibolite which is interlayered with the hornblende-quartz-chlorite schists.

The amphibolites contain variable amounts of hornblende, plagioclase, chlorite and actinolite-tremolite. Minor minerals are quartz, orthoclase, sericite, clinopyroxene, and traces of biotite, zoisite, epidote, sphene, garnet and magnetite. (see APPENDIX C for detailed petrographic descriptions). Plagioclase compositions vary from oligoclase (An12), to andesine/labradorite (An50). Locally the amphibolites may contain minor amounts of chlorite and epidote, especially near intrusive contacts and faults.

Although primary textures within the amphibolite appear to be absent, the fine-grained facies or fraction is believed to represent meta-basalt. The coarse-grained amphibolite probably represents a series of gabbroic or diabasic hypabyssal sills and dikes. Ultramafic xenoliths up to 30cm across are found within the coarse amphibolite.

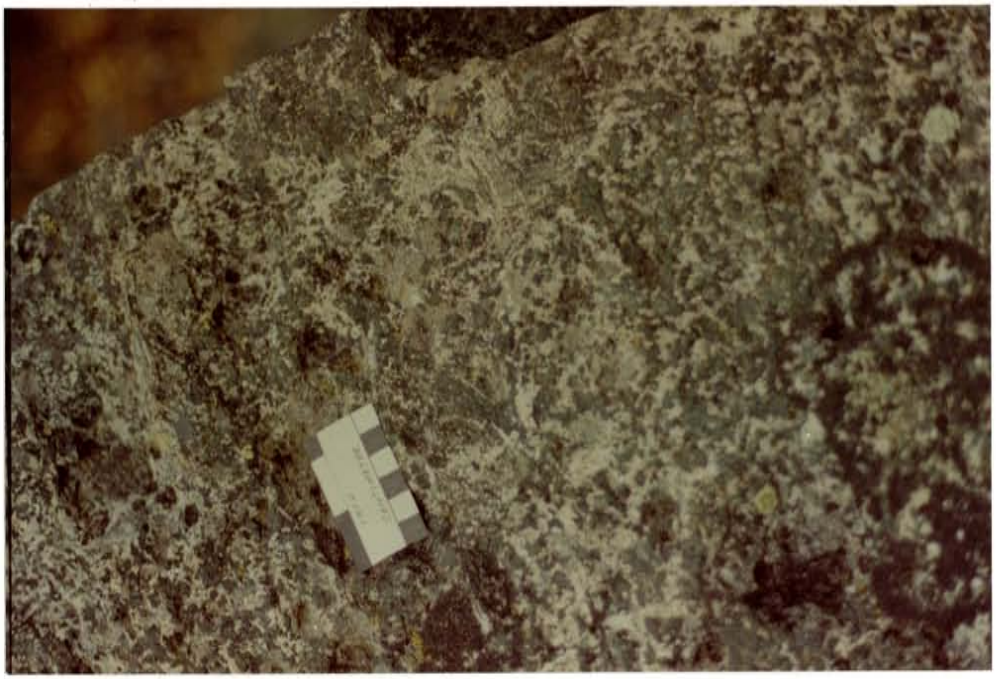

Figure 17. Coarse-grained amphibolite from lower Cow Creek Area 1.

Figure 18. "Pegmatitic" amphibolite from lower Cow Creek Area 1.

Hornblende-Quartz-Chlorite Schists

Hornblende-quartz-chlorite schists compose only a few percent of the total area of Precambrian rocks. They are commonly dark green to black but some have a mottled green and white coloring. Color is generally a function of plagioclase and quartz content: the higher the percentage of plagioclase and quartz, compared to hornblende and chlorite, the lighter the color.

Most of the rocks (Figure 19) are composed of hornblende, chlorite, quartz, plagioclase, magnetite and a trace of zircon. Foliation is well developed by millimeter sized plates of hornblende and chlorite which are aligned parallel to the regional foliation. Individual layers consisting of: quartz; plagioclase + hornblende; hornblende + chlorite; quartz + plagioclase; and hornblende + magnetite also give the rock a banded appearance. Magnetite occurs as both rounded grains and as an alteration product of hornblende. The individual layers of hornblende + chlorite (Figure 20) appear to be ultramafic, although no chemistry exists on these rocks. Individual layers vary in thickness from .5 mm (hornblende + magnetite) up to 2 cm (quartz, hornblende, plagioclase).

Remaining schists are characterized by their conformity with the above rocks. Texturally they contain granules and globules of chlorite. They are composed of hornblende, chlorite, quartz, plagioclase and magnetite. Hornblende and

Figure 19. Hornblende-Quartz-Chlorite Schist frow lower Cow Creek Area 1.

Figure 20. Ultramafic hornblende + chlorite lenses in the Hornblende-Quartz-Chlorite Schist from Area 1.

chlorite are in elongate lenses up to 1 cm long and 0.1 cm thick (Figure 21). Quartz and plagioclase have been recrystallized into fine-grained (<0.1 mm) aggragates which are now parallel to the developed foliation. Some hornblende has altered to magnetite and chlorite.

The hornblende-quartz-chlorite schists appear to represent mafic and ultramafic sediments, volcaniclastic rocks and subaqueous ashes which were all interbedded. They are intruded by both ultramafic and mafic rocks and possibly represent a remnant portion of the upper sea floor.

Figure 21. Hornblende + chlorite and quartz + plagioclase lenses in Hornblende-Quartz-Chlorite Schist from Area 1.

Granitic Rocks

Granitic rocks have been subdivided into six varieties based primarily upon mineralogical and textural differences. Limited chemistry is also available on some of these rocks (see geochemical section). The rocks vary in composition from diorites to granites and from unfoliated to strongly foliated. Most appear to be younger than the mafic and ultramafic rocks as evidenced by xenoliths of amphibolite (Figures 22,23) and ultramafic rock in the granites and crosscutting relationships. The exception to this is the diorite and quartz-diorite whose exact relation to other rocks is unknown. Intrusion of the granites has resulted in local sodium and potassium metasomatism near the contacts with the mafic and ultramafic units. Granitic rocks make up about 40 percent of the Precambrian rocks in the mapped area but are not included in the defined mafic-ultramafic complex. Granitic rocks are especially abundant in the south and east and the six varieties are presented in order of decreasing age in the following discussions.

Figure 22. Xenolith of amphibolite in granitic rock from Area 1.

Figure 23. Xenoliths of amphibolite in granitic rock from Area 1.

Tonalite-trondhjemite

A tonalite-trondhjemite body is defined on the basis of mineralogy and one chemical analysis (Robertson, J.M., in progress). It is intrusive into the ultramafic and amphibolitic rocks along the south and east part of the mapped area. Contacts are generally discordant to the foliation developed in the mafic and ultramafic rocks. Dikes up to 5 meters across can be traced directly from the tonalite-trondhjemite body into the mafic-ultramafic complex (see Plate 1). These dikes, unlike the main tonalite-trondhjemite body are generally concordant to the foliation in the mafic-ultramafic rocks. The unit is homogeneous, light gray, medium to coarse grained and well foliated. Flow-like structures are well developed around the xenoliths of amphibolite.

Mineralogically the tonalite-trondhjemite body is composed of quartz, sodic plagioclase, hornblende, biotite and microcline. Sericite, zoisite and magnetite occur as trace minerals. Ovoid to subhedral quartz and plagioclase eyes up to 2mm in diameter are common and elongate parallel to the developed foliation. Most are recrystallized into aggregates of smaller grains but are interpreted as representing grains of the original rock prior to metamorphic deformation.

Barker et.al. (1974, 1976) describe mid-Proterozoic trondhjemites from north-central New Mexico and south-central Colorado. J.M. Robertson (personal communication) has identified a number of mid-Proterozoic tonalite-trondhjemite bodies from the Pecos greenstone belt including this one from Cow Creek that exhibits trondhjemitic chemistry (Table 4a).

Diorite and Quartz-Diorite

Diorite and quartz-diorite together make up only a small percent of the area. Diorite is fine-grained, well-foliated and consists of plagioclase, actinolite-tremolite, biotite, quartz, epidote and magnetite. No chemical data exists on these rocks. The diorite is distinguished from the amphibolite in that it contains small amounts of visible quartz and more plagioclase. It is usually associated with amphibolite near or along the contacts with ultramafic units. The exact relationship between the diorite and the amphibolite is unclear.

Quartz-diorite is found in only one small outcrop. It consists of quartz, albite (An 8), K-feldspar, hornblende, biotite, chlorite and subordinate magnetite with a trace of zircon. Sericitization is selectively confined to the plagioclase and hornblende is altered to chlorite and biotite. The foliation in this body appears to be concordant to the regional northwest foliation of the mafic and ultramafic rocks. Its exact relationship to other units is unknown. It is distinguished from the tonalite-trondhjemite by less quartz and hornblende.

Foliated-granite

The foliated-granite is in fault contact with the tonalite-trondhjemite in the southern part of the map area. The contact is about 30 meters wide and contains breccia of both the foliated-granite and the tonalite-trondhjemite. The foliated-granite is a flesh pink microcline-biotite granite. It is commonly medium- to coarse-grained and in most places is well-foliated. It is a true granite containing quartz and microcline in approximately equal amounts, plagioclase (albite or oligoclase), biotite, hornblende, epidote and minor magnetite. Apatite, sphene, and zircon are accessory minerals. The foliated-granite is petrographically very similar to the microcline-biotite granite described by Miller and others (1963), which is part of the Embudo granite near the Truchas Peaks northwest of this map area. This body contains numerous small amphibolitic lenses on the east side of Cow Creek fault.

Foliated Quartz-monzonite

This body is a well-foliated pink equagranular medium-grained granite. It crosscuts mafic and ultramafic units in the northern part of the area. Most outcrops are extensively whethered and those that are found are unjointed. The body is well-foliated parallel to it's intrusive contacts with the mafic and ultramafic rocks. This foliation is formed by alignment of "quartz eyes", biotite and hornblende.

Mineralogically the rocks consist of 30 percent each of quartz, plagioclase and microcline, with about 5 percent each of biotite and hornblende. Minor minerals include magnetite and garnet. Technically the rock is a quartz-monzonite. Both microcline and plagioclase have been sericitized and the rock exhibits both mortar and cataclastic textures. Chemical data on the mafic and ultramafic rocks show that the body caused potassic and sodic metasomatism during it's intrusion. Petrographic evidence for this is large K-feldspar crystals in the amphibolite which become more abundant closer to the intrusion and it's dikes.

Unfoliated-granite

This body has informally been called the Pecos granite by Mathewson (in progress) and Condie (1979). It is intrusive into the mafic and ultramafic rocks in the northern part of the mapped area. In this area, however, it is also cut by the Cow Creek fault and therefore outcrops are extensively sheared and altered. In fresh exposure on the east side of the Cow Creek fault, the body is unfoliated and is in intrusive contact with the foliated-granite.

This body is primarily a medium- to coarse-grained, pink to tan, hornblende-biotite granite. It is non-porphyritic and contains 15-20 percent quartz 30-40 percent potassic feldspar, 20-30 percent plagioclase with subordinate hornblende and magnetite. Zircon is also present. Hornblende is in various stages of alteration to biotite and chlorite. Plagioclase is andesine (An 45) and is slightly altered to sericite. Most grains show curved, embayed or scalloped boundaries and the overall texture is granoblastic. Myrmekitic texture is seen in some plagioclase.

Cow Creek: Area 2

Ultramafic rocks of Area 2 are limited to two small outcrops within an extensive amphibolitic terrane (PLATE 2) and probably represent less than one percent of the total area of Precambrian rock. The ultramafics are mineralogically similar to the ultramafic rocks of Area 1 but contain more magnetite and less tremolite.

Amphibolites make up about 70 percent of the Precambrian rocks of the mapped area, decreasing in abundance to the southwest where they are intruded by a biotite-granite. Contacts between the amphibolite and biotite-granite appear both concordant and discordant. Mineralogically the amphibolites are similar to those of Area 1, however, almandine garnet is also found. Most amphibolites of Area 2 are fine-grained and well-foliated in a west-northwesterly direction. Foliation dips are nearly vertical.

Quartz-sericite schists occur as conformable units up to 15 meters thick of unknown length within the amphibolitic terrane. They are well-foliated parallel to the regional foliation. The predominant mineralogy is quartz, plagioclase, sericite, hornblende, biotite and minor potassic feldspar. Garnet, magnetite and zircon are also present in minor amounts. Quartz "eyes" up to 1 x 5 mm are aligned parallel to foliation. Other metacrysts include

plagioclase, potassium feldspar and garnet. The matrix is composed of fine-grained quartz and sericite and is also well-foliated.

The southwestern part of Area 2 is dominated by a well-foliated biotite-granite. Foliation is caused by alignment of biotite and hornblende. Mineralogically the rock consists of quartz, microcline, plagioclase, biotite and hornblende. Chlorite, sericite, zircon, magnetite and sphene occur in small amounts. The biotite-granite contains xenoliths of amphibolite and is believed to represent the latest Precambrian intrusive episode in Area 2. It preceeded regional metamorphism, however, as is demonstrated by a pervasive west-northwest foliation.

QUATERNARY DEPOSITS

Alluvium

Present stream terraces and associated deposits are mapped as Quaternary alluvium. The majority of the alluvial units are exposed in the bottom of Cow Creek in the northeastern and southeastern part of mapped Area 1. Other alluvial units are found in Rito Chaparito Creek in the northwestern part of the mapped area.

Quaternary alluvium is generally composed of Precambrian, and to a minor extent Paleozoic rocks. No Quaternary alluvium was mapped in Area 2 as the streams are immature and often run on bedrock.

Landslide Deposits

Three large deposits in the west and central parts of Area 1 are interpreted as landslide deposits on the basis of the size of fragments, and lack of any other viable explanation for their origin. The westernmost deposit consists of large angular blocks of Paleozoic rubble which have moved downslope along low-angle slide planes. Precambrian rocks are obscured in the area. The other two landslide deposits consist primarily of angular to subangular Precambrian ultramafic blocks up to 1.5 meters in diameter. No matrix was found as it was probably washed

away by rains. In the central part of Area 1 the two deposits are each irregular in shape but roughly 200 meters on a side. They occur on two topographically high benches, one directly above and to the east of the other, and therefore the two deposits may be related to the same landslide.

GEOCHEMISTRY

Thirty-five ultramafic and mafic rocks from the two separate Cow Creek field areas were analyzed for whole rock chemistry. In addition 4 samples (2 ultramafics and 2 amphibolites) were analyzed for rare earth elements by neutron activation methods described by Gordon et.al (1968) and Condie and Lo (1971). Those samples, for which complete major element data is available, are presented in Table 2. Rare earth data are presented in Table 5, and together with the major element data were used in constructing Figures 24-39. Before plotting however, all analyses were recalculated to 100 percent after subtracting volatiles (H2O and CO2).

CIPW norms were calculated with the aid of a computer program and are presented in Table 3. Because Fe+2 and Fe+3 were not distinguished analytically, the amount of FeO was calculated using the method of Irvine and Baragar (1971).

Alteration

The rocks of Cow Creek could have been altered by any one or combination of the following processes. 1) Sea floor alteration (halmyrolisis) during formation of the rocks. 2) Alteration during devitrification of any glassy material that may have existed. 3) Sodium or potassium enrichment by

Table 2

Whole Rock and Trace Metal Chemistry

Ultramafic Rocks	A2-79-6	A2-79-7	A1-1	7-19-2	80-2-23	80-3-23	80-4-23	80-1-26	80-2-26	80-3-26	79-7-26	79-16-26	79-17-26	79-18-26	79-23-26	79-24-26	79-4-35	79-11-35
SiO_2	44.69	41.80	43.43	42.98	43.55	42.90	42.17	44.35	43.54	40.46	46.43	43.09	45.57	43.32	46.20	42.16	44.09	47.46
TiO_2	0.80	0.71	0.36	0.27	0.30	0.28	0.29	0.22	0.22	0.21	0.52	0.15	0.21	0.18	0.25	0.14	0.30	0.24
Al_2O_3	4.40	9.11	7.49	7.19	6.93	8.56	6.66	5.80	11.16	6.28	9.04	3.95	4.97	3.85	5.53	3.74	8.70	7.63
Fe_2O_3 Total	19.60	14.99	11.60	11.58	14.40	11.42	12.52	12.67	8.21	10.73	12.03	10.95	12.21	12.93	11.73	12.02	11.25	10.52
MgO	17.88	13.47	24.46	24.07	19.85	19.79	24.61	23.61	19.55	27.22	18.70	26.93	24.85	27.51	23.44	24.33	19.70	22.84
CaO	4.30	10.93	7.45	7.12	6.37	8.85	7.41	5.93	10.36	7.53	7.57	2.21	2.78	3.12	5.47	4.70	9.37	5.34
Na_2O	0.73	3.99	0.48	0.45	0.69	0.93	0.53	0.63	1.72	0.67	0.72	5.00	0.67	0.18	0.47	0.60	0.79	0.70
K_2O	ND	ND	ND	ND	ND	ND	ND	ND	0.96	ND	0.19	ND	0.09	ND	ND	0.13	ND	0.15
MnO	0.20	0.146	0.10	0.75	0.19	0.16	0.18	0.16	0.14	0.16	0.20	0.10	0.25	0.02	0.08	0.16	0.10	0.18
LOI[1]	4.37	4.73	4.74	5.89	5.58	5.01	5.40	6.34	4.06	6.89	3.33	7.74	6.94	8.27	6.04	6.01	4.32	4.63
P_2O_5 [2]	<0.04	0.11	0.08	<0.04	<0.04	<0.04	<0.04	<0.04	<0.04	<0.04	<0.04	<0.04	<0.04	<0.04	<0.04	0.04	<0.04	<0.04
Total	97.01	99.94	100.15	100.31	97.90	98.94	99.81	100.75	99.96	100.19	98.72	100.02	98.58	98.42	99.17	97.90	98.65	99.73
FeO Total[3]	19.04	14.18	10.95	11.04	12.96	10.28	11.27	11.40	7.39	9.65	11.36	10.68	11.99	12.91	11.34	11.78	10.73	9.96
Ni (ppm)[2]	190	140	540	720	670	640	910	860	650	970	417	860	910	1065	890	1040	1100	840
Cu (ppm)[2]	162	112	69	20	24	13	14	70	108	60	176	53	177	<10	107	<10	14	33
Zn (ppm)[2]	205	106	80	69	88	53	70	96	36	54	94	77	147	85	56	88	170	82
Co (ppm)[2]	165	102	84	98	109	96	97	105	67	83	126	123	124	129	113	120	111	99
Cr (ppm)[2]	99	161	443	293	187	163	84	230	115	263	388	73	132	238	216	109	168	366
Cu/Cu + Ni	0.46	0.44	0.11	0.03	0.03	0.02	0.02	0.08	0.14	0.06	0.29	0.06	0.16	0.01	0.11	0.01	0.01	0.04
CaO/Al_2O_3	0.98	1.12	0.99	0.99	0.92	1.03	1.11	1.02	0.93	1.20	0.84	0.56	0.56	0.81	1.01	1.26	1.08	0.70

[1] Determined by the New Mexico Bureau of Mines and Mineral Resources Lab, Socorro, New Mexico.

[2] Analysis by Atomic Absorbtion conducted by the New Mexico Bureau of Mines and Mineral Resources Lab, Socorro, New Mexico.

[3] Determined by method outlined by Irvine and Barager (1971).

ND Below the detection limit of X-ray fluorescence analysis.

Table 2

Whole Rock and Trace Metal Chemistry (Continued)

Amphibolites	A2-79-2	A2-79-5	A2-79-8	A2-79-9	BP-1	80-1-23	80-4-26	80-5-26	79-12-26	79-14-26	79-15-26	79-19-26	79-20-26	79-21-26	79-22-26	80-1-35	80-2-35
SiO_2	45.08	44.65	45.57	45.28	43.28	47.09	46.24	46.40	45.77	45.71	46.82	46.00	47.49	45.57	46.11	45.04	47.07
TiO_2	1.17	1.07	0.53	1.06	0.80	0.46	0.38	0.34	0.35	0.41	0.24	0.34	0.35	2.33	0.39	0.31	0.32
Al_2O_3	13.17	10.96	12.38	12.12	13.84	14.54	14.38	14.96	14.24	14.15	14.88	13.94	15.23	12.35	13.81	12.08	12.41
Fe_2O_3 Total	13.22	14.53	12.14	12.72	10.78	8.30	7.01	8.67	8.41	9.27	7.16	9.49	8.23	9.90	9.44	9.44	9.15
MgO	7.39	10.23	10.34	8.30	11.75	11.84	12.30	10.87	12.77	12.36	10.21	12.21	12.90	14.17	12.52	15.91	12.17
CaO	12.66	12.23	11.71	11.42	15.41	14.21	15.05	15.28	12.60	13.13	12.27	13.03	13.20	11.46	12.45	11.64	12.95
Na_2O	1.45	1.32	2.01	2.53	2.52	2.17	1.63	1.83	1.58	1.91	4.46	1.57	1.73	1.72	1.53	0.84	2.42
K_2O	0.24	0.15	0.04	0.85	0.38	0.22	0.15	0.05	0.48	0.09	0.87	0.29	0.43	0.05	1.25	0.12	0.56
MnO	0.25	0.21	0.21	0.24	0.21	0.15	0.15	0.15	0.11	0.14	0.10	0.14	0.14	0.16	0.15	0.15	0.14
LOI[1]	2.49	2.77	2.70	2.98	0.80	0.84	1.53	1.40	1.83	1.96	1.88	1.48	1.09	1.51	1.37	2.62	2.35
P_2O_5 [2]	0.09	ND	<0.04	<0.04	<0.04	<0.04	<0.04	<0.04	<0.04	<0.04	ND	<0.04	<0.04	<0.04	<0.04	<0.04	<0.04
Total	97.21	98.12	97.67	98.04	99.81	99.50	98.86	99.99	98.20	99.17	98.88	98.53	100.79	99.71	99.06	98.19	99.58
FeO Total[3]	12.57	13.71	11.50	12.05	9.70	6.11	6.30	6.00	7.86	8.58	6.64	8.80	7.42	9.07	8.70	8.49	6.43
Ni (ppm)[2]	60	80	180	110	83	223	210	210	330	250	330	795	280	320	305	540	250
Cu (ppm)[2]	50	408	<10	118	13	42	81	71	44	132	99	1243	108	95	149	76	20
Zn (ppm)[2]	125	77	85	81	25	38	54	29	59	50	50	70	50	80	52	47	44
Co (ppm)[2]	65	109	78	93	43	47	54	52	96	80	70	99	87	85	67	68	54
Cr (ppm)[2]	263	160	333	165	225	486	443	260	429	251	273	387	367	436	302	201	282
Cu/Cu + Ni	0.45	0.83	0.05	0.52	0.14	0.16	0.28	0.25	0.12	0.35	0.23	0.61	0.44	0.22	0.33	0.12	0.07
CaO/Al_2O_3	0.96	1.12	0.95	0.94	0.94	1.06	1.05	1.02	0.88	0.93	0.82	0.93	0.87	0.93	0.90	0.96	1.04

Table 3

Normative Mineralogy

Ultramafic Rocks	A2-79-6	A2-79-7	A1-1	7-19-2	80.2-23	80-3-23	80-4-23	80-1-26	80-2-26	80-3-26	79-7-26	79-16-26	79-17-26	79-18-26	79-23-26	79-24-26	79-4-35	79-11-35
OR	0	0	0	0	0	0	0	0	5.952	0	1.192	0	0.597	0	0	0.834	0	0.952
AB	6.811	5.819	4.266	4.098	6.352	8.559	4.795	5.717	2.599	5.375	6.486	16.671	6.239	1.691	4.266	5.543	7.165	6.307
AN	9.593	6.884	19.364	18.803	17.390	20.858	16.921	14.005	20.894	15.341	22.053	0	11.356	10.748	14.080	7.835	21.585	18.247
NE	0	15.036	0	0	0	0	0	0	6.856	0.378	0	2.984	0	0	0	0	0	0
AC	0	0	0	0	0	0	0	0	0	0	0	4.839	0	0	0	0	0	0
NS	0	0	0	0	0	0	0	0	0	0	0	4.314	0	0	0	0	0	0
WO	5.788	19.611	8.229	7.906	7.127	11.117	9.278	7.357	13.698	10.382	7.381	5.009	1.597	2.676	6.403	7.417	11.742	4.107
EN	37.377	13.026	21.634	21.747	28.693	17.407	17.113	30.392	10.329	7.776	33.195	3.676	42.332	38.255	41.938	41.642	20.897	39.852
FS	21.864	5.155	5.113	5.827	11.302	5.141	4.551	8.692	1.983	1.572	10.363	0.859	11.351	9.804	10.938	11.354	6.089	9.385
FO	8.146	14.219	29.999	29.659	17.957	25.357	34.028	23.366	28.584	45.887	11.258	48.769	18.156	26.446	14.923	17.410	22.106	14.315
FA	5.251	6.202	7.813	8.758	7.795	8.253	9.973	7.364	6.048	10.221	3.873	12.554	5.366	7.469	4.290	5.232	7.098	3.715
MT	3.486	12.684	2.749	2.618	2.677	2.652	2.655	2.568	2.526	2.535	2.998	0	2.533	2.464	2.588	2.411	2.660	2.556
IL	1.664	1.346	0.728	0.556	0.617	0.563	0.596	0.447	0.440	0.442	1.054	0.306	0.441	0.380	0.517	0.287	0.613	0.478
Total	99.980	99.982	99.894	99.972	99.908	99.908	99.909	99.908	99.908	99.909	99.852	99.980	99.969	99.932	99.943	99.964	99.953	99.914

Table 3

Normative Mineralogy (Continued)

	A2-79-2	A2-79-5	A2-79-8	A2-79-9	BP-1	80-1-23	80-4-26	80-5-26	79-12-26	79-14-26	79-15-26	79-19-26	79-20-26	79-21-26	79-22-26	80-1-35	80-2-35
Amphibolites																	
OR	1.494	0.957	0.239	5.343	0	1.302	0.892	0.298	2.971	0.535	5.342	1.783	2.554	2.970	7.614	0.775	3.384
AB	13.093	11.822	18.120	17.341	0	11.996	9.796	9.821	13.086	13.100	8.725	13.633	13.542	14.884	8.242	7.509	12.774
AN	30.719	24.991	26.208	20.571	25.835	29.800	32.551	33.134	31.669	30.830	18.633	31.209	32.785	25.122	27.938	30.408	22.103
NE	0	0	0	2.993	11.753	3.604	2.393	3.267	0.471	1.996	16.454	0.085	0.682	0	2.779	0	4.501
WO	15.203	16.472	14.876	16.706	19.130	17.369	18.510	18.395	14.025	15.304	18.541	14.953	13.882	13.808	14.920	12.635	18.360
EN	16.503	16.311	11.856	9.636	12.803	12.336	13.728	12.536	9.956	10.541	13.109	10.116	9.942	15.245	10.235	19.359	12.430
FS	12.530	10.528	6.783	6.311	4.902	3.516	2.982	4.419	2.846	3.529	3.831	3.689	2.701	1.474	3.495	5.400	4.518
FO	2.220	7.529	10.889	8.744	11.921	12.352	12.551	10.588	16.297	14.965	9.274	15.014	15.737	14.648	15.350	15.718	13.241
FA	1.858	5.356	6.865	6.312	5.030	3.880	3.005	4.113	5.134	5.521	2.987	6.033	4.712	1.561	5.777	4.832	5.304
MT	4.003	3.846	3.017	3.859	3.366	2.861	2.756	2.687	2.712	2.803	2.549	2.698	2.697	5.640	2.773	2.661	2.666
IL	2.362	2.154	1.074	2.161	1.534	0.984	0.745	0.650	0.688	0.803	0.477	0.669	0.668	4.524	0.765	0.613	0.630
LC	0	0	0	0	1.777	0	0	0	0	0	0	0	0	0	0	0	0
CS	0	0	0	0	1.858	0	0	0	0	0	0	0	0	0	0	0	0
Total	99.985	99.966	99.927	99.978	99.909	99.909	99.908	99.908	99.854	99.928	99.923	99.881	99.903	99.876	99.888	99.909	99.908

TABLE 4

	A**	B	K**	M**	O**	P**	W**	ct**	ot**	ob**
SiO_2	44.0	52.73	46.1	52.2	47.8	45.2	46.0	50.7	49.3	47.1
TiO_2	0.27	0.85	0.34	0.80	0.56	0.71	0.25	2.0	1.8	2.7
Al_2O_3	5.27	9.83	3.0	14.8	3.47	3.54	5.73	14.4	15.2	15.3
Fe_2O_3*	12.2 T	NR	6.23	11.52T	6.43	0.46	3.97	3.2	2.4	4.3
FeO*	10.95T	10.80T	4.82	10.36T	5.90	8.04	5.72	9.8	8.0	8.3
MgO	32.5	10.10	33.9	7.95	27.1	37.5	32.8	6.2	8.3	7.0
CaO	5.48	9.99	4.74	10.17	7.45	3.08	5.15	9.4	10.8	9.0
Na_2O	0.32	2.65	0.17	2.44	0.52	0.57	0.24	2.6	2.6	3.4
K_2O	0.04	0.46	0.03	0.28	0.05	0.13	0.02	1.0	0.24	3.4
MnO	0.22	0.22	0.19	0.20	0.20	0.14	0.20	0.20	0.17	0.17
P_2O_5	NR	0.06	NR	NR	NR	NR	NR	NR	NR	NR
Total	100.3	97.69	99.52	100.36	99.48	99.37	100.08	99.5	98.81	100.67
Ni(ppm)	NR	NR	1600	NR	1200	1600	NR	NR	NR	NR
Cr(ppm)	NR	NR	2400	NR	2600	3000	NR	NR	NR	NR

A, Peridotitic Komatiite from Australia (Naldrett and Turner, 1977).
B, Basaltic Komatiite, Barberton type (Viljoen and Viljoen, 1969).
K, Peridotitic Komatiite, Komati Formation (Viljoen and Viljoen, 1969).
M, Basaltic Komatiite, Munro township (Naldrett and Turner, 1977).
O, Peridotitic Komatiite, Sandspruit Formation (Viljoen and Viljoen, 1969).
P, Pyrolite (Ringwood, 1966).
W, Quench Textured Peridotite, Western Australia (Nisbet et al., 1977)
ct, Average continental tholeiite (Nocholds, 1954).
ot, Average oceanic tholeiite (Nocholds, 1954).
ob, Average olivine basalt (Nocholds, 1954).

*, Symbol "T" means calculated as total iron
**, Recalculated to 100 percent after correction for volitiles
NR, Not Reported

Table 4a

Selected Analyses from the Pecos Greenstone Belt Region

	1	2	3	4	5	6	7
SiO_2	43.2	59.0	49.8	53.1	76.8	75.8	75.21
TiO_2	0.10	0.44	0.61	1.25	0.11	0.09	0.15
Al_2O_3	9.14	14.0	14.8	13.9	12.9	13.1	13.57
Fe_2O_3 T	14.2	8.98	10.4	12.9	1.28	1.15	1.43
FeO T	12.8	NR	9.4	11.6	NA	NA	NA
MgO	21.9	11.8	8.30	5.03	0.87	0.35	0.36
CaO	7.77	11.0	12.1	9.8	0.87	0.82	1.03
Na_2O	0.72	1.64	2.16	2.89	3.86	3.85	5.83
K_2O	0.08	0.38	0.33	0.73	3.12	4.99	0.56
MnO	0.17	0.17	0.18	0.19	NA	NA	0.01
P_2O_5	NR	NR	NR	NR	NA	NA	0.03
LOI	NR	0.74	1.19	0.92	NA	NA	0.52
Total	97.3	99.0	99.88	100.69	99.7	100.1	95.69
Ni (ppm)	724	79.1	41	26.3	11.3	25.4	9
Cr	241	914	275	109	NA	NA	NA
Co	90.4	48.6	48.1	42.6	NA	NA	8
Cu	34.8	51.3	67.3	55.5	27.4	21.4	90
Zn	102	66.4	92.7	126	28.7	61.1	12

1 - Average of 3 ultramafic samples from Area 1 collected and analyzed by Mathewson, in progress

2 - H-7-122, from Mathewson, in progress

3 - Pecos A, from Mathewson, in progress

4 - Pecos B, from Mathewson, in progress

5 - Embudo Granite, from Mathewson, in progress

6 - Pecos Granite, from Mathewson, in progress

7 - Pecos Tonalite-Trondhjemite, from Robertson, in progress

NA - Not Analyzed

TABLE 5

Trace Element Concentrations

	79-23-26	79-18-26	79-22-26	79-12-26	RP-5-2*	RP-5-5*	H-7-122*	Pecos A*	Pecos B*
Rb	11.00	10.49	12.24	21.99	6.7	3.7	10.7	8.2	18
Ba	83	78	115	99	95.3	13.9	86.9	129	437
Cs	.005	0.21	3.30	8.53	1.14	0.16	8.07	9.9	2.47
Ta	0.11	0.14	0.20	0.11	0.16	0.00	0.08	0.19	0.51
Th	0.98	0.16	0.19	0.08	0.09	0.02	0.45	0.45	1.95
La	1.79	2.25	1.05	1.93	2.40	1.56	1.56	5.40	20.8
Ce	3.70	2.84	5.84	5.69	6.06	3.35	8.8	9.78	47.5
Sm					0.57	0.26	1.47	1.91	5.41
Eu	0.47	0.50	0.76	0.50	0.59	0.25	1.10	1.00	2.20
Tb	0.20	0.22	0.57	0.45	0.10	0.07	0.44	0.54	0.98
Yb	0.74	0.67	2.60	2.95	0.49	0.15	1.60	2.01	4.20
Lu	0.11	0.10	0.32	0.33	0.11	0.02	0.30	0.36	0.68

*from Mathewson, in progress

contact metamorphic effects of any of the several granitic plutons in the area. 4) Hydrothermal alteration associated with the volcanogenic exhalitive sulfide deposits in the Pecos greenstone belt. and 5) Regional metamorphism. Alteration in the Cow Creek rocks is evidenced by minerals such as sericite and chlorite which are present in most rocks. Several authors, Burwash and Krupicka, (1969), Hart, (1969), Hart et.al., (1974), Condie, Viljoen and Kable, (1977), and Smith, (1968), have discussed major and minor element mobilization during seafloor alteration and metamorphism. They have concluded that metamorphic alteration during low grade metamorphism effects both the LIL elements as well as the alkalis but does not appreciably affect the bulk chemistry in the rest of the rock. Halmyrolisis tends to enrich potassium and oxidize iron to Fe2O3, but the effect on the other major elements appears to be small. Sodium and potassium have been enriched in several of the Cow Creek samples which were collected near the contact with the tonalite-trondhjemite unit. This enrichment is attributed to metasomatism and is restricted to the immediate vicinity of the contacts with the mafic and ultramafic rocks. These samples are easily distinguished from unaltered samples when plotted on a Na2O+K2O vs SiO2 diagram such as Figure 38. In all of the other chemical variation diagrams used in this section the Cow Creek rocks consistently plot in relatively tight groups, therefore it

is believed by the author that major element alteration has been minimal in the Cow Creek area. This is also supported by the normative mineralogy as presented in Table 3.

Ultramafic Rocks and Amphibolites

Table 4 contains chemical analyses from mafic and ultramafic rocks from Archean, Proterozoic and Phanerozoic terranes throughout the world. Table 4a contains analyses from similar rocks from within the Pecos greenstone belt. These analyses are presented to give readers a quick reference to similar rocks which will aid in following discussions.

In Figure 24, a plot of weight percent TiO2 vs. MgO, from Naldrett and Cabri (1976), the dashed outlined area represents the komatiitic field as defined by samples from the Barberton region of South Africa, the Yilgarn and Pilbra blocks in Australia and Munro Township in Ontario, Canada. Samples which plot within or near the field outlined are generally considered to be komatiitic. It is important to notice that both Area 1 and Area 2 Cow Creek ultramafic rocks meet this criteria. There is, however, a distinct separation on the diagram between the rocks of Area 1 and those of Area 2. In addition the amphibolites of Area 2 contain more than twice the amount of TiO2 as the amphibolites of Area 1.

Figure 25 is a plot of weight percent Al2O3 vs. FeO/FeO+MgO also from Naldrett and Cabri (1976). Samples which plot above the line are defined as komatiitic if they also meet the criteria of the TiO2 vs. MgO plot in Figure 24. It is again interesting to note the distinct separation

Figure 24

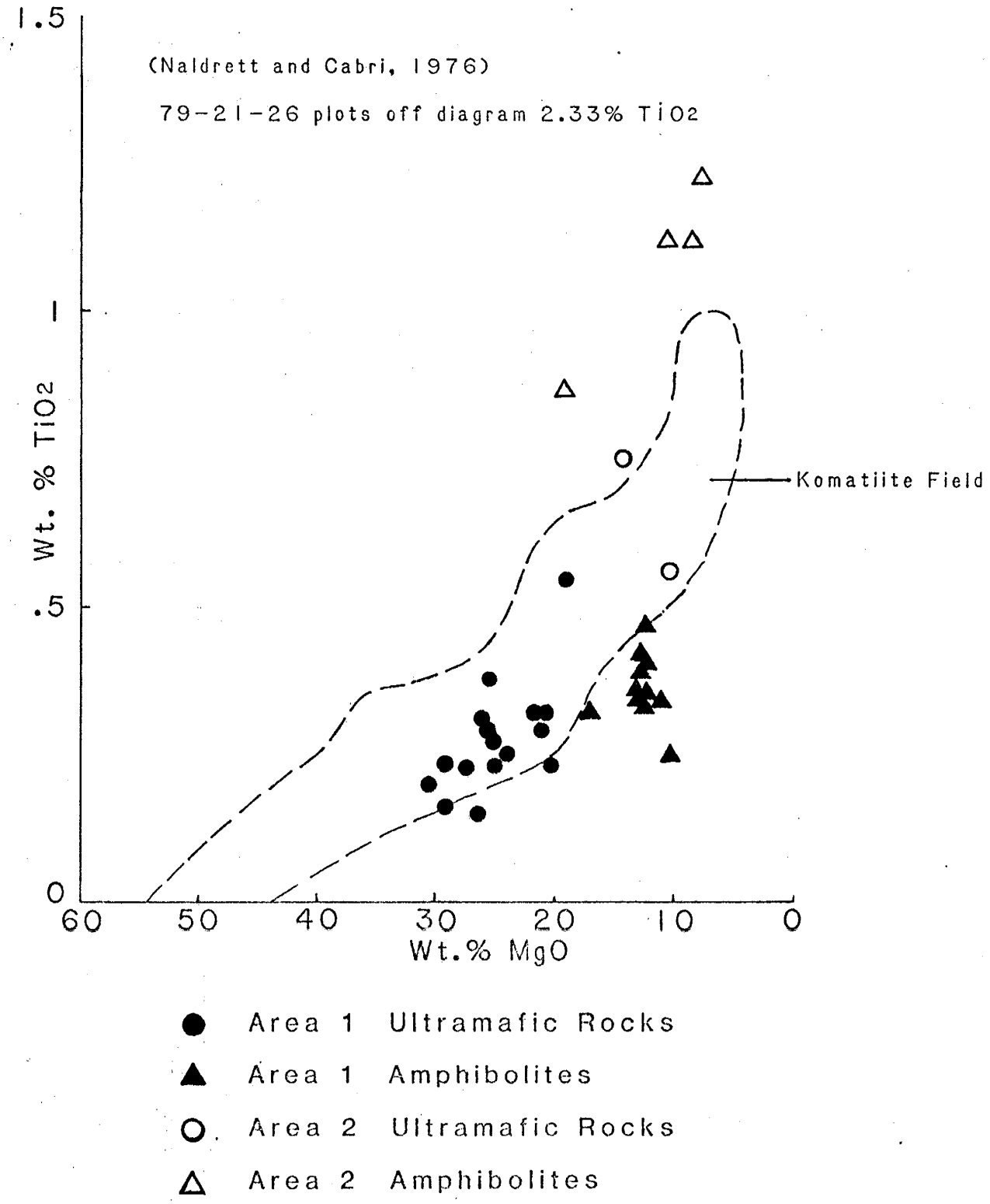
1.5
(Naldrett and Cabri, 1976)
79-21-26 plots off diagram 2.33% TiO2
1
.5
0
Wt. % TiO2
Komatiite Field
60
50
40
30
20
10
0
Wt.% MgO
Area 1 Ultramafic Rocks
Area 1 Amphibolites
Area 2 Ultramafic Rocks
Area 2 Amphibolites

Figure 25
(Naldrett and Cabri, 1976)

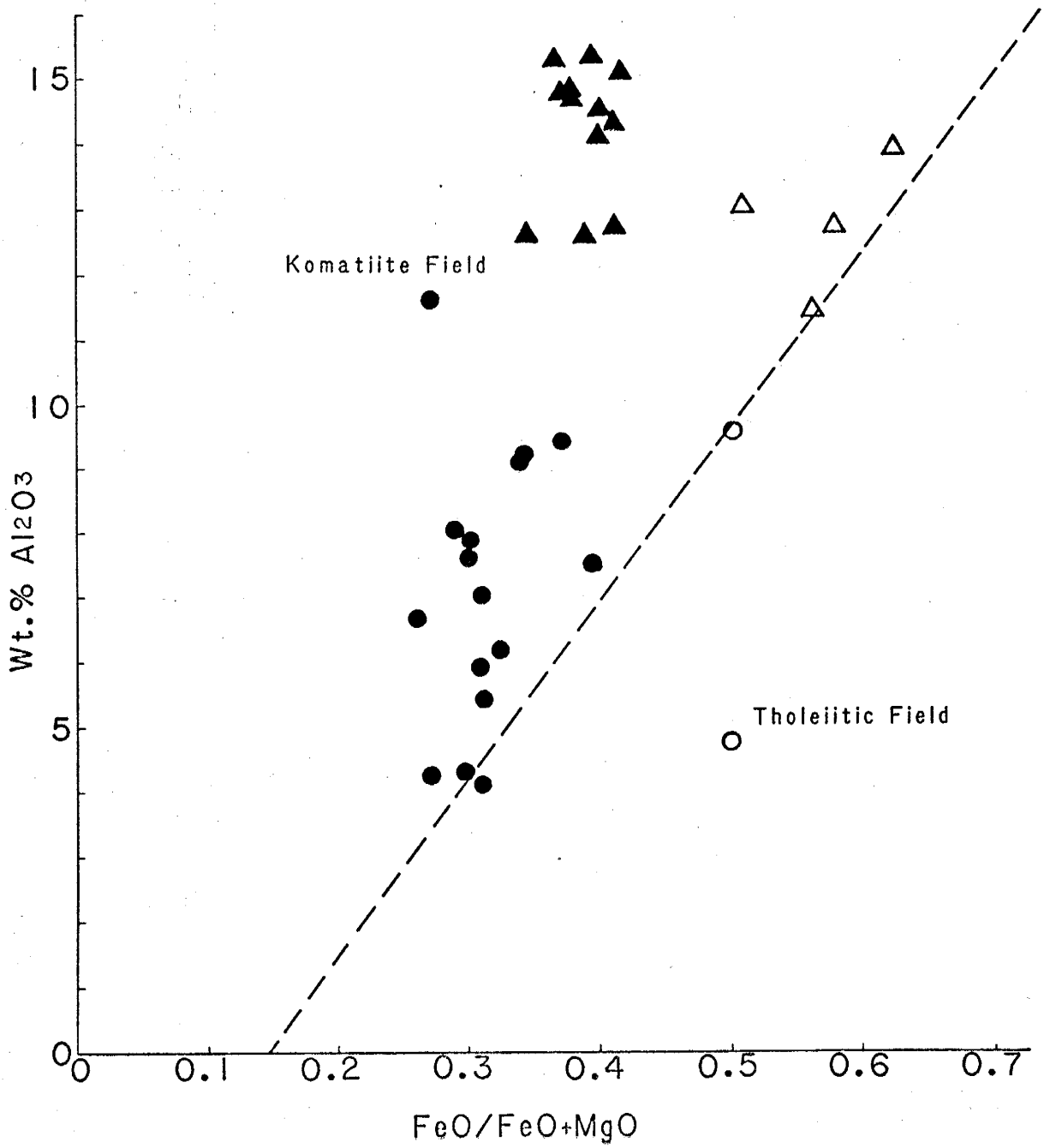

● Area 1 Ultramafic Rocks

▲ Area 1 Amphibolites

○ Area 2 Ultramafic Rocks

△ Area 2 Amphibolites

of the samples in Area 1 from those of Area 2. Also notice that one Area 2 ultramafic sample does not fit this criteria.

Figure 26 is a Jensen(1976) cation plot. As with the plots discussed previously, the ultramafic rocks of Cow Creek clearly plot within the ultramafic and basaltic komatiitic fields. This plot has its advantages over the standard AFM diagram (Figure 37) which may show a tholeiitic trend to the Cow Creek rocks but lacks the ability to distinguish between different volcanic trends other than tholeiitic and calcalkaline.

On the Jensen plot the Cow Creek Area 1 amphibolites overlap the basaltic komatiite field and the high magnesium tholeiite field. The chemical gap between the two field areas is again evident and appears to be real. Also notice that one of the ultramafics from Area 2 plots away from the other Area 2 rocks. Selected amphibolite analyses from the Pecos greenstone belt to the west of Cow Creek (Robertson, J.M., in progress) are plotted on this diagram for comparison between the Cow Creek rocks and the rest of the greenstone belt.

Viljoen and Viljoen (1969a) used CaO/Al2O3 ratios to distinguish between various types of ultramafic rocks in South Africa. Komatiites according to their definition possess CaO/Al2O3 ratios greater than 1.0. Since a CaO/Al2O3 ratio of greater than 1.0 would exclude some of their original samples and would exclude many other rocks

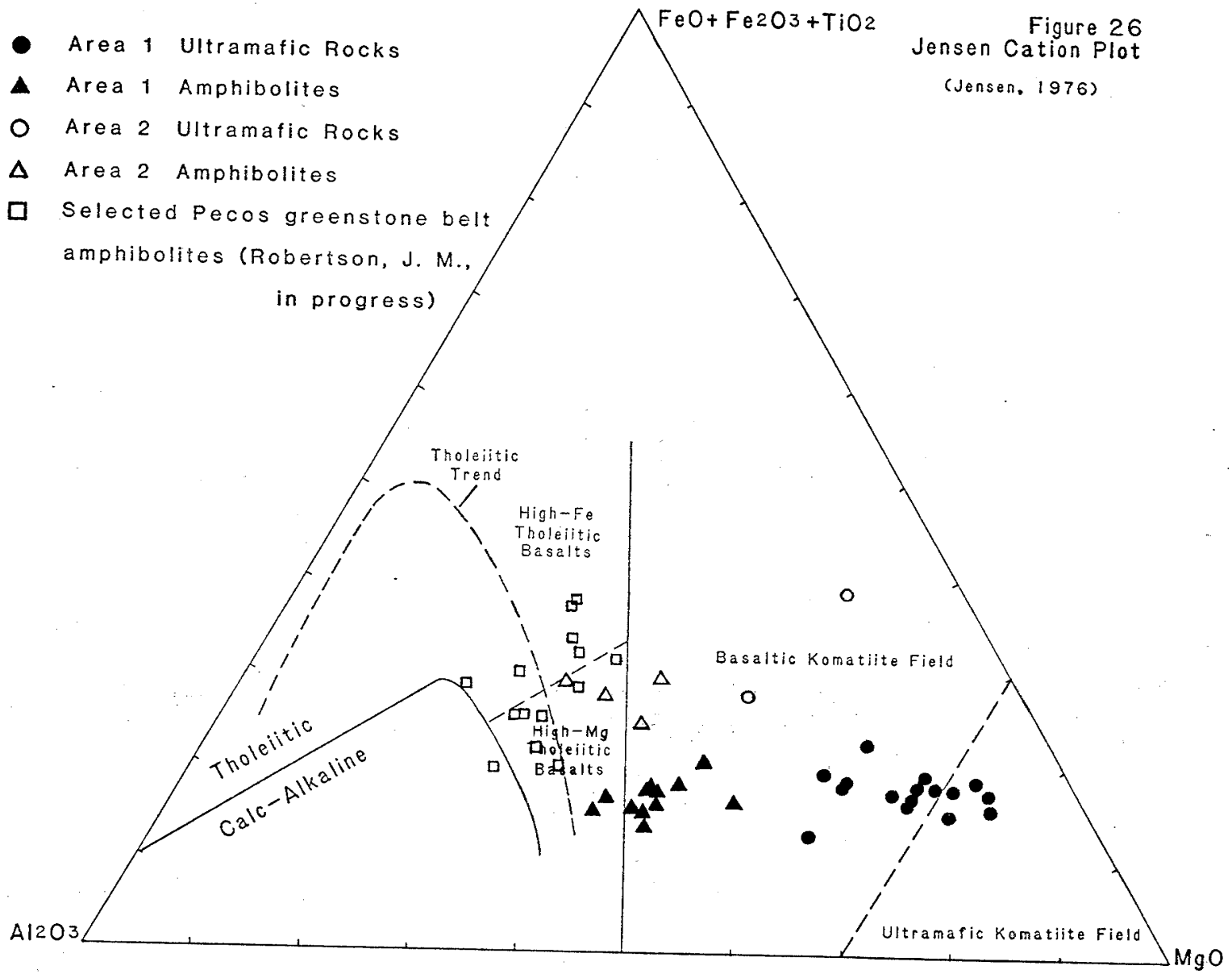

Figure 26
Jensen Cation Plot
(Jensen, 1976)

worldwide with other grossly similar chemical and physical characteristics, Nisbet et. al. (1977) and Arndt et. al. (1977) have amended the ratio to be greated than 0.8. Figure 27 is a plot of CaO vs. Al2O3 after the Viljoens (1969a), and includes a 0.8 line after Nisbet et. al. Almost all Cow Creek ultramafic rocks plot well above the 0.8 line. Several of the Cow Creek ultramafic rocks however do not have CaO/Al2O3 ratios of greater than 0.8. One of two possibilities may account for this: Clinopyroxene accumulation or lack of accumulation in the magma at the source, or Ca addition or Al removal during metamorphism. Neither possibility can be supported nor discounted at this point.

The Viljoens (1969a) also used a ternary plot of MgO,CaO,Al2O3 to distinguish between various types of meta-tholeiites, ultramafic komatiites, peridotitic komatiites, peridotites and picrites. Figure 28 has the various fields which they describe as well as a slightly modified komatiite-tholeiite trend after Condie (1980, in press). Nearly all Area 1 and Area 2 ultramafic and mafic rocks fall within the komatiite-tholeiite trend. It is also interesting to notice that all amphibolite samples plot within or near the tholeiitic end of the diagram as described by Condie or near the meta-tholeiite field described by the Viljoens.

Figure 27
(Viljoen and Viljoen, 1969a)
(modified by Arth et.al., 1977)
BK – Basaltic Komatiite

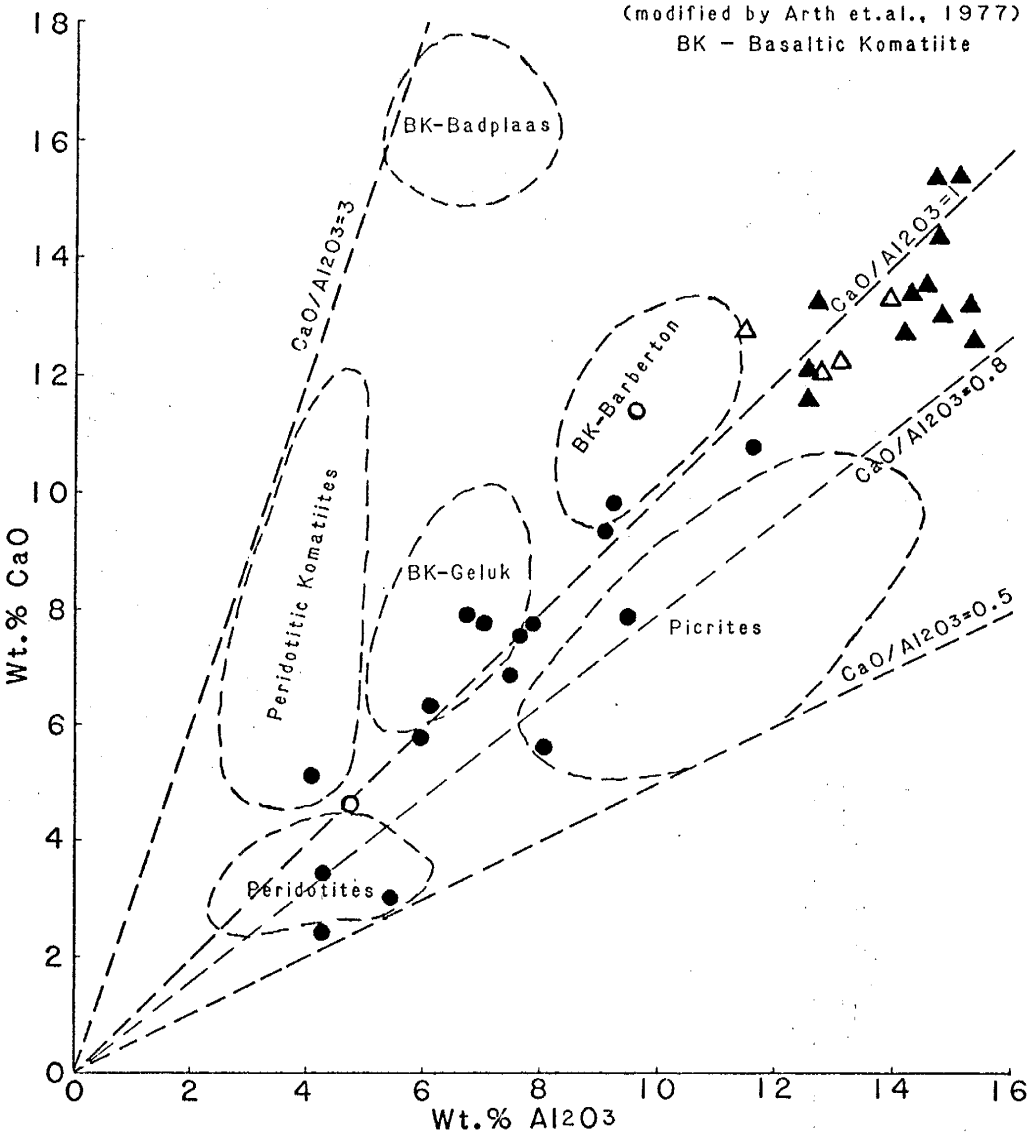

● Area 1 Ultramafic Rocks
▲ Area 1 Amphibolites
○ Area 2 Ultramafic Rocks
△ Area 2 Amphibolites

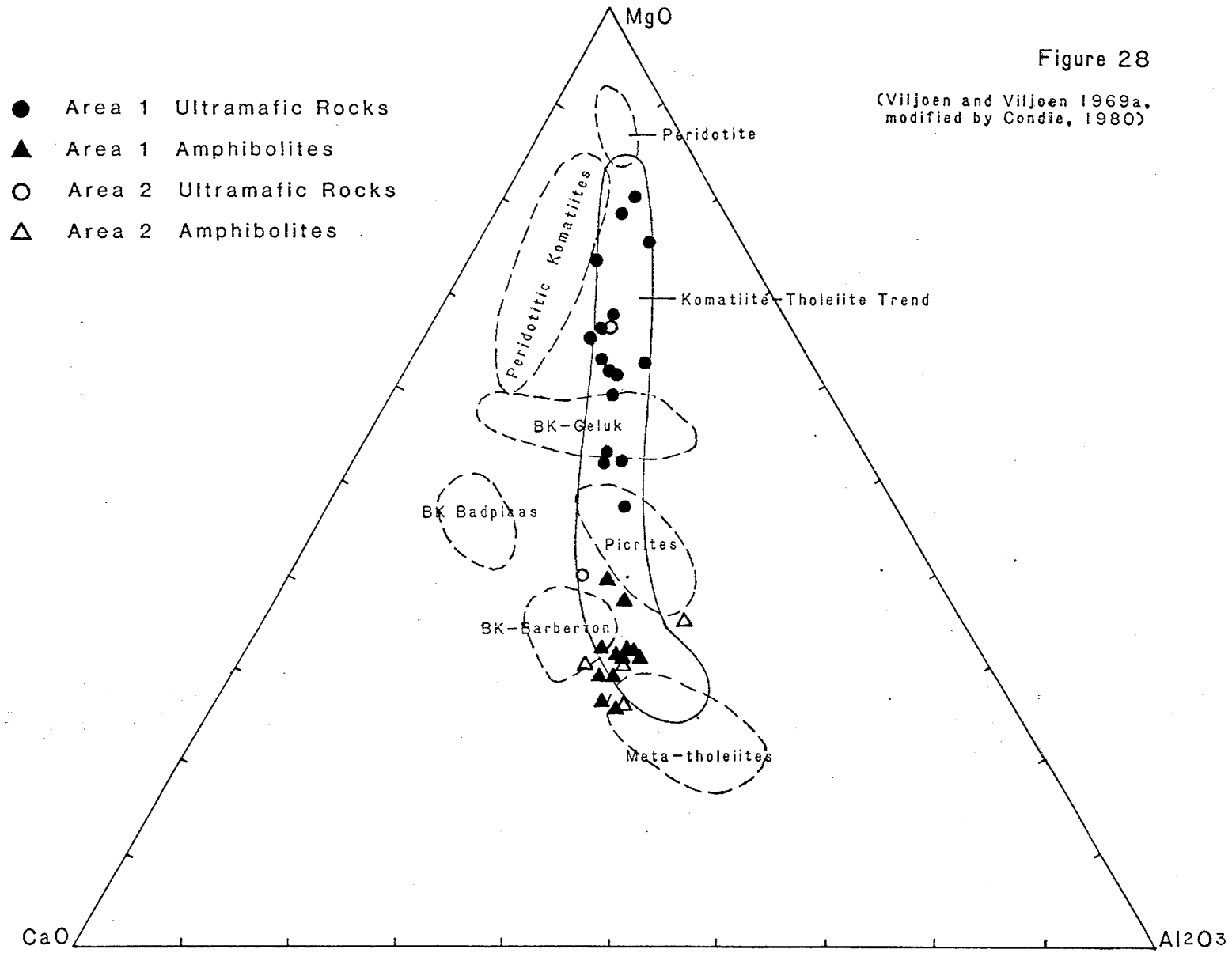

Figure 28

(Viljoen and Viljoen 1969a, modified by Condie, 1980)

The Viljoens (1969a) diagram of MgO vs. FeO (Figure 29) also distinguishes the komatiite trend. None of the Cow Creek samples plot near the Peridotite field however they do fall within or near the komatiite trend. One ultramafic sample from Area 2 however, does not follow this.

Muir (1979) used a series of trace and major element chemical variation diagrams to distinguish between intrusive and extrusive ultramafic rocks. His extrusive ultramafic rocks consisted of peridotitic komatiites from South Africa, Australia and Canada. Intrusive rocks include dunites and lherzolites. All types and degrees of alteration were considered. After considering both chemical and physical characteristics of all types of ultramafic rocks, Muir established what he considered to be intrusive (I) and extrusive (E) fields which are indicated on his diagrams (Figures 30-35). These fields are established with 92-96 percent accuracy. Almost all Cow Creek ultramafic rocks plot within the extrusive fields on all of Muir's diagrams.

Figures 36 and 36a are chondrite-normalized REE diagrams for ultramafic and mafic rocks of Cow Creek. Plotted along with the 4 analyses done by the author are two analyses of ultramafic rocks from Cow Creek, one Area 2 amphibolite, and two amphibolite analyses from the middle and southern part of the Pecos greenstone belt after Mathewson (in progress). Notice the overall flat patterns, and the slightly positive Eu anomaly in the ultramafic rocks. The positive Eu anomaly may or may not be real

Figure 29
(Viljoen and Viljoen, 1969a)

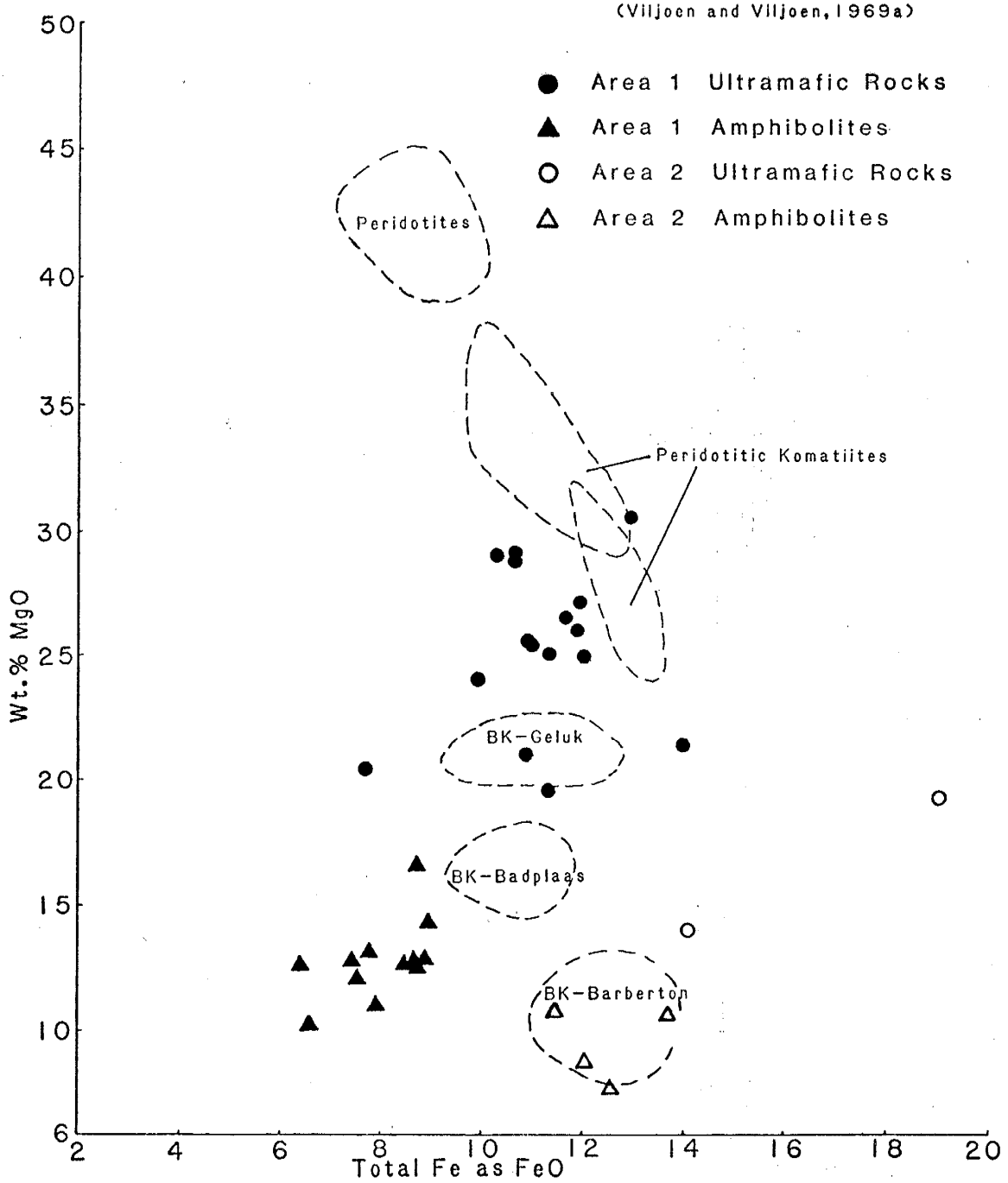

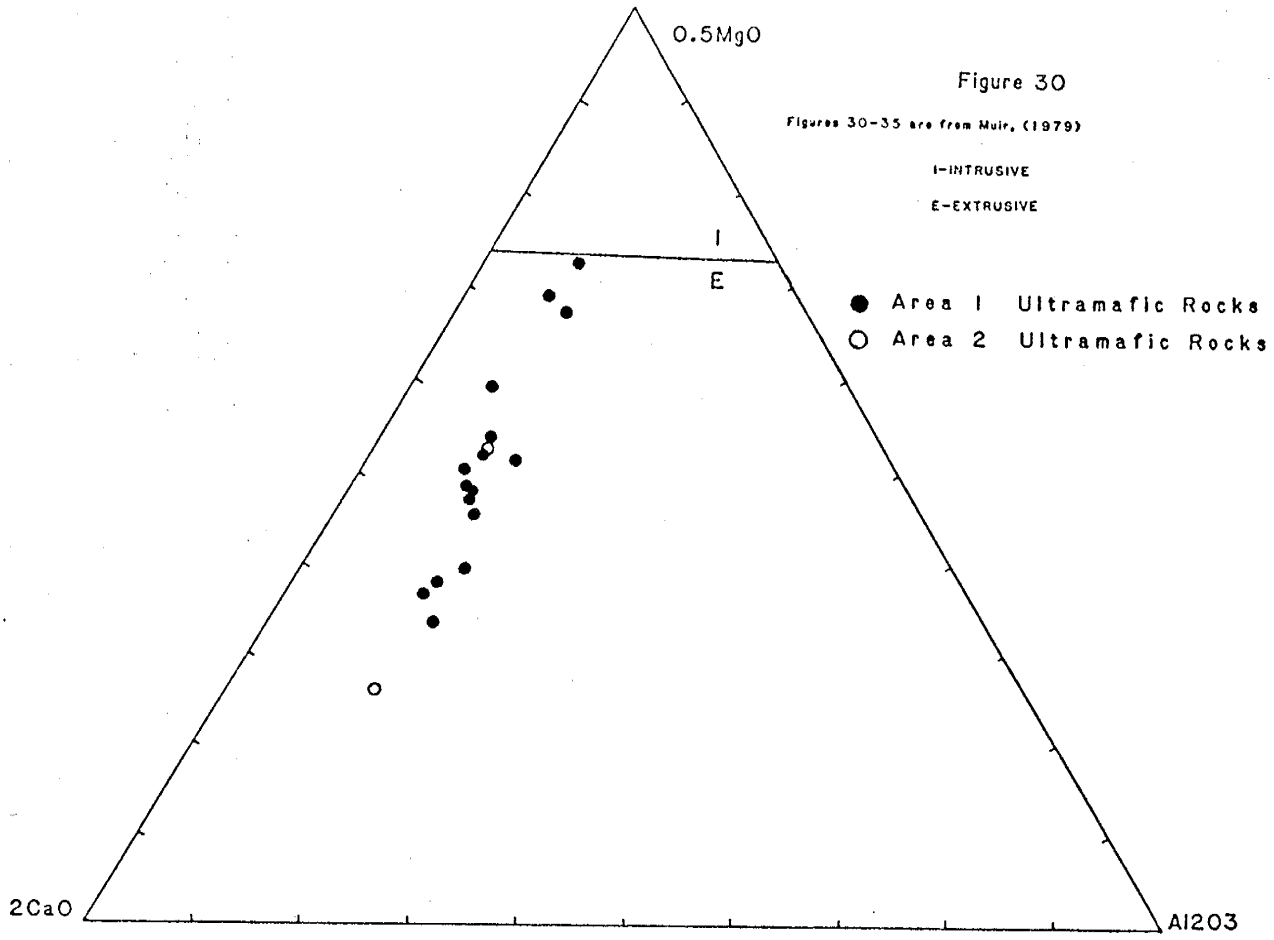

Figure 30

Figures 30-35 are from Muir, (1979)

I-INTRUSIVE

E-EXTRUSIVE

● Area 1 Ultramafic Rocks

○ Area 2 Ultramafic Rocks

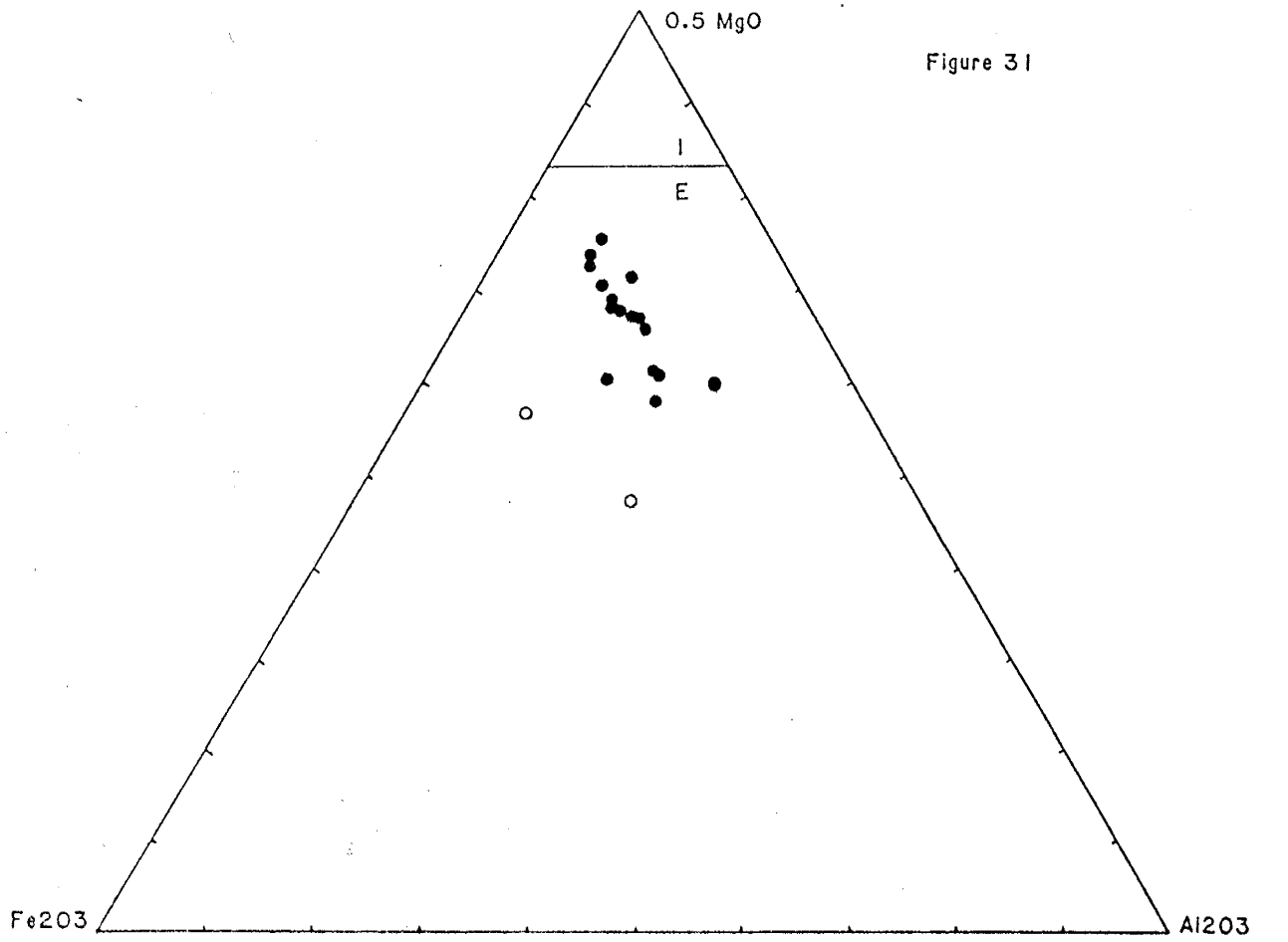

Figure 31

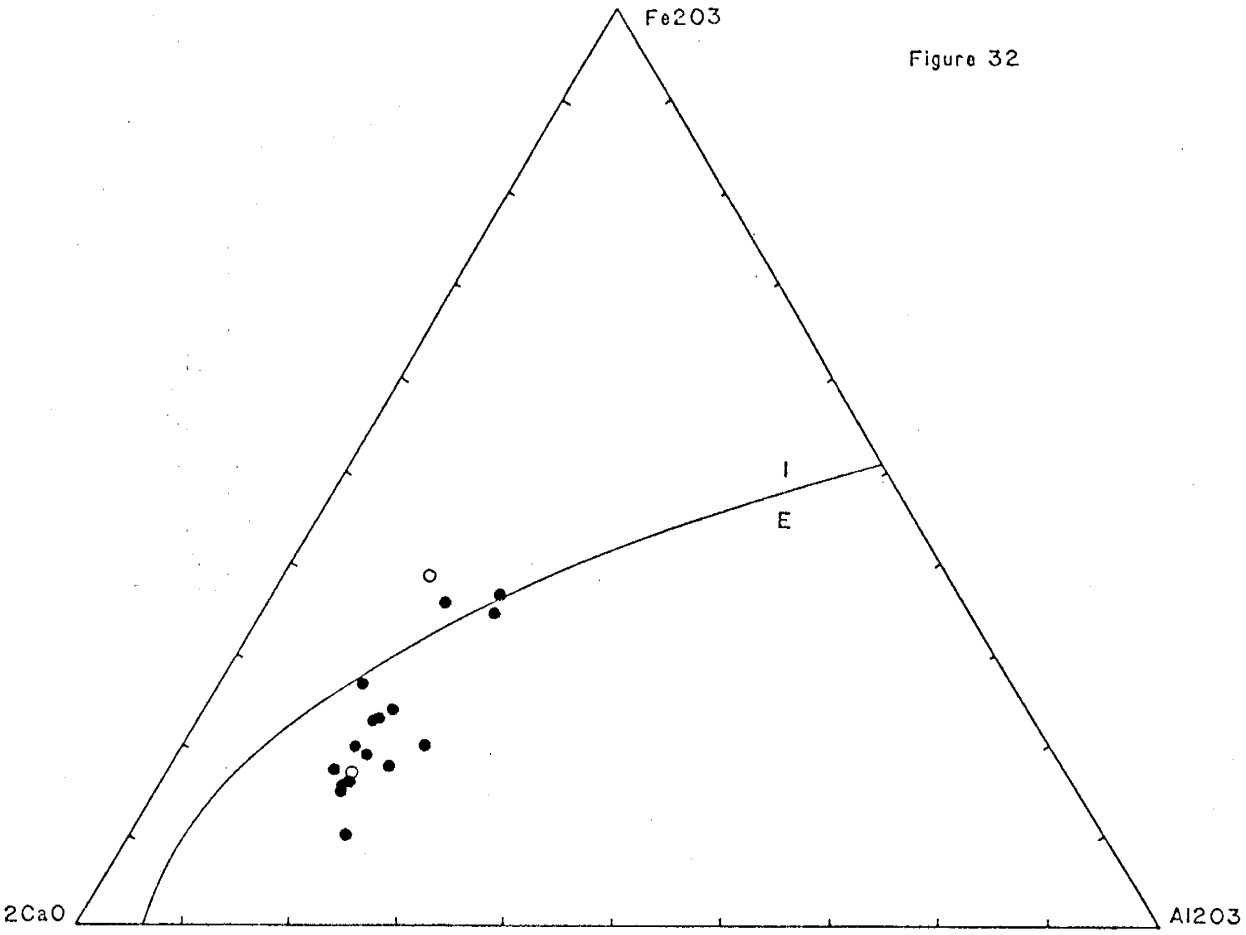

Figure 32

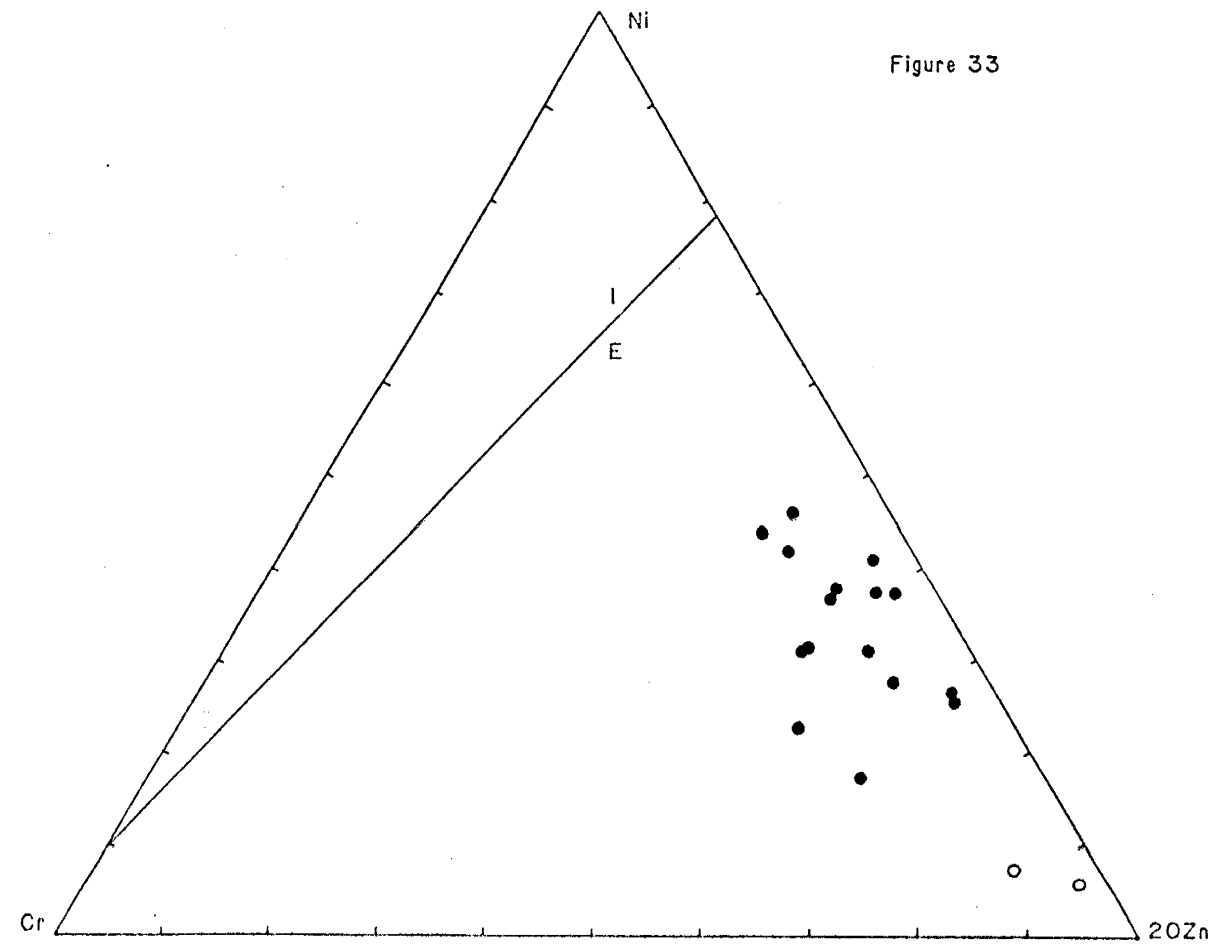

Figure 33

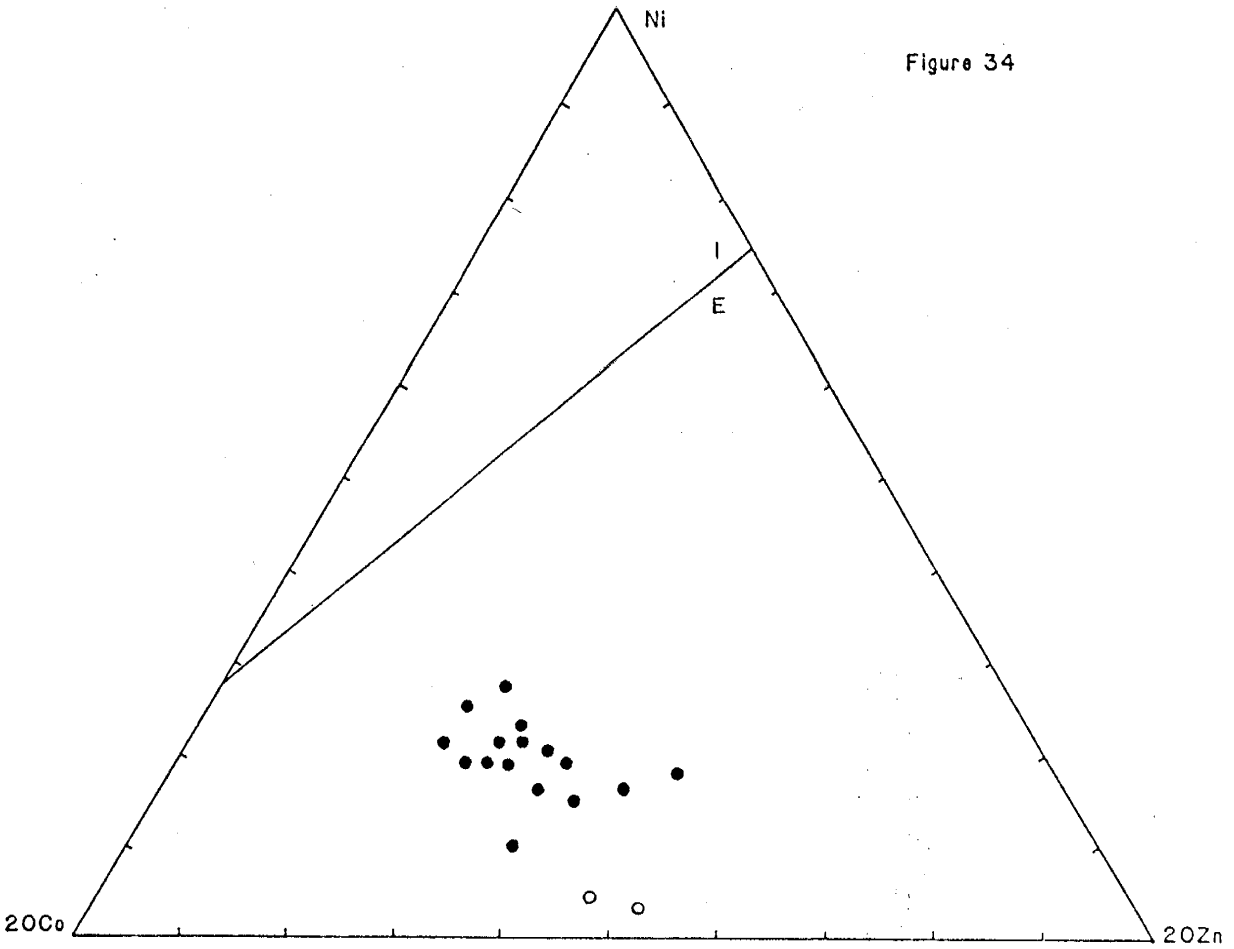

Figure 34

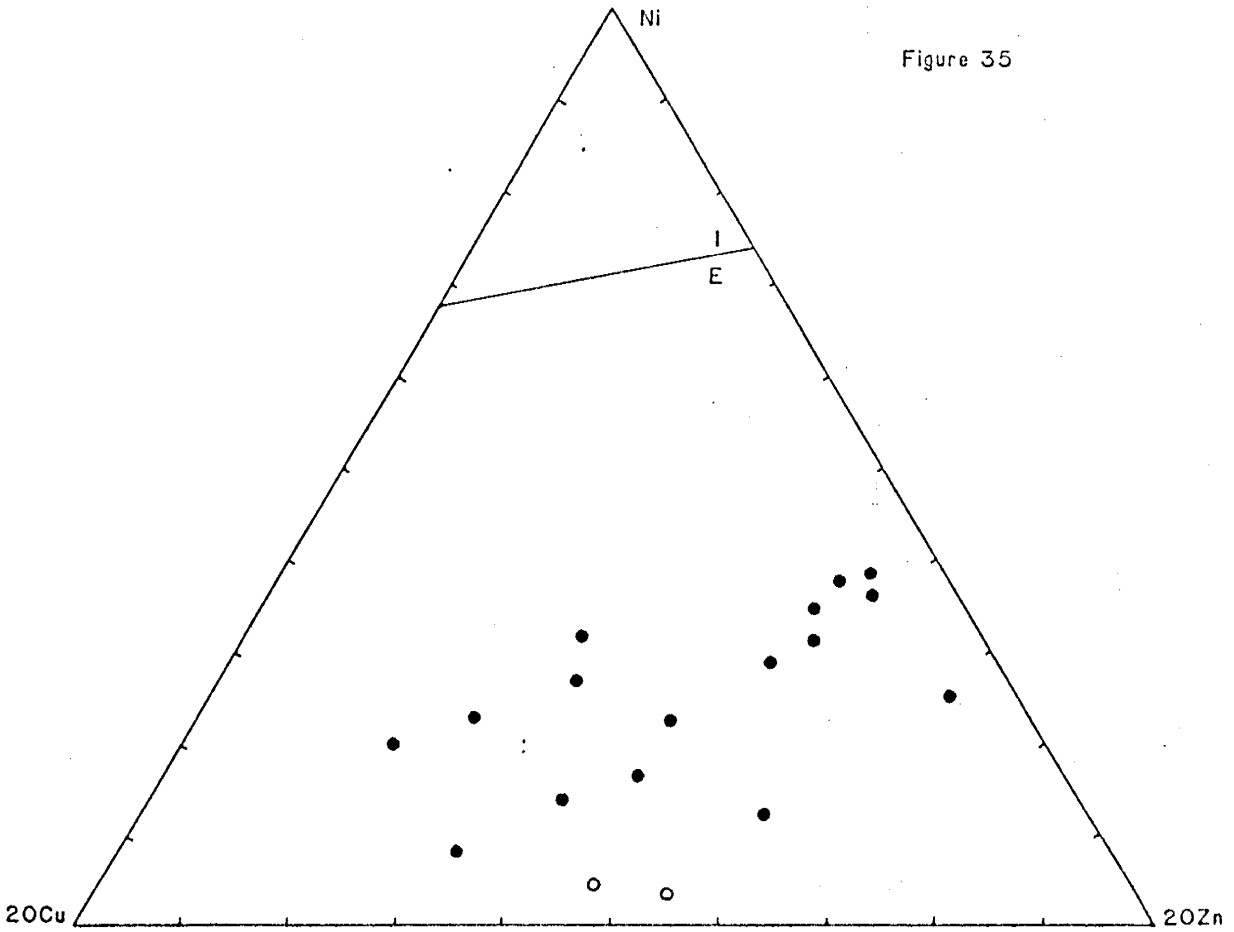

Figure 35

however, as REE analysis by neutron activation methods, below 10x are often suspect. In the amphibolite analyses there is also a slight depletion of light REE. Notice that the ultramafic rocks plot near or within the Komatiitic field as defined by Arth et.al. (1977).

Figure 37, from Irvine and Baragar (1971), is a standard AFM diagram used to distinguish between tholeiitic and calcalkaline volcanic rocks. Samples from the Pecos greenstone belt (after Robertson, J.M., in progress) are ploted along with the rocks from both Area 1 and Area 2. Almost all samples plot within the tholeiite field. Those few samples that do not plot within the tholeiite field appear to be enriched in the alkali elements as a result of close contact with a granitic body.

The Viljoens (1969a) also used a plot of Na2O+K2O vs. SiO2 to distinguish between the alkalic, tholeiitic and ultramafic rocks of South Africa. Figure 38 clearly shows that the Cow Creek amphibolites have tholeiitic affinities. The 3 samples that plot within the alkali field of Figure 39 are clearly enriched in sodium (Table 2).

Determination of tectonic setting of amphibolites has been attempted by Pearce et.al. (1977), using whole rock geochemistry (Figure 39). It is important to notice here that the amphibolites of Area 2 (triangles) plot within the oceanic island field while the amphibolites of Area 1 (circles) plot within the MORB field. The same samples from the Pecos greenstone belt (squares, used in figure 31) are

Ultramafics

Figure 36

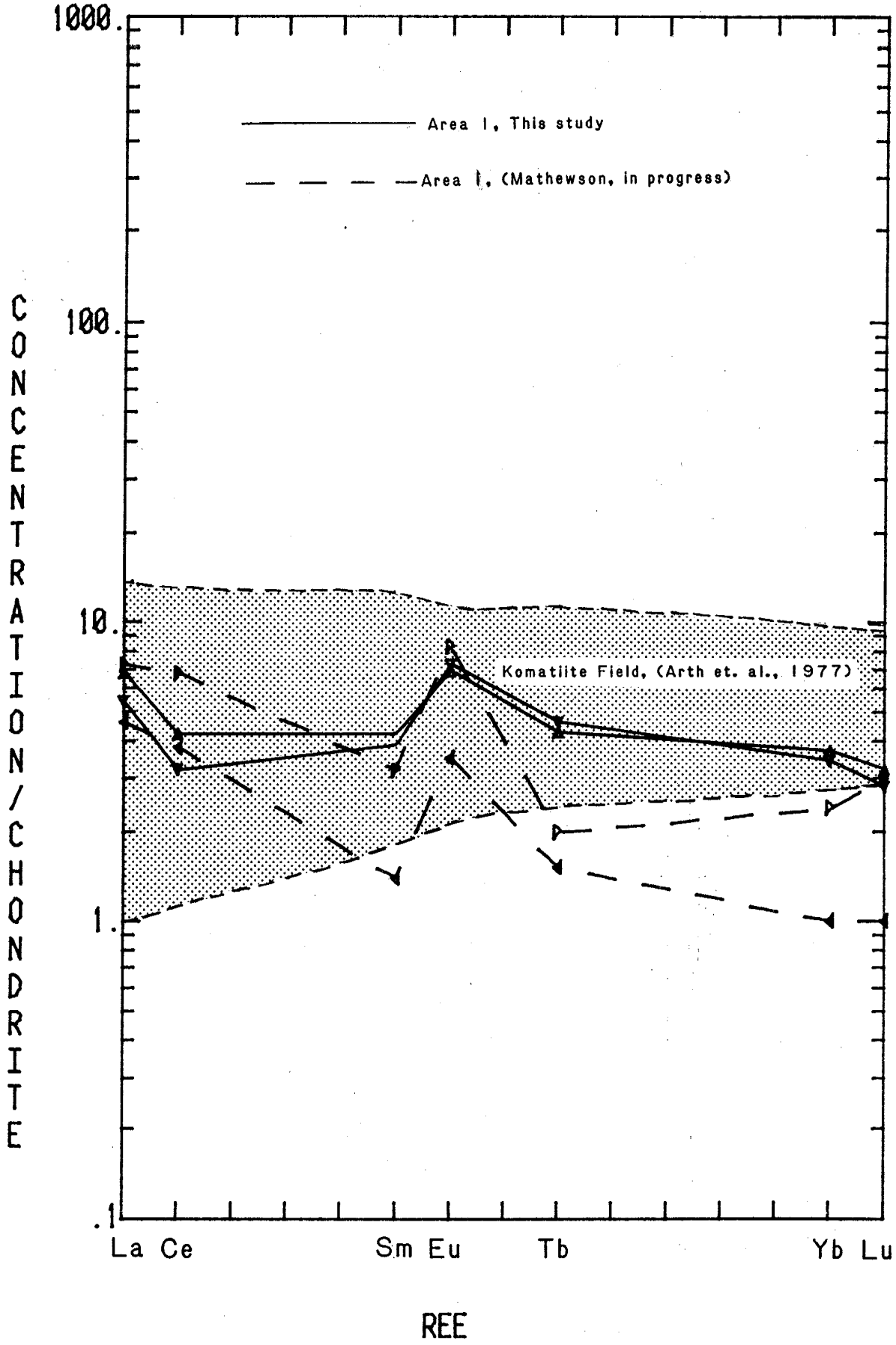

Amphibolites

Figure 36a

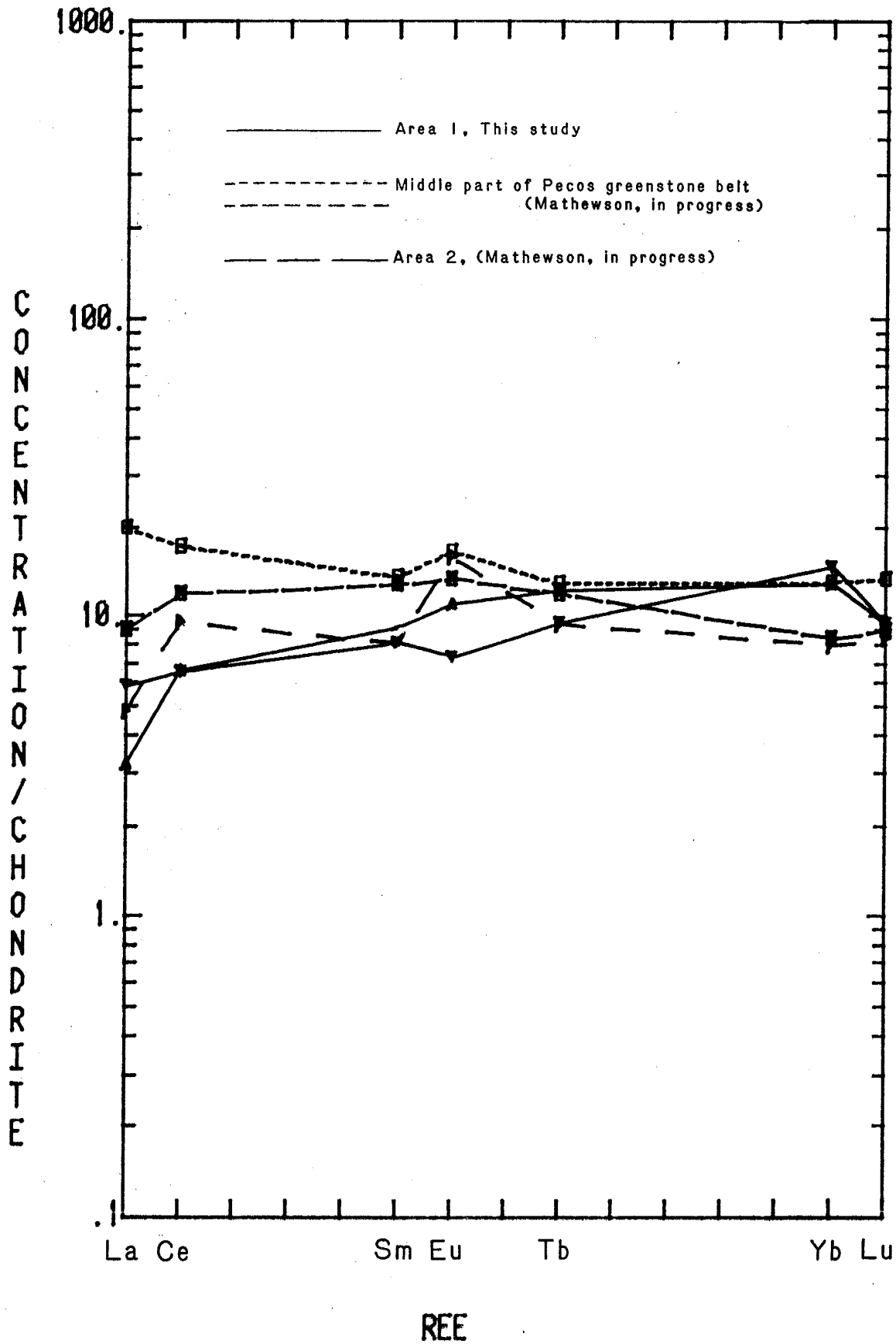

Figure 37

(Irvine and Barager, 1971)

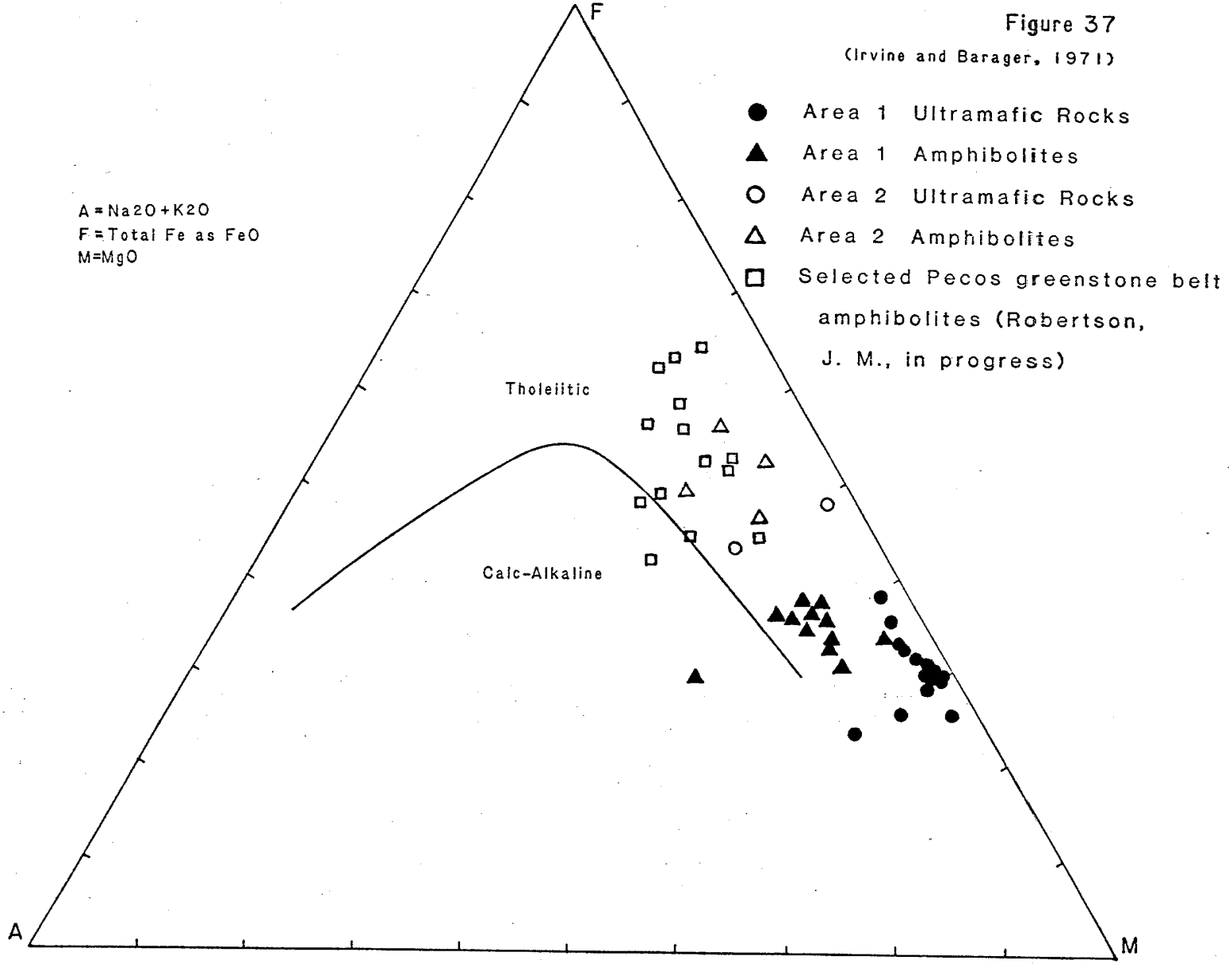

Figure 38

(Viljoen and Viljoen, 1969a)

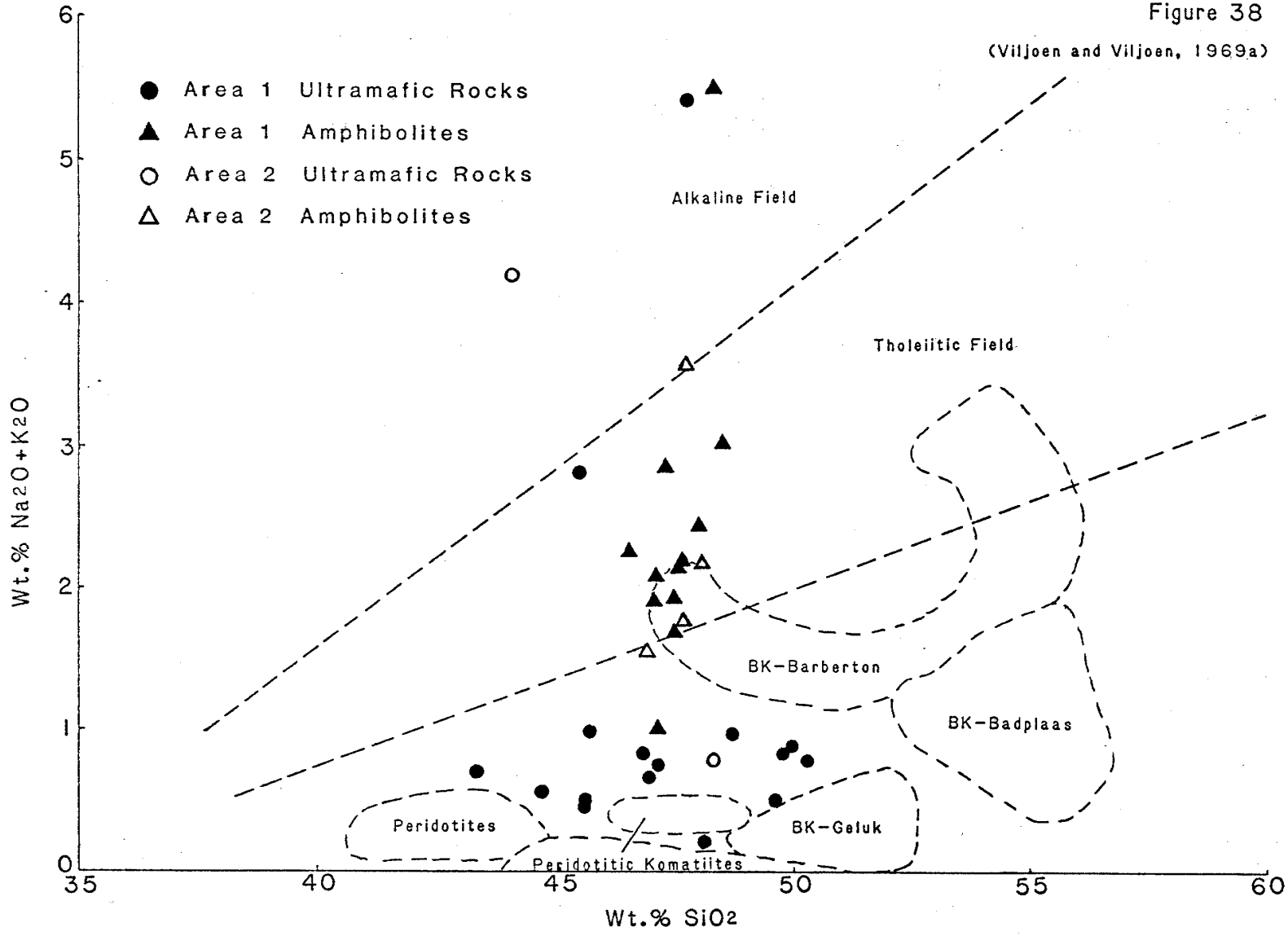

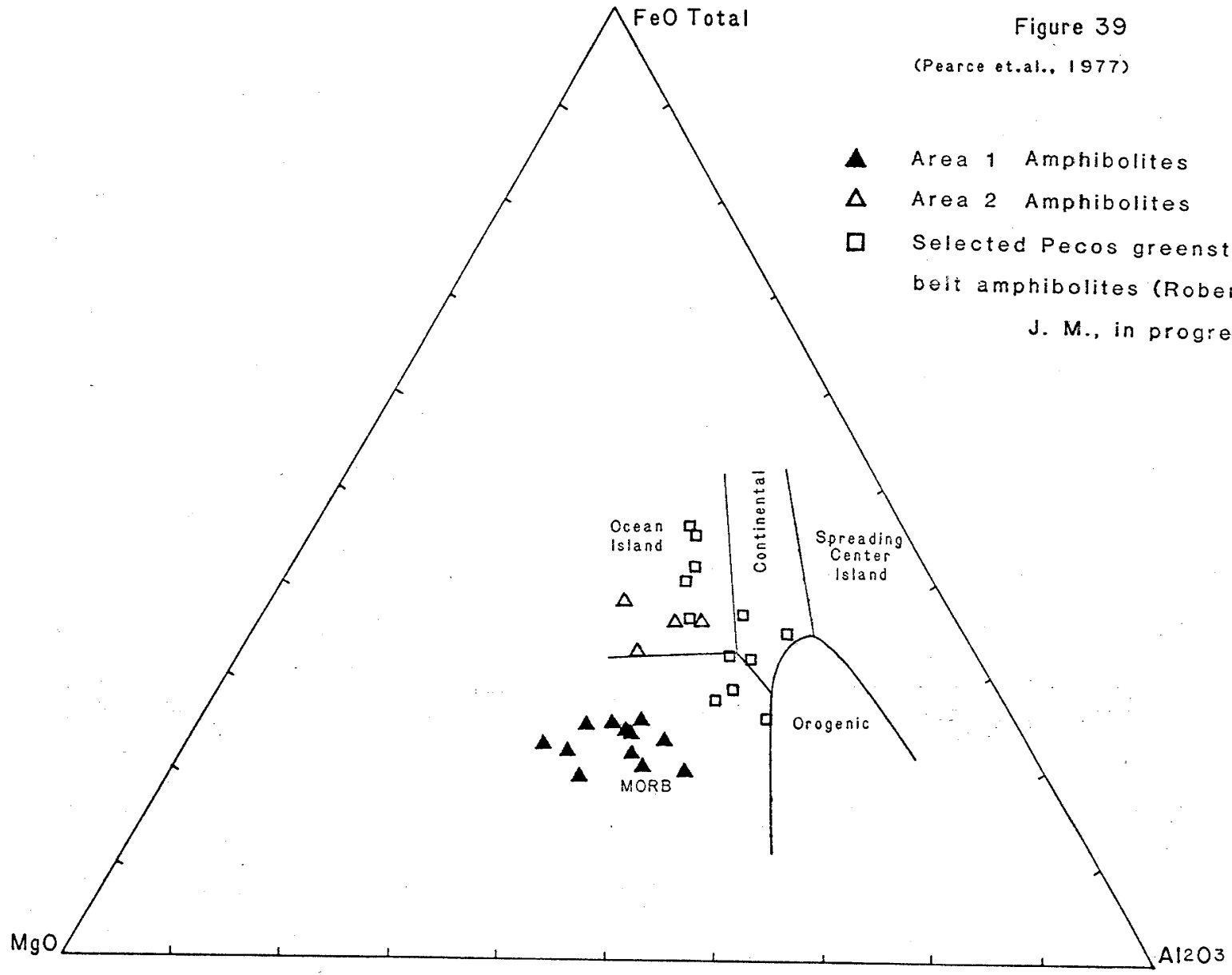

Figure 39

(Pearce et.al., 1977)

▲ Area 1 Amphibolites

△ Area 2 Amphibolites

□ Selected Pecos greenstone belt amphibolites (Robertson, J. M., in progress)

ploted with the Cow Creek rocks for comparison. It should be kept in mind that Pearce et.al. used data from Phanerozoic volcanics in constructing the diagram and caution should be used in fitting Precambrian data to it.

Granitic Rocks

Chemical analyses from the Pecos granite along Cow Creek (Mathewson, in progress), the Cow Creek tonalite-trondhjemite (Robertson, J.M., in progress) and the Embudo granite are all included. No interpretation was attempted as the emphasis of the thesis is confined to the mafic-ultramafic rocks.

METAMORPHISM

The Precambrian rocks of Cow Creek appear to have undergone at least one major period of regional dynamothermal metamorphism to the lower amphibolite facies which caused jointing and subsequent retrograde metamorphism to the greenschist facies. Because retrograde minerals are superimposed over the original metamorphic assemblages, identification of stable assemblages is difficult. Retrograde mineral reactions which have been identified include chloritization of biotite, chlorite and tremolite after hornblende and sericitization of feldspars.

Mafic Rocks

Mafic rocks of Cow Creek appear to have been regionally metamorphosed to amphibolites of the lower amphibolite facies. Amphibolite facies mineral assemblages which are observed include hornblende + oligoclase + epidote + quartz and hornblende + andesine + epidote + quartz. According to Miyashiro (1973): Since actinolite (tremolite) occurs in greenschist facies metabasites and coexists with hornblende in the transition zone to an epidote-amphibolite facies zone, the boundary between the greenschist and epidote-amphibolite facies lies at the temperature where the dominant calcic amphibole changes from actinolite (tremolite) to hornblende. This is at approximately 500

degrees C at 3 Kbar. Since hornblende and tremolite alternate as the dominant amphibole in the Cow Creek rocks, it is believed that at least this degree of metamorphism was reached. After metamorphism to the epidote-amphibolite facies, subsequent retrograde metamorphism produced the assemblage actinolite (tremolite) + chlorite + epidote + albite which is characteristic of greenschists, Miyashiro (1973). Actinolite may be absent and quartz may be present in certain rocks. Biotite may also be present in amounts up to 10 percent. Almandine garnet is present in one sample but does little except to establish a lower limit for temperature and pressure (500 degrees C at 0.5 Kbar, Miyashiro (1973)). Almandine garnet is thought to require reducing conditions for formation (Hsu, 1968, referenced in Miyashiro (1973), p. 260). If true it is not exactly understood what role this would play in the metamorphism of the Cow Creek rocks.

Plagioclase has compositions ranging from albite, An8, to andesine/labradorite, An50. Since mineral assemblages in the Cow Creek area are indicative of both greenschist and amphibolite facies, the high anorthite content of some rocks is not considered unusual. Condie and Budding (1979), have noticed the same high anorthite contact in Precambrian rocks in south and central New Mexico. They attribute it to incomplete recrystallization of mafic rocks formed at initially high temperatures, and subsequently metamorphosed to greenschist facies. Winkler (1976) and Miyashiro (1973)

both state that the anorthite content increases with metamorphic grade, although they also point out that this is not always true and other criteria must be used in conjunction with the anorthite content before an accurate determination of metamorphic grade can be made.

Because excess silica is a criteria for ploting on the ACF diagram, Miyashiro (1973), and because none of the Cow Creek ultramafic rocks exhibit free quartz, only amphibolites from the Cow Creek area have been plotted (Figure 40). The initial oxide compositions (Table 3) are corrected for accessory minerals (sphene, muscovite, sericite, biotite and magnetite) as outlined by Winkler (1976, p.37-40). The mafic rocks plot very near the anorthite-hornblende and the epidote-actinolite joins, indicating that assemblages of both amphibolite and greenschist facies could be expected. These predicted mineralogies agree very well with the observed mineralogies (APPENDIX C) seen in the Cow Creek rocks. Because the major rock types involved in metamorphism in Cow Creek (ultramafics and mafics) are easily altered, only a few primary textures have been preserved. Most have been obscured by the development of a pervasive foliation, and decussate texture. Some small scale folding is found.

Cataclasis, the final stage of dynamothermal metamorphism, is evident by bent twin lamellae in plagioclase and hornblende, strain fractures, mortar texture, exsolution of feldspars into perthite lamellae and minor sericitization of feldspars.

Figure 40

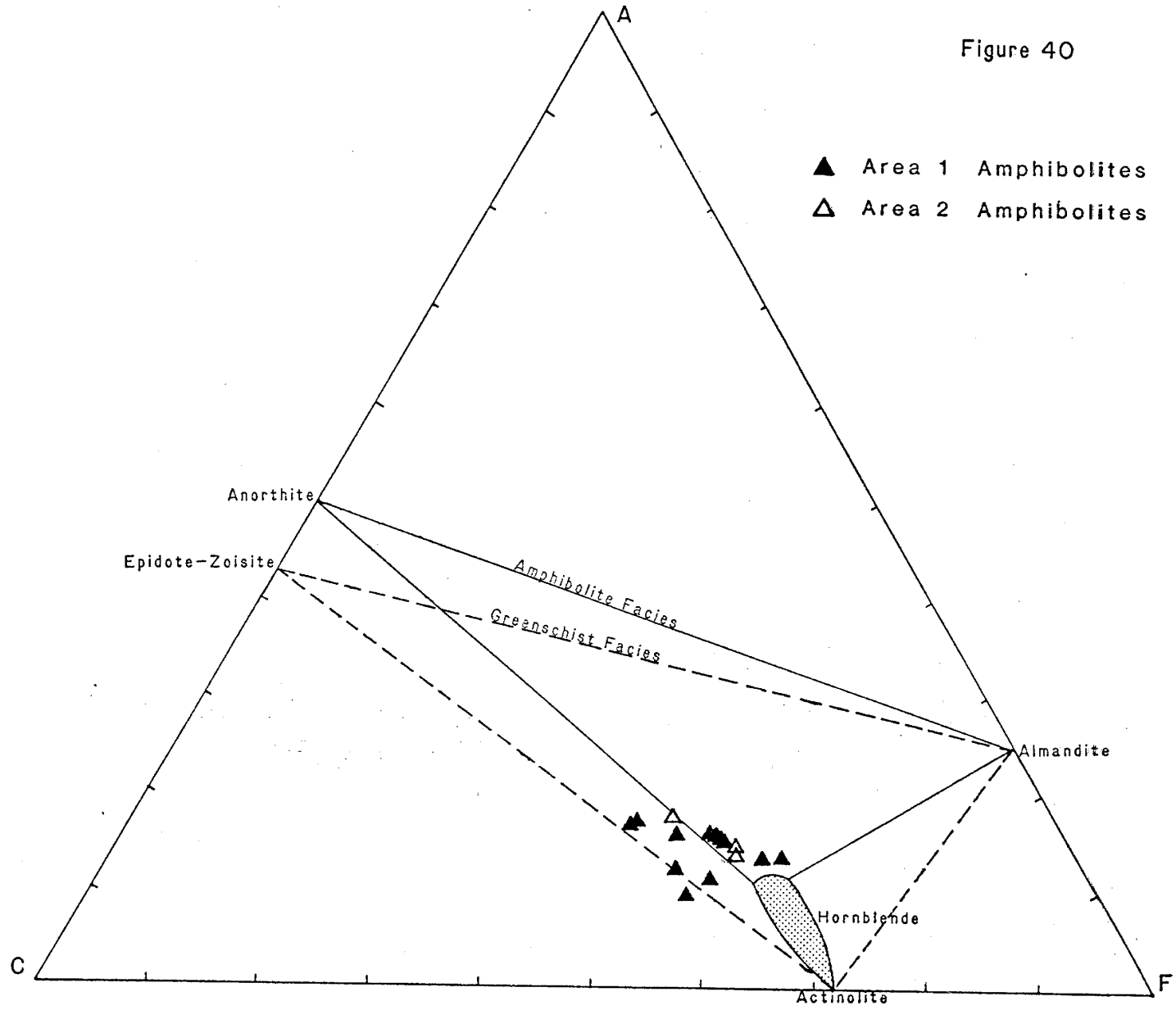
A
Area 1 Amphibolites
Area 2 Amphibolites
Anorthite
Epidote–Zoisite
Amphibolite Facies
Greenschist Facies
Almandite
Hornblende
C
F
Actinolite

Ultramafics Rocks

Metamorphism of ultramafic rocks requires the presence and access of H2O and/or CO2. H2O, commonly available from surface percolation and various mineralogical breakdowns, converts ultramafic rocks to serpentinites consisting of antigorite (variety of serpentine), talc, quartz, and magnetite, Winkler (1976). This reaction can take place within 100 meters of the surface as seen in the Belingwe greenstone belt, Rhodesia, Nisbet et.al., (1977). Because ultramafic rocks are so easily weathered, the above assemblage may be assumed to closely approximate the preburial lithologic assemblage of the Cow Creek ultramafic rocks.

To define the maximum metamorphic facies reached in Cow Creek by using ultramafic mineral assemblages is difficult. Certain minerals, nonetheless, can be easily eliminated from consideration as indicators of metamorphic grade. The presence of Al203 gives rise to high-Mg chlorite in metamorphosed ultramafic rocks, Winkler (1976). This high-Mg chlorite is stable into medium and even high grades of metamorphism where it often occurs with enstatite, forsterite and magnetite, Evans and Trommsdorff (1970). Antigorite which forms at essentially surficial conditions is also stable to high grades of metamorphism, Evans and Trommsdorff (1970). Diopside can form at temperatures

between 370 and 470 degrees C, at pressures between 0.2 and 5 Kb, and together with serpentine and in the absence of CO2 will persist to high temperatures in the presence of other minerals, Evans and Trommsdorff, (1970). Low CO2 activity in the Cow Creek ultramafics is indicated by the presence of serpentine and lack of magnesite, dolomite and quartz, Winkler (1976). Since high-Mg chlorite, antigorite and diopside (clinopyroxene) are stable in a wide variety of temperatures they are not used in the determination of the metamorphic facies. As temperature increases diopside undergoes the following reaction, Winkler (1976):

5 serpentine + 2 diopside = 1 tremolite + 6 forsterite + 9 H2O

This tremolite forming reaction requires the activity of H2O to have been high to initially form serpentine. High H2O activity is indicated in the Cow Creek rocks because mineral assemblages which fill fractures (tremolite and chlorite) are the same as those assemblages in the country rock, Evans and Trommsdorff (1970). The reaction to form tremolite and forsterite first occurs at amphibolite facies temperatures and pressures, Evans and Trommsdorff (1970). If the assumption is made that tremolite and forsterite were stabilized together at a temperature of 500-600 degrees C, then altered by retrograde reactions the current mineral assemblages in the Cow Creek rocks would be expected.

It must be pointed out that because determination of metamorphic grade in ultramafic rocks is difficult, the possibility exists that the 600 degree temperature was reached, exceeded or was not reached at all. The Mg-rich olivine, forsterite, could be present at a lower temperature in the rock if it was present as an original constituent. For normative mineralogy see Table 3. Alteration at slightly lower temperatures would also be expected to produce the same mineral assemblages as are now seen. Tremolite can be formed by alteration of clinopyroxene and forsterite as is some high-Mg chlorite according to the alteration sequence in Table 6.

In conclusion the ultramafic and mafic mineral assemblages probably indicate metamorphic grades of at least epidote-amphibolite facies, which have been retrograded to greenschist facies. The temperature range of 450 to 600 degrees C is indicated at pressures from 1 to 4 Kbar, Winkler (1976), Miyashiro (1973) for the epidote-amphibolite facies metamorphic event.

TABLE 6

Outline of Alteration Sequence
(Nisbet et al., 1977)

	→ Increasing alteration →					
Olivine	→	serpentine and magnetite, chlorite in less ultramafic komatiites	→	serpentine, magnetite tremolite, talc and/or chlorite	→	random aggregate of serpentine, tremolite, talc chlorite, magnetite
Clinopyroxene	→	clinopyroxene (except fine plumose sheaves replaced by tremolite)	→	tremolite and chlorite	→	random aggregate of serpentine, tremolite, talc chlorite, magnetite
Groundmass	→	Devitrified glass too fine grained to resolve optically Igneous textures visible	→	chlorite, tremolite, serpentine, talc and ore		random aggregate of serpentine, tremolite, talc chlorite, magnetite No igneous textures visible

STRUCTURE

The structure of both areas is fairly complex, reflecting remnant Precambrian foliations and small-scale folding associated with the regional dynamothermal metamorphism. At least one post-metamorphic felsic intrusive has caused migmatization and small scale folding along it's intrusive borders in Area 1. A pre-metamorphic felsic body is intruded into the rocks of Area 2 and now reflects the regional west to northwest foliation pattern.

Foliation

Foliations are best developed in medium-grained highly chloritized ultramafic units and some medium-grained amphibolites. Throughout both mapped areas foliations generally strike in a west-north-west to northwest direction and dip either steeply to the south or nearly vertically. Exceptions are seen. The cause of this foliation is believed to be a regional dynamothermal metamorphic event. A separate, second northeast foliation is seen in the mafic and ultramafic units of Area 1 within a few hundred feet of the tonalite-trondhjemite contact. This second foliation generally strikes approximately parallel to the intrusive contact and dips from 32 to 85 degrees away from it.

Intrusion of the tonalite-trondhjemite also created a prominent internal foliation. This foliation is parallel to subparallel to the intrusive contact and dips rather steeply beneath the mafic-ultramafic complex in most places (Plate 1). This internal foliation in the tonalite-trondhjemite is believed to reflect a primary flow structure developed within the unit during its molten stage. The foliated-granite also probably recieved it's foliation during this metamorphic event.

Joints

At least three sets of joints are recognized in the Cow Creek Area 1 rocks. One generally strikes northerly, one westerly and the third either northwesterly of north easterly. Dips vary from 30 degrees to vertical. Because outcrop in the area was limited to about 10 percent and because joints only appeared in a few outcrops information is limited. The joints may have been formed during the waning stages of the metamorphic event or could also have been formed by any other event up to Tertiary time.

Faults

No faults were found in Area 2 (Plate 2) so the following discussion relates only to Area 1. Faults are presented in their chronological order as interpreted by the author.

The oldest major fault to occur in the study area separates the tonalite-trondhjemite from the foliated-granite. This fault forms a brecciated zone approximately 30 meters wide composed of fragments of both rock types. Striations on shear planes striking parallel to the strike of the fault are seen throughout the zone and indicate vertical or near vertical movement. Much of the sheared rock exhibits cataclastic textures, although some undeformed rock fragments are found.

Possibly contemporaneously with the faulting of the foliated-granite a second parallel to sub-parallel fault formed. This second fault is now completely obscured by alluvium deposited by Cow Creek. Indirect evidence for this fault is in the form of shear planes along both sides of Cow Creek in the central part of the mapped area. These shear planes exhibit vertical striations which are totally serpentinized. Further circumstantial evidence is indicated by comparing the overall character of the rocks on the southeast side of the creek to that of the rocks on the northwest. The rocks on the southeast represent the best exposures of polygonal fractures, fine-grained margins,

pillow-like structures and cumulus textures. These features along with the thin alternating amphibolite/ultramafic/amphibolite character of the rocks, are in sharp contrast to the more massive character of the rocks on the northwest side of the creek.

The most prominent structural feature in the area is the Cow Creek fault and is located in the eastern part of the mapped area. This fault forms a brecciated zone up to 150 meters wide. It strikes almost due north-south and appears to dip vertically (Plate 1). The age relationships of this fault are difficult to determine although it crosscuts all Precambrian units in the mapped area. Mathewson (in progress) mapped the Cow Creek fault as connecting to another north-south fault that is exposed in Bear Creek to the north. He further mapped this fault as crosscutting Paleozoic strata. Between this "Bear Creek" fault and Cow Creek he infers that the Cow Creek fault also cuts Paleozoic rocks. No evidence to support or discount this interpretation was found during this study.

Minor faulting is present in the northwest part of the area along the northeast side of Rito Chaparito. These faults definitely cut the Paleozoic strata and appear vertical and down to the north. They may or may not be related to the Laramide Orogeny which formed the Sangre de Cristo Mountains.

Folding

Small scale folding (Figure 41), on a centimeter scale, is occasionally seen. Larger scale folding however, may be obscured by the extensive vegitative cover and lack of good outcrop or may be absent.

Figure 41. Small scale folding in ultramafic rock of Area 1.

DISCUSSION

Nature of the Ultramafic Rocks:

The identification of any rock type should be carefully based on both physical and chemical criteria. One must, however, be careful when working in metamorphic terranes. Because of the extensive recrystallization and amount of deformation that occurs, original textural features are often obscured or obliterated. In the rocks of Cow Creek this is the case, although some relict textural features remain. As stated previously it is not believed that any alteration has greatly affected the whole rock chemistry although some local sodium and potassium enrichment has occurred.

Ultramafic rocks of many types occur in a variety of tectonic settings, as presented in Table 1 and described by Naldrett and Cabri, (1976). Determination of tectonic setting requires a comprehensive look at the regional geologic picture. In New Mexico the regional geology seems to confine possible Precambrian tectonic settings to extensional types such as, 1) Paleo-rift, or 2) a paleo-back-arc basin - Island-arc assemblage, Condie (1980), Condie and Budding, (1979), Robertson, J.M., personal communication, Condie, personal communication). If either of the two postulated settings is correct, the Cow Creek ultramafic rocks formed in an active orogenic area, at least according to Naldrett and Cabri's, (1976) definitions.

The Cow Creek ultramafic rocks do not appear to be Alaskan type complexes because they lack concentric zoning and are not surrounded by an extensive gabbroic terrane (further discussion of Alaskan type bodies is given in Wyllie (1967). Alpine-type bodies can also be eliminated from consideration based on the following observations: a) Cow Creek rocks do not fit the chemical criteria for alpine type bodies as defined by Irvine and Findlay (1977). b) It is believed that alpine-type bodies are emplaced as solid mantle material and they often occur as breccias along thrust faults. The Cow Creek rocks do not exhibit any evidence of having ever been involved in thrusting and appear to have been emplaced as a silicate melt. c) Alpine-type bodies are characterized by podiform chromite deposits which are lacking in the Cow Creek rocks. and d) Mafic plutonic rocks associated with alpine-type bodies are Calc-alkaline (Thayer in Wyllie (1967)) and from Figures 26 and 37 it can be seen that the amphibolites of Cow Creek are clearly tholeiitic.

Ultramafic bodies emplaced in active orogenic areas, contemporaneous with eugeosynclinal volcanism as seen in Table 1 are divided into the tholeiitic suite and komatiitic suite. The tholeiitic suite is subdivided into the picritic subtype and anorthositic subtype. The latter can be eliminated simply based on the present mineralogy of the Cow Creek rocks. The Picritic subtype can also be eliminated

since the present mineralogy and normative mineralogy (Table 3) suggest that the Cow Creek rocks could have not contained enough olivine to have been picrites. Further differences are indicated chemically. The Cow Creek rocks consistently have less CaO, Al2O3 and TiO2 than do picritic rocks, some analyses are given in Wyllie (1967). If the Cow Creek rocks do not belong to the tholeiitic suite, they must be komatiitic.

Komatiites are defined by using both chemical and textural criteria. Chemical criteria have been well defined by various authors, Brooks and Hart (1974), Nisbet et. al. (1977), Viljoen and Viljoen (1969a), etc., and the criteria of Brooks and Hart as modified by Nisbet et. al. are used in this study. Komatiites are characterized by high MgO content (>9.0 percent), high CaO/Al2O3 ratios (>0.8, Nisbet et. al. (1977)), TiO2 and K2O <0.9 percent, SiO2 is less than 53 percent and Al2O3 is less than 10 percent. Arndt et. al. (1977) subdivide this classification on the basis of MgO. They identify peridotitic komatiites as having >20 percent MgO, pyroxenitic komatiites as having MgO between 12 and 20 percent, and basaltic komatiites as having MgO between 9 and 12 percent. Many authors, Viljoen and Viljoen (1969a), Naldrett and Cabri (1977), Jensen (1976), Condie (1980), Muir (1979) and others, have used chemical variation diagrams in successful and unsuccessful attempts to distinguish komatiites from other types of ultramafic rocks. Figures 24 to 39 have been presented elsewhere in this

thesis. It can be seen from these and an examination of Table 2 that the majority of the Cow Creek ultramafic rocks clearly meet all chemical criteria to be classified as either pyroxenitic or peridotitic komatiites.

Only one textural feature is used in defining komatiites. This texture reflects rapid crystal growth and is called "spinifex texture". The texture is formed when large lath-like olivine or clinopyroxene crystals are created by quenching or rapid cooling of the ultramafic liquid. Spinifex texture is well-documented by the Viljoens (1969a and 1969b) and Pyke et. al. (1973). This texture has not been positively identified in the Cow Creek rocks, although its presence is suggested in several places in both hand specimen and thin section. Figure 10 is a photo of a hand specimen and Figure 10a is a photomicrograph of radiating tremolite, probably after clinopyroxene. In Figures 42 and 42a Figure 10a is compared to amphibole spinifex (probably after clinopyroxene) from komatiitic rocks in the Archean Pilbra block of western Australia. Extensive recrystallization due to metamorphism and alteration in the Cow Creek rocks may account for the differences. Other textural features which are suggestive of komatiites but are not definitive include chilled-margins and pillow-structures. Cumulus textures have also been described from the lower parts of flows and in hypabyssal equivalents of komatiites in both the Munro Township and western Australia. Fine-grained margins suggestive of

Figure 42. (Figure 10a)

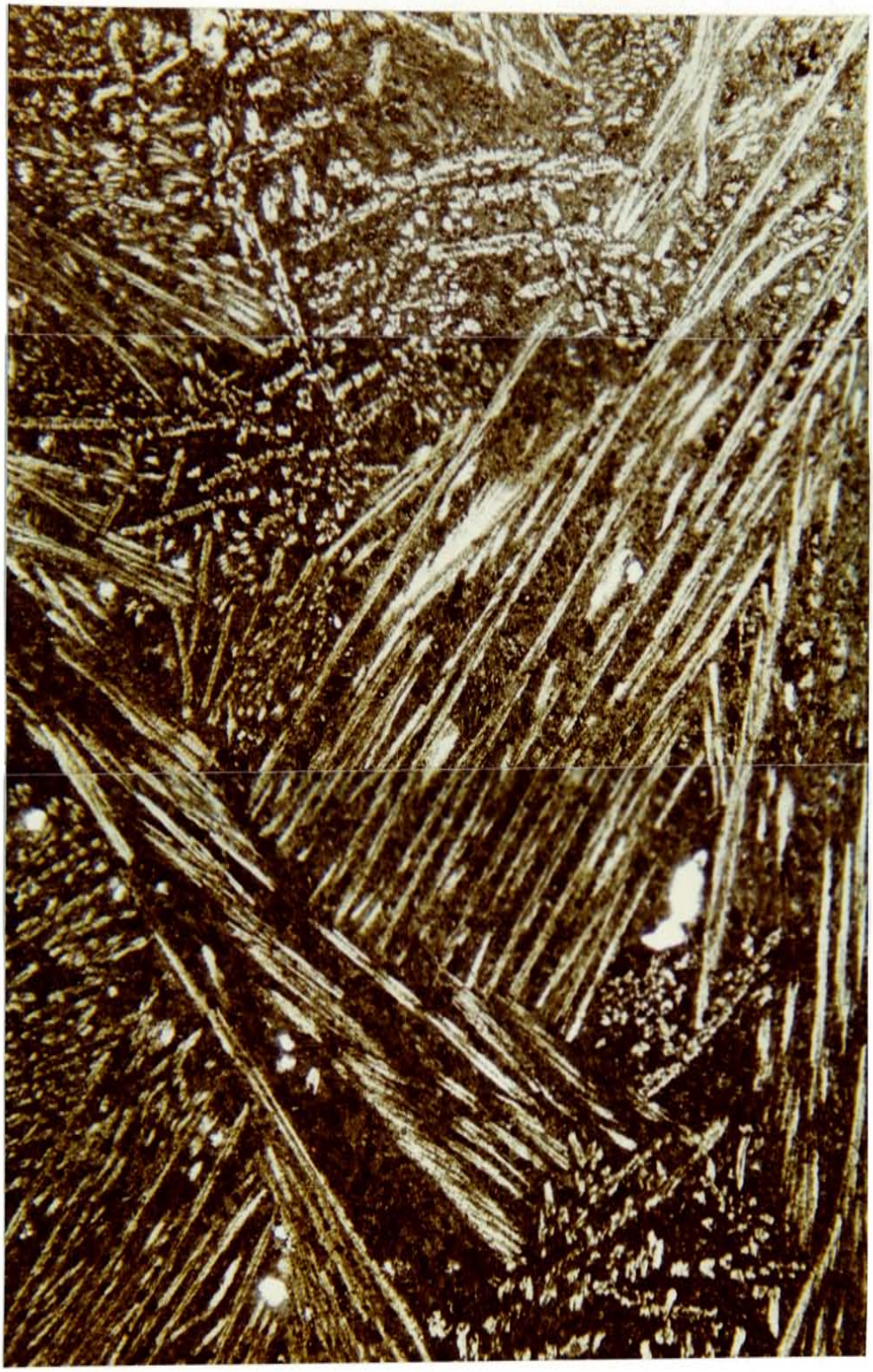

Figure 42a. Photomicrograph of amphibole spinifex, probably after clinopyroxene, from western Australia, 10x, plain light.

chilled-margins (Figure 8), cumulus textures (Figure 11) and pillow-like structures (Figures 6 and 7) have all been identified in the Cow Creek rocks. A 3 meter thick polyhedrally jointed flow-like ultramafic unit has been found in Cow Creek (Figure 43). This unit appears to closely resemble the majority of flows in the Munro township of Ontario, Canada, Figure 44, from Arndt et. al. (1977).

Cow Creek ultramafic rocks appear to exhibit many of the textural features (lacking only well documented spinifex texture) suggestive of komatiites.

Figure 43

Figure 44

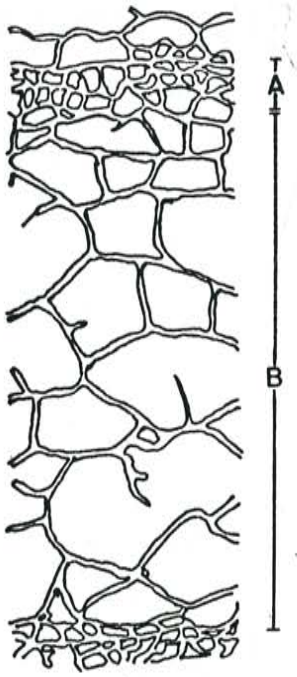

Figure 43. Polyhedral jointing in an ultramafic flow from Cow Creek, Area 1.

Figure 44. Type "C" flow from the Munro Township, Ontario, Canada. (from Arndt et. al., 1977)

A) Chilled flow top with fine polyhedral jointing.

B) Main part of flow, medium to fine peridotite with coarse polyhedral jointing.

Relationship of Ultramafic to Mafic Rocks:

The occurrence of ultramafic rocks and mafic rocks together in the basal sections of Archean greenstone belts has been well documented (Viljoen and Viljoen, 1969a; Arndt, Naldrett and Pyke, 1977; Bickle, Martin and Nisbet, 1975; Nesbitt and Sun, 1976; McCall, 1973; and others). This association often consists of high-Mg tholeiitic basalts interbedded with basaltic or peridotitic komatiites. Peridotitic komatiites of Proterozoic or younger age are uncommon, although a few pyroxenitic and basaltic varieties have been reported from Newfoundland (Barton, 1975), India, (Gupta et.al., 1980), and the Cape Smith Fold Belt of northern Canada, (Francis and Hynes, 1979). Francis and Hynes used the Jensen Cation Plot (Figure 26) to define a differentiation trend from ultramafic komatiites to high-Mg tholeiites thus suggesting a chemical link between the two rock types based on cation chemistry. This trend is exactly the same as that displayed by the Cow Creek Area 1 rocks.

The AFM diagram has also been used by several authors, Gupta et.al. (1980) and McCall (1973) in attempts to define chemical trends and establish genetic links between various rock types. McCall (1973) attempts to show differentiation trends from komatiites to tholeiites. He suggests that the highly magnesian komatiitic rocks of South Africa discussed by the Viljoens (1969a, and 1969b) might be an extension of the abyssal tholeiite association. Whether or not he is

correct is open to debate but Figure 37 seems to suggest that the ultramafic rocks of Cow Creek may be a highly magnesian extension of the mafic tholeiitic rocks.

Rare earth element patterns of the ultramafic and mafic rocks of Cow Creek are similar (see Figures 36 and 36a). The ultramafics have slightly positive Eu anomalies and an overall flat pattern. The amphibolites also have a overall flat pattern and are slightly depleted in light REE, which is common in many basaltic komatiites. This evidence seems to suggest that the ultramafic and mafic rocks, at least at one time, may have shared a common parent magma.

Naldrett and Cabri (1976) suggest a method whereby both mafic and ultramafic magmas could arrive in the same place at essentially the same time and share a common origin. Figure 45 is after Naldrett and Cabri (1976) as modified after Clarke and Ringwood (1964) and Green (1975).

Mantle material at point A will have a temperature slightly above the solidus and result in its being approximately 5 percent molten. Any slight perturbation might cause a mass of this material, perhaps several tens of kilometers in diameter, to move upward as a diapir. Thermal conductivities of the rocks being intruded are so low that the rise of the magma is essentially adiabatic, along ABCD. The tendency to rise would be reinforced by the hot material expanding as it moves upward into a lower pressure environment and therefore assumes a lower density than its surroundings. By the time the diapir reaches point B, 25 to

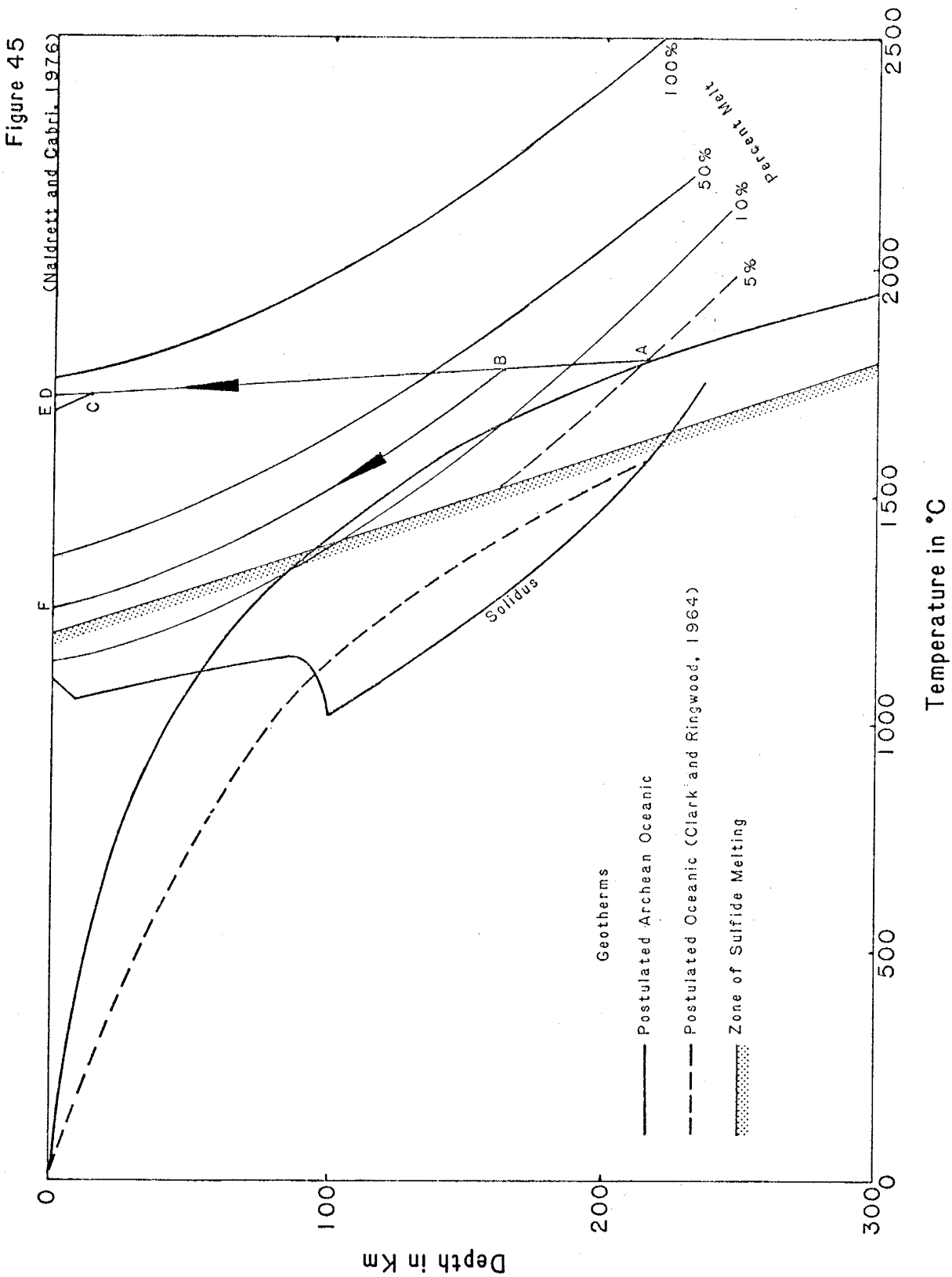
Figure 45
(Naldrett and Cabri, 1976)
Depth in Km
Temperature in °C
0
100
200
300
500
1000
1500
2000
2500
Percent Melt
100%
50%
10%
5%
Solidus
A
B
C
D
E
F
Geotherms
Postulated Archean Oceanic
Postulated Oceanic (Clark and Ringwood, 1964)
Zone of Sulfide Melting

30 percent would have been liquid and this liquid of basaltic composition would have separated from the unmelted residuum to rise to the surface along the non-adiabatic curve BF. Continued rise of the unmelted residuum of the diapir from B to C would result in a further melting. Perhaps as much as an additional 30 percent. (The contours are no longer directly applicable to this depleted refractory material). Separation of a second more magnesian liquid at C gives rise to intrusion or extrusion of a high-temperature ultramafic magma at point E. In this manner both a relatively low temperature basaltic (high-Mg-tholeiite) magma and a high temperature (komatiitic) magma could share a common origin and still solve the two magma dilemma.

The above lines of evidence, Jensen Cation Plot (Figure 26), AFM diagram (Figure 37), REE plots (Figures 36 and 36a) and the work of Naldrett and Cabri (1976, Figure 45) combined with field relations discussed in earlier sections, suggest that the Cow Creek mafic and ultramafic rocks could have originally shared a common parent rock.

Significance of Komatiites and Relations to the rest of the Pecos greenstone belt:

Many rock types can exhibit komatiitic chemistry, therefore, for a rock to be considered komatiitic it must be shown that the rock was emplaced as a silicate melt. This is done by textural evidence such as spinifex texture, pillow structures, chilled margins etc. Once their extrusive, volcanic nature is established, as with the Cow Creek rocks, the question that arises is, how do these rocks relate to the regional Precambrian geologic picture?

Komatiites have been interpreted as forming in varied tectonic settings by authors other than Naldrett and Cabri. A back-arc marginal basin environment is favored by Brooks and Hart (1974), Bickle et. al. (1975) and Condie and Harrison (1976), sea floor, Glickson (1971), and Gale (1973), meteor impact, Green (1972) and primative crust, Viljoen and Viljoen (1969b). Since, as pointed out by Brooks and Hart (1974), it is clear that other rocks of peridotitic komatiite chemistry occur in diverse tectonic regimes, (for example, alpine- and high-temperature peridotites, peridotite-nodules, sea floor peridotites, and ophiolite complexes) throughout geologic time, the general chemical character is not helpful in specifying the tectonic setting.

In order to speculate about the possible tectonic setting of the Pecos greenstone belt at the time of emplacement of the Cow Creek komatiites, field relations must be heavily relied upon. Quartzites overlie the more typical greenstone terrane composed of bimodal volcanics, volcaniclastics and sedimentary rocks. The bimodal volcanics in the Pecos greenstone belt (described by Robertson, J.M., in progress) tend to indicate a extensional environment. The greenstone belt lacks andesites and graywackes, Robertson and Moench (1979), and therefore it is most likely that the Pecos greenstone belt represents a series of bimodal volcanics, volcaniclastics, and subaqueous sediments which have been deposited in an extensional environment. This is also supported by Condie (1980), and Condie and Budding (1979). It must be emphasized that the presence of komatiites neither adds nor subtracts evidence from this interpretation.

The Cow Creek ultramafic and amphibolitic rocks appear to be chemically related to the mafic rocks of the Pecos greenstone belt as shown in Figures 26, 36a and 37. Francis and Hynes (1979), discuss the relationship between komatiitic rocks and their relationship to the tholeiitic suite using the Jensen Cation Plot. In Figure 26 it can be seen that the same relationship exists for the Cow Creek rocks and therefore it is suggested that the Pecos greenstone belt amphibolites are chemically related to the Cow Creek rocks.

ECONOMIC POTENTIAL OF THE COW CREEK ROCKS

Most major nickel, nickel-copper, chrome and platinum deposits are associated with ultramafic or very mafic rocks. Naldrett (1973) discussed the various types of ultramafic bodies and their potential for economic sulfide deposits. He concluded, after examining most nickel and nickel-copper deposits worldwide, that alaskan-type and alkalic ultramafic bodies appear to be poor bets as exploration targets. Chrome and platinum deposits are usually associated with large layered mafic-ultramafic intrusions and are therefore not likely in the Cow Creek rocks. Again on the basis of existing deposits, he also concluded that Archean and early-Proterozoic (> 1.7 b.y.) ultramafic bodies are more likely hosts for massive nickel and nickel-copper sulfides than younger bodies and that extrusive lens-like ultramafic bodies occurring in Archean and early Proterozoic greenstone belts form one of the most important classes of ultramafic rocks in terms of their potential as hosts for nickel and nickel-copper ores. In Figure 46, Naldrett and Cabri (1976) attempted to use Cu/Cu+Ni ratios to characterize ultramafic komatiites from other ore bearing types of mafic and ultramafic rocks. The Cow Creek ultramafics clearly plot within the komatiitic field and therefore fit this criteria, as being good potential sources of nickel or nickel-copper sulfides. Sulfide ores in ultramafic komatiites are, however, generally confined to the olivine bearing variety,

Figure 46

(Naldrett and Cabri, 1976)

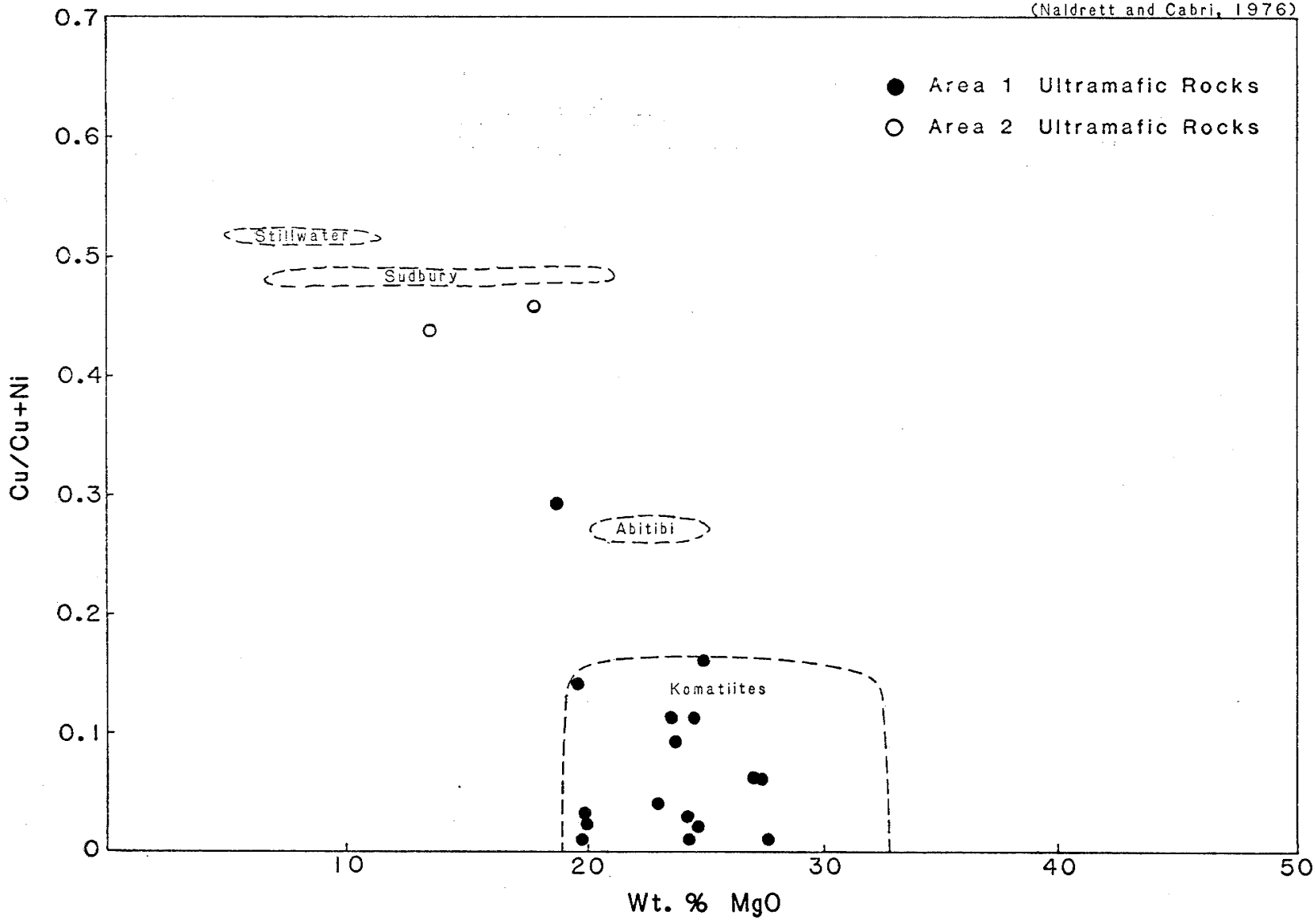

and also exhibit a close association to carbonaceous material. Olivine was probably a minor constituent in the Cow creek rocks as evidenced by the lack of olivine alteration products (such as serpentine and talc), anomalously low values for nickel and chrome when compared to olivine bearing komatiites (compare Table 2 to Table 4), normative mineralogy (Table 3) and comparison of MgO contents. Carbonaceous material is conspicuously absent in the Cow Creek rocks.

Future Prospects for Cow Creek

Since rock exposure is at best, only 10 percent, there is a chance that sulfides remain undiscovered in the Cow Creek Complex, and that sampling of the ultramafic rocks has been somehow biased. If however, as indicated by trace metal concentrations, lack of alteration products, MgO contents and normative mineralogy (Table 3), the Cow Creek komatiites are olivine poor and were not associated with carbonaceous material, the outlook is only fair at best.

Possible exploration methods for the future could include a detailed geochemical study including the method outlined by Naldrett and Gasparrini (1971). This method points out that the high sulfur fugacity associated with sulfur-rich magmatic ores requires a high oxygen fugacity in the environment of the ores. This high oxygen fugacity zone

in turn may be recognized by a high Fe 3+ : Fe 2+ ratio in coexisting chrome spinel. No spinels were seen during this study. Sulfide-rich country rocks, zones of nickel depletion in peridotite and peridotite characterized by chrome spinel with a high Fe 3+ : Fe 2+ ratio are apparently good omens in the exploration for nickel sulfide deposits associated with peridotites. As can be seen from Figure 47, ultramafic komatiites form good exploration targets for nickel sulfides of economic concentration with the exceptions being the Sudbury irruptive and intrusive equivalents of flood basalts. Since exploration of disseminated deposits such as found in the Stillwater and Duluth complexes carry heavy environmental consequences, massive sulfide deposits (such as those associated with ultramafic komatiites) mineable by underground methods will be the way of the future.

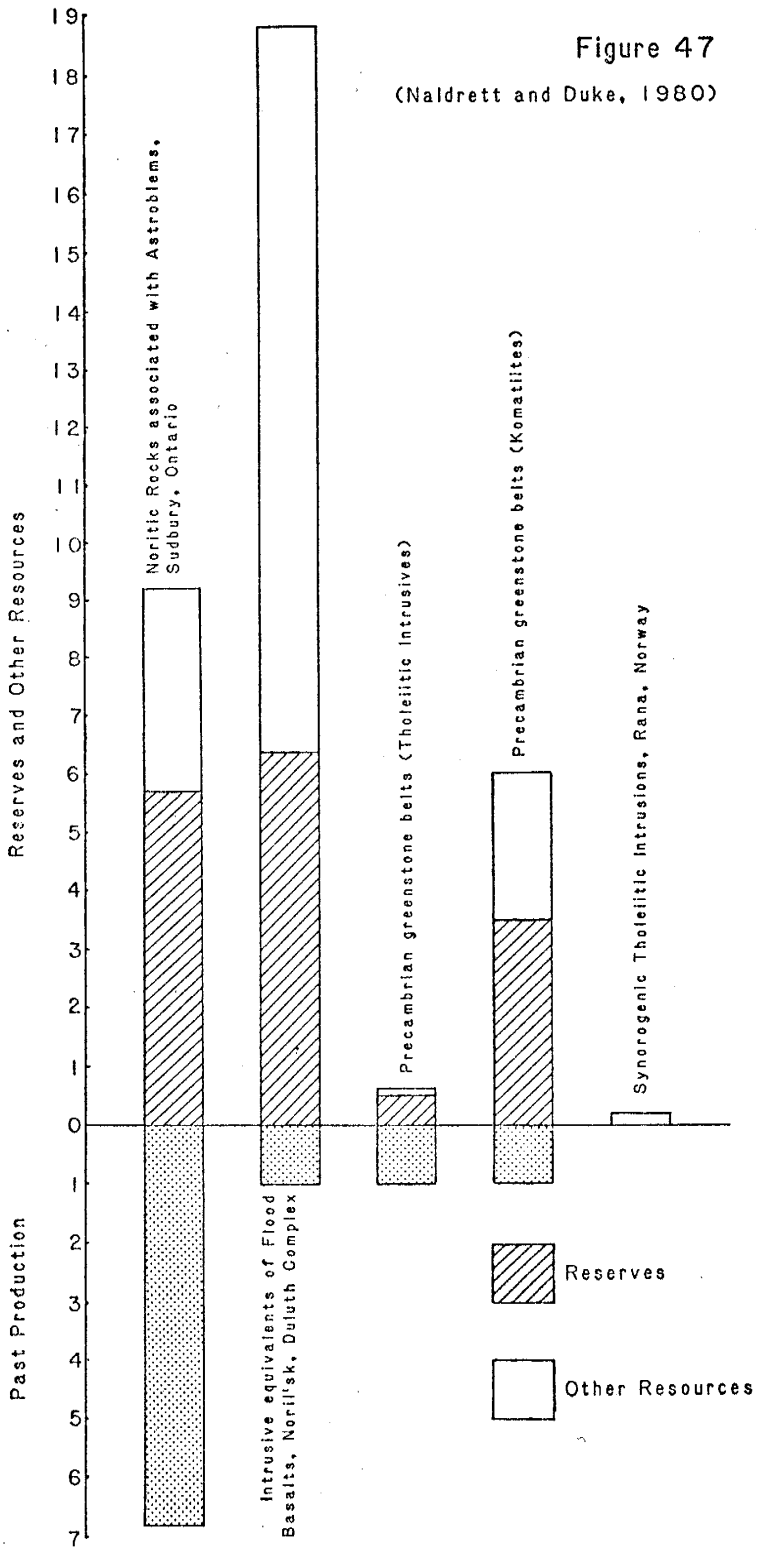
Figure 47
(Naldrett and Duke, 1980)
Reserves and Other Resources
Past Production
19
18
17
16
15
14
13
12
11
10
9
8
7
6
5
4
3
2
1
0
1
2
3
4
5
6
7
Noritic Rocks associated with Astroblems, Sudbury, Ontario
Intrusive equivalents of Flood Basalts, Noril'sk, Duluth Complex
Precambrian greenstone belts (Tholeiitic Intrusives)
Precambrian greenstone belts (Komatiites)
Synorogenic Tholeiitic Intrusions, Rana, Norway
Reserves
Other Resources

GEOLOGICAL HISTORY AND CONCLUSIONS

The geologic history of the Cow Creek rocks include events from middle Precambrian to early Tertiary time. These include at least six intrusive events, two deformational events, one major progressive metamorphic event and one retrograde metamorphic event. The major events in this history are outlined below.

1) The oldest rocks in the area are believed to be the mafic and ultramafic sediments and volcaniclastic rocks. These rocks are crosscut by both mafic and ultramafic intrusive rocks which are inturn intruded by granitic rocks. These rocks were deposited on an unknown surface now totally obliterated by subsequent metamorphic, structural and intrusive events. The sediments and volcaniclastics may have been subaqueous as suggested by their thin laminar and fine grained character.

2) Intrusion and extrusion of the ultramafic and mafic rocks occurred after or during deposition of the sediments and volcaniclastics. Contemporaneous with sedimentation was also some extrusive activity. Evidence of this relationship includes metabasalts which are interbedded with the sediments and volcaniclastics, chilled margins, polygonally fractured flows, pillow-like structures, xenoliths of amphibolite in ultramafic rock, cumulus textures and crosscutting relations.

3) Following the ultramafic and mafic igneous activity diorites and quartz diorites were intruded. The genetic relationship if any to the mafic and ultramafic rocks is unknown.

4) The intrusion of the tonalite-trondhjemite formed crosscutting relations with the mafic-ultramafic complex. If the tonalite-trondhjemite of Cow Creek represents part of a subvolcanic intrusive complex and is correlative to the tonalites in other parts of the Pecos greenstone belt, it is probably about 1718 million years old.

5) Foliated Quartz-monzonite cuts across the foliation in the mafic and ultramafic rocks and it's intrusion was probably the next event to occur. Associated dikes are all discordant to mafic and ultramafic contacts. Major sodium and potassium enrichment occurred locally near these dikes.

6) Embudo granite emplacement at 1638, Fullagar and Shiver (1973), to 1400 million years, Long (1974), occurred in a widespread event throughout the Pecos greenstone belt region. The foliated-granite is believed to be correllative to this intrusive episode.

7) Burial and regional dynamothermal metamorphism is the next recorded event. The major foliation was established which is now in a northwesterly direction. The sedimentary, volcaniclastic, ultramafic, mafic, diorite and quartz diorite rocks all reflect this period of deformation and metamorphism to the lower amphibolite facies.

8) Emplacement of the Pecos Granite (Unfoliated-Granite) is believed to represent the latest Precambrian activity in the mapped area. The unit is unmetamorphosed and undeformed attesting to its post metamorphic and deformational emplacement.

9) Uplift and erosion of all of the Precambrian rocks occurred after emplacement of the Pecos granite. This was followed by the unconformable deposition of the Paleozoic and younger rocks.

10) Formation of the Cow Creek fault is post Pennsylvanian if it crosscuts Paleozoic strata to the north of the mapped area. It cuts the faults of event 9 and crosscuts the Pecos granite.

Conclusions

Some fundamental conclusions that can be drawn from this study are:

1) The ultramafic rocks of Cow Creek, based on whole rock geochemistry, textural evidence and rare earth patterns, appear to be both extrusive pyroxenitic and peridotitic komatiites and their intrusive hypabyssal equivalents. They are believed to be among the first of their kind found in North America. These komatiites are also among the few of their age (1.7-1.8 B.Y.) found in the world

2) The ultramafic rocks of Cow Creek were probably extruded and intruded into subaqueous sediments which had been deposited in an extensional environment such as a continental rift or back-arc basin.

3) The Cow Creek ultramafic and mafic rocks appear to have shared a common origin, however, they could have been erupted and intruded by separate magma chambers of varying temperature and composition. This is based upon cation chemistry and rare earth data. The Cow Creek rocks further appear to be related not only spatially but genetically to the mafic rocks of the Pecos greenstone belt. This is apparent in the Jensen Cation Plot (Figure 26), the REE plots (Figures 36 and 36a), and the AFM diagram (Figure 37).

4) The Cow Creek ultramafic rocks may or may not hold economic concentrations of nickel or nickel-copper sulfides. Due to the extensive vegetation and weathering none was found exposed at the surface, however, modern geochemical and geophysical methods may be able to discover nickel sulfides at depth.

REFERENCES

Arndt, N.T., Naldrett, A.J., and Pyke D.R., 1977, Komatiitic and Iron-Rich Tholeiitic Lavas of Munro Township, Northeast Ontario: Journal of Petrology, v.18, Part 2, p.319-369.

Arth, Joseph G., Arndt, Nicholas T., and Naldrett, Anthony J., 1977, The Genesis of Archean Komatiites from the Munro Township, Ontario: Trace-Element Evidence: Geology, v.5, no.10, p.590-594.

Barker, F., Peterman, Z.E., Henderson, W.T., and Hildreth, R.E., 1974, Rubidium-strontium dating of the tonalite-trondhjemite of the Rio Brazos, New Mexico, and the Kroenke granodiorite, Colorado: U.S. Geological Survey Journal of Research, v.2, p.705-709.

------, Arth, J.G., Peterman, Z.E. and Friedman, I., 1976, The 1.7-1.8 b.y.-old tonalite-trondhjemites of southwestern Colorado and northern New Mexico: geochemistry and depth of genesis: Geological Society of America Bulletin, v.87, p.189-198.

Barrett, F.M., Binns, R.A., Groves, D.I., Marston, R.J., and McQueen, K.G., 1977, Structural History and Metamorphic Modification of Archean Volcanic-Type Nickel Deposits, Yilgarn Block, Western Australia: Economic Geology, v.72, p.1195-1223.

Barton, J.M. Jr., 1975, The Mugford Group Volcanics of Labrador; Age, Geochemistry, and Tectonic Setting: Canadian Journal of Earth Sciences, v.12, p.1196-1208.

Bickle, M.J., Martin, A., and Nisbet, E.G., 1975, Basaltic and Peridotitic Komatiites and Stromatolites Above a Basal Unconformity in the Belingwe Greenstone Belt, Rhodesia: Earth and Planetary Science Letters, v.27, p.155-162.

------, Ford, C.E., and Nisbet, E.G., 1977, The Petrogenesis of Peridotitic Komatiites; Evidence from High-Pressure Melting Experiments: Earth and Planetary Science Letters, v.37, p.97-106.

Baltz, E.H. and Bachman, G.O., 1956, Notes on the geology of the southeastern Sangre de Cristo Mountains, New Mexico: New Mexico Geological Society Guidebook 7, p.96-108.

-----, 1972, Geologic Map and cross-sections of the Gallinas Creek area, Sangre de Cristo Mountains, San Miguel County, New Mexico: U.S. Geological Survey Miscellaneous Geologic Investigation Map I-673.

-----, 1978, Resume of the Rio Grande depression in north-central New Mexico: New Mexico Bureau of Mines and Mineral Resources Circular 163, p.210-228.

Brooks, C., and Hart, S.R., 1974, On the Significance of Komatiite: Geology, v.2, no.2, p.107-110.

Burwash, R.A. and Krupicka, J., 1969, Cratonic reactivation in the Precambrian basement of western Canada. I. Deformation and Chemistry: Canadian Journal of Earth Science, V.6, p.1381-1396.

Cawthorn, R. Grant, and McIver, J.R., 1977, Nickel in Komatiites: Nature, v.266, p.716-718.

Clark, S.P. and Ringwood, A.E., 1964, Density distribution and constitution of the mantle: Reviews in Geophysics, v.2, p.35-88.

Clarke, D.B., and O'Hara, M.J., 1979, Nickel, and the Existence of High-MgO Liquids in Nature: Earth and Planetary Science Letters, v.44, p.153-158.

Coleman, R.G., ed., 1977, Ophiolites, Ancient Oceanic Lithosphere?: New York, Springer-Verlag Publishers, 229 p.

Condie, K.C., 1976a, Plate Tectonics and Crustal Evolution: New York, Pergamon Press Inc., 288 p.

------, 1976b, Trace-element geochemistry of Archean greenstone belts: Earth Science Reviews, v.12, p.393-417.

------, 1980a, Archean Greenstone Belts: Amsterdam, Elsevier Publishing Co., (in press)

------, 1980b, The Tijeras Greenstone: Evidence for Depleted Upper Mantle Beneath New Mexico during the Proterozoic: (in press)

------, and Budding, A.J., 1979, Geology and Geochemistry of Precambrian Rocks, Central and South-Central New Mexico: New Mexico Bureau of Mines and Mineral Resources Memoir 35, 58p. figures.

------, and Harrison, N.M., 1976, Geochemistry of the Archean Bulawayan Group, Midlands Greenstone Belt, Rhodesia: Precambrian Research, v.3, p.253-271.

------, and Lo, H.H., 1971, Trace element geochemistry of the Louis Lake batholith of early Precambrian age, Wyoming: Geochimica et Cosmochimica Acta, v.35, p.1095-1120.

------, Viljoen, M.J., and Kable, E.J.D., 1977, Effects of Alteration on Element Distributions in Archean Tholeiites from the Barberton Greenstone Belt, South Africa: Contributions to Mineralogy and Petrology, v.64, p.75-89.

Cox, K.G., Johnson, R.L., Monkman, L.J., Stillman, C.J., Vail, J.R., and Wood, D.N., 1965, The Geology of the Nuanetsi Igneous Province: Royal Society of London, Philosophical Transactions, ser.A, v.257, p.71-218.

Evans, B.W., and Trommsdorff, V., 1970, Regional Metamorphism of Ultramafic Rocks in the Central Alps: Paragenesis in the System CaO-MgO-SlO2-H2O: Schwiez. Mineralogische und Petrographische Mitteilungen, v.50, p.481-492.

Francis, Donald M., and Hynes, Andrew J., 1979, Komatiite-Derived Tholeiites in the Proterozoic of New Quebec: Earth and Planetary Science Letters, v.44, p.473-481.

Fullagar, P.D., and Shiver, W.S., 1973, Geochronology and petrochemistry of the Embudo Granite, New Mexico: Geological Society of America Bulletin, v.84, p.2705-2712.

Gale, G.H.,1973, Paleozoic Basaltic Komatiites and Ocean-Floor Type Basalts from Northeastern Newfoundland: Earth and Planetary Science Letters, v.18, p.22-28.

Glickson, A.Y., 1971, Primative Archean element distribution patterns: Chemical evidence and geotectonic significance: Earth and Planetary Science Letters, v.12, p.309-320.

Gordon, G.E., Randle, K., Goles, G.G., Corliss, J.B., Beeson, M.H., and Oxley, S.S., 1968, Instrumental activation analysis of standard rocks with high resolution ()-ray detectors: Geochimica et Cosmochimica Acta, v.32, p.369-396.

Grambling, Jeffrey A., 1979, Precambrian Geology of the Truchas Peaks Region, North-Central New Mexico, and some Regional Implications: New Mexico Geological Society, 30th Field Conference, Guidebook, Santa fe County, p.135-143.

Green D. H., 1972, Archean greenstone belts may include terrestrial equivalents of Lunar Maria: Earth and Planetary Science Letters, v.15, p.263.

-----, 1975, Genesis of Archean Peridotitic Magmas and Constraints on Archean Geothermal Gradients and Tectonics: Geology, v.3, no.1, p.15-18.

Groves, D.I., Barrett, F.M., Binns, R.A., and McQueen, K.G., 1977, Spinel Phases Associated with Metamorphosed Volcanic-Type Iron-Nickel Sulfide Ores from Western Australia: Economic Geology, v.72, p.1224-1244.

Gupta, A., Basu, A., and Grosh, P.K., 1980, The Proterozoic ultramafic and mafic lavas and tuffs of the Dalma greenstone belt, eastern India: Canadian Journal of Earth Science, v.17, p.210-231.

Irvine, T.N., and Baragar, W.R.A., 1971, A Guide to the Chemical Classification of Common Volcanic Rocks: Canadian Journal of Earth Sciences, v.8, p.523-548.

------, and Findlay, T.C., 1977, Alpine-Type Peridotite with Particular Reference to the Bay of Islands Igneous Complex: Publications of the Earth Physics Branch, the Ancient Oceanic Lithosphere, Canadian Contribution no. 8 to the Geodynamics Project, p.97-128

Jenkins, Ron., 1976, An Introduction to X-ray Spectrometry, London, New York, and Rheine, Heyden Son Publishers, 163p.

Jensen, L.S., 1976, A New Cation Plot for Classifying Subvolcanic Rocks: Ontario Division of Mines, Misc. Paper 66, 22p.

Kent, S.C., 1980, Precambrian Geology of the Tusas Mountain Area, Rio Ariba County, New Mexico: (M.S. Thesis) Socorro, New Mexico, New Mexico Institute of Mining and Technology.

Kerr, Paul F., 1977, Optical Mineralogy: New York, McGraw Hill, 492 p.

Lajoie, J., and Gelinas, L., 1978, Emplacement of Archean Peridotitic Komatiites in La Motte Township, Quebec: Canadian Journal of Earth Science, v.15, p.672-677.

Long, P.E., 1974, Contrasting types of granitic rocks in the Dixon-Penasco area, northern New Mexico: New Mexico Geological Society Guidebook 25, p.101-108.

Mathewson, D., (in progress), Precambrian geology and mineral deposits of San Miguel County, New Mexico: (Ph.D. thesis) Socorro, New Mexico, New Mexico Institute of Mining and Technology.

McCall, G.J.H., 1972, The Nickel-Sulfide-Bearing Ultramafic Rocks and Their Environment in the Archaean of Western Australia: 24th International Geological Congress, Section 1, Precambrian Geology, p.354-362.

McIver, J.R., 1975, Aspects of Some High Magnesia Eruptives in Southern Africa: Contributions to Mineralogy and Petrology, v.51, p.99-118.

Miller, John P., Montgomery, Arthur, and Sutherland, Patrick, K., 1963, Geology of Part of the Southern Sangre de Cristo Mountains, New Mexico, New Mexico Bureau of Mines and Mineral Resources, Memoir 11, 106p.

Miyashiro, A., 1973, Metamorphism and Metamorphic Belts, London, George Allen and Unwin Ltd., 492 p.

Montgomery, A., 1953, Precambrian Geology of the Picuris Range, North-Central New Mexico: New Mexico Bureau of Mines and Mineral Resources, Bulletin 30, 89 p.

Muir, T.L., 1979, Discrimination between Extrusive and Intrusive Archean Ultramafic Rocks in the Shaw Dome Area Using Selected Major Trace Elements: Canadian Journal of Earth Sciences, v.16, p.80-90.

Naldrett, A.J., 1973, Nickel Sulfide Deposits-Their Classification and Genesis, with Special Emphasis on Deposits of Volcanic Association; Canadian Mining and Metalurigical Bulletin, v.66, no.739, p.45-63.

--------, and Duke, J.M., 1980, Platinum Metals in Magmatic Sulfide Ores: Science, v.208, p.1417-1424.

--------, and Cabri, L.J., 1976, Ultramafic and Related Mafic Rocks: Their Classification and Genesis with Special Reference to the Concentration of Nickel Sulfides and Platinum-Group Elements: Economic Geology, v.71, p.1131-1158.

--------, and Gasparrini, E.L., 1971, Archean Nickel Sulfide Deposits in Canada: Their Classification, Geological Setting and Genesis with Some Suggestions as to Exploration: Special Publication of the Geological Society of Australia, no.3, p.201-226.

Nesbitt, Robert W., and Sun, Shen-Su, 1976, Geochemistry of Archean Spinifex-textured Peridotites and Magnesian and low-magnesian Tholeiites: Earth and Planetary Science Letters, v.31, p.433-453.

Nisbet, Euan G., Bickle, M.J., and Martin, A., 1977, the Mafic and Ultramafic Lavas of the Belingwe Greenstone Belt, Rhodesia: Journal of Petrology, v.18, part 4, p.521-566.

Nockolds, S.R., 1954, Average Chemical Composition of Some Igneous Rocks: Geological Society of America Bulletin, v.65, p.1007-1032.

Pearce, T.H., Gorman, B.E., and Birkett, T.C., 1975, The TiO2-K2O-P2O5 Diagram: A Method of Discriminating Between Oceanic and Non-Oceanic Basalts: Earth and Planetary Science Letters, v.24, p.419-426.

Pyke, D.R., Naldrett, A.J., and Eckstrand, O.R., 1973, Archean Ultramafic Flows in Munro Township, Ontario: Geological Society of America Bulletin, v.84, p.955-978.

Riesmeyer, W.D., 1978, Precambrian geology and ore deposits of the Pecos Mining District, San Miguel and Santa fe Counties, New Mexico (M.S. Thesis): Albuquerque, University of New Mexico, 215 p.

---------, and Robertson, J.M., 1979, Precambrian Geology and Ore Deposits of the Pecos Mine, San Miguel County, New Mexico: New Mexico Geological Society, 30th Field Conference, Guidebook, Santa Fe County, p.175-179.

Ringwood, A.E., 1966, The Chemical Composition and Origin of the Earth: in P.M. Hurley editor. Advances in Earth Sciences. Cambridge: Massachusetts Institute of Technology Press. p.287-326.

Robertson, J.M., and Moench, R., 1979, The Pecos Greenstone Belt, a Proterozoic Volcano-Sedimentary Sequence in the Southern Sangre de Cristo Mountains, New Mexico: New Mexico Geological Society, 30th Field Conference, Guidebook, Santa Fe County, p.165-173.

Smith, R.E., 1968, Redistribution of Major Elements in the Alteration of Some Basic Lavas During Burial Metamorphism: Journal of Petrology, v.9, part 2, p.191-219.

Spry, A., 1969, Metamorphic Textures: New York, Pergamon Press, 350p.

Thayer, T.P., 1967, Chemical and Structural Relations of Ultramafic and Feldspathic Rocks in Alpine Intrusive Complexes: in Wyllie, P.J., ed.,Ultramafic and related rocks: New York, John Wiley Publishers, p222-239.

Trommsdorff, V., Evans, B.W., 1974, Alpine Metamorphism of Peridotitic Rock: Schweizer. Mineralogische und Petrographische Mitteilungen, v.54, p.333-352.

Van Schmus, W.R. and Bickford, M.E., 1980, Proterozoic Evolution of the Midcontinent Region, North America: Precambrian Plate Tectonics, Elsevier Publishers, Amsterdam (in Press).

Viljoen, M.J., and Viljoen, R.P., 1969a, The Geology and Geochemistry of the Lower Ultramafic Unit of the Onverwacht Group and a Proposed New Class of Igneous Rocks: Transactions of the Geological Society of So. Africa, Upper Mantle Symposium, 1969, paper no. 4, p.55-86.

-------, and -------, 1969b, Evidence for the Existence of a Mobile Extrusive Peridotitic Magma from the Komati Formation of the Onverwacht Group: Transactions of the Geological Society of So. Africa, Upper Mantle Symposium, paper no. 5, p.87-121.

Weaver, B.L., and Tarney, J., 1979, Thermal Aspects of Komatiite Generation and Greenstone Belt Models: Nature, v.279, no.5715, p.689-692.

Windley, B.F., 1977, The Evolving Continent, New York, John Wiley and Sons, Publ., 385 p.

Winkler, H.G.F., 1976, Petrogenesis of Metamorphic Rocks: New York, Springer-Verlag Publishers, 334p.

Wyllie, P.J., ed., 1967, Ultramafic and Related Rocks: New York, John Wiley and Sons Inc., a collection of 30 papers on ultramafic and ultrabasic rocks, 464p.

APPENDIXES

APPENDIX A

Sample Preparation Procedure

Sample preparation was conducted by the writer at the New Mexico Bureau of Mines and Mineral Resources Lab in Socorro, New Mexico.

Samples were crushed from hand sized samples to about 3 cm. in an Allis Chalmers Jaw Crusher. The crusher was scraped and scrubbed with a wire brush between each sample. At this stage, contamination was not much of a problem due to the amount of sample. After grinding in the jaw crusher each sample was hand picked to remove any anomalous quartz or weathered pieces. Only the unaltered unweathered sample went beyond this point. All residue was labeled as contaminate and was used to "contaminate" each of the next grinders and crushers before the actual sample was crushed.

Crushing from 3cm to 1cm was done in a DFC No. 1 Jaw Crusher. This crusher was scrubed with a wire brush and "contaminated" before each sample. Between the crushing of contaminate and the sample, the crusher was blown clean with compressed air and scrubbed with a wire brush.

To crush from 1cm to 3-5mm, a Lemaire Instruments Model 150 Jaw Crusher was used. This crusher is constructed of porcelain jaws, thus making cleaning and crushing easy. The crusher was "contaminated" and cleaned before each sample and each sample was crushed four times.

Grinding from 3-5mm to 1mm was accomplished in a disc type pulverizer with porcelain jaws. Like before, it was "contaminated" and cleaned before each sample. Each sample was pulverized twice. The contaminate was disregarded at this point.

To grind from 1mm to 400 mesh a Micro Materials Corp. Microjet 5 Automatic Mortar and Pestal was used. The mortar and pestal are made of agate. The pestal is motorized and turns at 3000 rpm. The mortar and pestal were cleaned with water and acetone before each use. Each sample was ground for 3-4 minutes which proved sufficient time for complete grinding and homogenization.

Contamination

By contaminating each piece of equipment with contaminate from the sample to be run, unwanted contamination was kept to a minimum. The Microjet 5 mortar and pestal did not require contamination with the sample as the cleaning of agate with water and acetone is sufficient to eliminate any residue from any previous sample.

Briquetting:

Briquettes were made using undiluted samples. This eliminates a correction. Boric acid was used as a binder. Each sample was compressed to 20 tons of pressure and left for 3-5 minutes to allow escape of gases. A minimum of 2 grams of sample was used for each briquette to insure sufficient thickness for the x-ray fluoresence whole rock determination.

APPENDIX B

Error Analysis in X-ray Fluoresence and Neutron Activation Calculations

The total error in x-ray fluoresence and neutron activation techniques is calculated by taking the square root of the sum of the squares of all of the individual errors (equation 1).

Equation 1: $$E = \sqrt{\sum e_c^2 + e_o^2 + e_I^2 \cdots e_{RMS}^2}$$

The individual errors used in the calculations include: counting error, (e_c) equation 2.

Equation 2: $$e_c = 100/(N)^{1/2}$$

N=counts in net peak

Operator error (e_o) assumed to be 1%

Instrument or electronic error (e_I) assumed to be 1 to 5%

Error due to flux inhomogeneties (Neutron Activation only) assumed to be < 1%

Errors in Chemistry (Neutron Activation only) assumed to be < 1%

Sample Geometry error (Neutron Activation only) assumed to be < 1%

Accuracy of standard is assumed to be from 1-10%

Sample preparation error in x-ray fluoresence calculations (e_s) was determined by counting 4 replicate samples and determining the percent associated with each element. Sample preparation error on neutron activation is assumed to be 1%.

Absolute RMS error in x-ray fluoresence is an accurate measurement of the amount of error in the calibration curve. This is done by evaluating the difference between concentrations of standards calculated from the curve and the concentrations used to construct it. (Equation 3)

Equation 3: RMS error = $\sqrt{\sum_{i}^{n} \frac{(C_i - C_n)^2}{n}}$

Ci = calculated concentration of ith element

Mi = measured concentration of ith element

n = number of standards

Because neutron activation techniques rely on radioactive decay, certain other corrections must be taken into account. These include corrections for the difference between the weight of the sample and the weight of the standard, decay corrections and corrections for dead time. All of these are taken into account in the computer program (NEUTRON) in the computer at the New Mexico Institute of Mining and Technology.

Assigning Error

To assign the appropriate error to a calculated wt% oxide the total error (E) should be multiplied by the oxide wt%: For example, a sample containing 50% SiO2 has and overall 2.23% error. Therefore, 50% x.0223= + 1.115% SiO_2.

Errors were calculated and averaged from two analyses made of the standards several days apart. The results are given in tabular for below along with appropriate comments on specific problems.

Oxide	E	Largest Contributing Factors
SiO_2	2.23%	Ultramafic Standards DTS-1, PCC-1, and Std. BR (amphibolite)
TiO_2	1.43%	Operator and Instrument error
Al_2O_3	1.59%	Operator and Instrument error, Std. DTS-1 which contains only 0.24% Al_2O_3
Fe_2O_3	1.43%	Operator and Insturment error
MgO	1.73%	Operator and Insturment error and Std. AGV-1 with 1.53% MgO
CaO	1.53%	Operator and Instrument error
Na_2O	1.53%	Operator and Instrument error
K_2O	1.51%	Operator and Instrument error
MnO	1.42%	Operator and Instrument error

Lower Limit of Detection: (Jenkins, 1976)

$$LLD \simeq \frac{3}{m}\sqrt{\frac{I_{Bkg}}{T_{Bkg}/2}}$$

m = number of counts per 1 per cent of oxide

I_{Bkg} = average number of counts in background

T_{Bkg} = Time counting background

Oxide	LLD	Comments
SiO_2	.100%	
TiO_2	.0036%	
Al_2O_3	.084%	
Fe_2O_3	.070%	
MgO	.113%	
CaO	.0222%	
Na_2O	.074%	Undetectable in many ultramafic samples
K_2O	.0066%	Undetectable in many ultramafic samples
MnO	.0076%	

APPENDIX C

THIN SECTION DESCRIPTIONS

* modal percent given in parenthesis when determined

Sample type	Sample #	Major Minerals *	Minor Minerals *	Texture	Comments
Amphibolite	79-12-26	Hornblende (50) Chlorite (10) Plagioclase (22)	Orthoclase (3) Sercite (5) Epidote (5) Sphene, Mag	Mortar	
Amphibolite	79-15-26	Hornblende (30) Plagioclase (30) Tremolite (15) Sercite (15)	Epidote (3) Zircon Magnetite	Decussate	High Na due to nearby intrusion
Amphibolite	79-19-26	Tremolite (35) Hornblende (30) Oligoclase (20)	Chlorite (5) Sericite (3) Clinopyroxene (5) Magnetite	Granoblastic	
Amphibolite	79-20-26	Chlorite (30) Hornblende (24) Plagioclase (30)	Sericite (7) Orthoclase (3) Tremolite (5) Biotite, Pyrite	Decussate	
Amphibolite	79-21-26	Hornblende (70) Plagioclase (20)	Chlorite, Sericite (10) Zircon, Biotite, Pyrite	Decussate	Hornblende altering to Biotite
Amphibolite	79-22-26	Hornblende (45) Plagioclase (25) Sericite (10) Biotite (10)	Chlorite (5) Pyroxene. Zoisite, Epidote, Magnetite	Decussate	Hornblende altering to Biotite then chlorite
Amphibolite	80-1-35	Hornblende (40) Plagioclase (35) Chlorite (20)	Tremolite (5) Sericite Quartz	Granoblastic	Sericitization confined to fractures
Amphibolite	80-2-35	Hornblende (40) Plagioclase (30) Chlorite (10)	Quartz (5) Tremolite (5) Sericite (5) Epidote (5)	Mortar	Plagioclase is heavily sericitized
Amphibolite	80-4-26	Hornblende (45) Plagioclase (40) Chlorite (15)	Quartz, Zircon	Granoblastic	Hornblende altering to Chlorite
Amphibolite	80-5-26	Hornblende (40) Plagioclase (45) Clorite (15)	Quartz, Zircon, Zoisite	Granoblastic	
Amphibolite	80-1-23	Hornblende (25) Plagioclase (40) Tremolite (10) Chlorite (15)	Quartz, Clinozoisite, zoisite	Decussate	Some Feldspars have Myrmetitic texture
Volcaniclastic	SP-6	Quatrz (30-40) Hornblende (50-55)	Plagioclase (2-5) Chlorite Magnetite		See photo
Volcaniclastic	SP-7	Quartz (30) Hornblende (50) Chlorite (10) Plagioclase (10)	Biotite, Zircon, Magnetite Sericite		See photo
Sediment	SP-7	Quartz, Hornblende, Plagioclase	Magnetite in layers		Compositional lavering

APPENDIX C cont.

THIN SECTION DESCRIPTIONS

* modal percent given in parenthesis when determined

Sample type	Sample #	Major Minerals *	Minor Minerals *	Texture	Comments
Ultramafic	79-7-26	Hornblende (40) Clinopyroxene (15) Chlorite (35)	Quartz (5) Feldspars (5) Clinozoisite, Sphene, Magnerite	Mortar	Chlorite is after Hornblende & Pyroxene
Ultramafic	79-16-26	Chlorite (60) Tremolite (30) Hornblende (8)	Pyroxene, Plagioclase, Biotite Zoisite, Magnetite	Decussate	Relict amphibole Porphyroblasts
Ultramafic	79-17-26	Chlorite (48) Tremolite (25) Clinopyroxene (10) Hornblende (8)	Antigorite (5) Plagioclase(2) Biotite (1) Carbonate, Magnetite	Decussate	
Ultramafic	79-18-26	Chlorite (50) Tremolite (25) Diopside (10) Orthopyroxene (10)	Antigorite (5) Magnetite	Decussate	Porphyroblasts of Pyroxene
Ultramafic	79-23-26	Chlorite (97)	Hornblende (1) Magnetite (2)	Medium grained aggregates	Chlorite is non-chrome variety
Ultramafic	79-24-26	Tremolite (60) Chlorite (30)	Biotite (5) Epidote (2) Hornblende (1) Magnetite	Matrix is Decussate	Long Tremolite needles up to 2mm long
Ultramafic	79-4-35	Chlorite (30) Hornblende (30) Tremolite (10) Antigorite (10)	Orthopyroxene (7) Clinozoisite (10) Magnetite(2)	Matrix shows mortar texture	Tremolite recrystallized after Pyroxenes
Ultramafic	79-11-35	Tremolite (45) Chlorite (35) Hornblende (15)	Carbonate (5) Plagioclase, Magnetite	Decussate	Hornblende after pyroxene as porphyroclasts
Ultramafic	80-1-26	Chlorite (60) Tremolite (15) Hornblende (10)	Magnetite (5)	Well foliated	Magnetite forming as 3x3mm
Ultramafic	80-2-26	Hornblende (25) Plagioclase (30) Clinopyroxene (10) Tremolite (20)	Sericite (10) Biotite, Zoisite Quartz, Magnetite	Granoblastic	alteration of Hornblende
Ultramafic	80-3-26	Hornblende (50) Chlorite (30) Tremolite (20)		Decussate	
Ultramafic	80-2-23	Chlorite (50) Tremolite (30) Hornblende (20)	Zoisite, Magnetite	Decussate	Magnetite forming from Hornblende
Ultramafic	80-3-23	Chlorite (60) Tremolite (30) Hornblende (10)	Magnetite	Fiberous	Tremolite laths in Chlorite matrix
Ultramafic	80-4-23	Tremolite (60) Chlorite (30) Hornblende (10)	Magnetite	Fiberous	
Ultramafic	Chilled Margin 7-24-5	Hornblende (50) Chlorite (25) Biotite (10) Tremolite (10)	Quartz, Epidote (2) Zoisite (1) Magnetite	Overall Decussate	Good skeletal Tremolite

APPENDIX C cont.

THIN SECTION DESCRIPTIONS

* modal percent given in parenthesis when determined

Sample type	Sample #	Major Minerals *	Minor Minerals *	Texture	Comments
Amphibolite	A2-79-2	Chlorite (30) Hornblende (25) Plagioclase (30) Quartz (8)	Tremolite, Carbonate (2) Epidote (1) Zircon	Pokidioblastic Hornblende decussate	Some Quartz may be secondary
Amphibolite	A2-79-5	Hornblende (70) Chlorite (20)	Tremolite, Quartz (4) Plagioclase (1) Carbonate	Matrix Granoblastic	
Ultramafic	A2-79-6	Chlorite (35) Hornblende (30) Tremolite (10) Magnetite (15)	Antigorite (5) Hemetite Plagioclase	Chlorite as aphanitic Matrix	Helicitic Hornblende
Ultramafic	A2-79-7	Hornblende (60) Chlorite (25) Tremolite (10)	Clinozoisite, Quartz, Plagioclase, Magnetite (3)	Mortar	High Na in Hornblende & Plagioclase
Amphibolite	A2-79-8	Hornblende (60) Chlortie (20) Plagioclase (12)	Tremolite (5) Quartz (2) K-Feldspar, Antigorite, Magne-	Unfoliated Decussate	Probably Metabasalt
Amphibolite	A2-79-9	Hornblende (43) Chlorite (30) Plagioclase (15)	Quartz (5) Tremolite (3) tite Carbonate (3) Zircon, Sphene	Granoblasitc	Some Quartz secondary Some Feldspar serici- tized

APPENDIX D

Sample Location Map

Area I

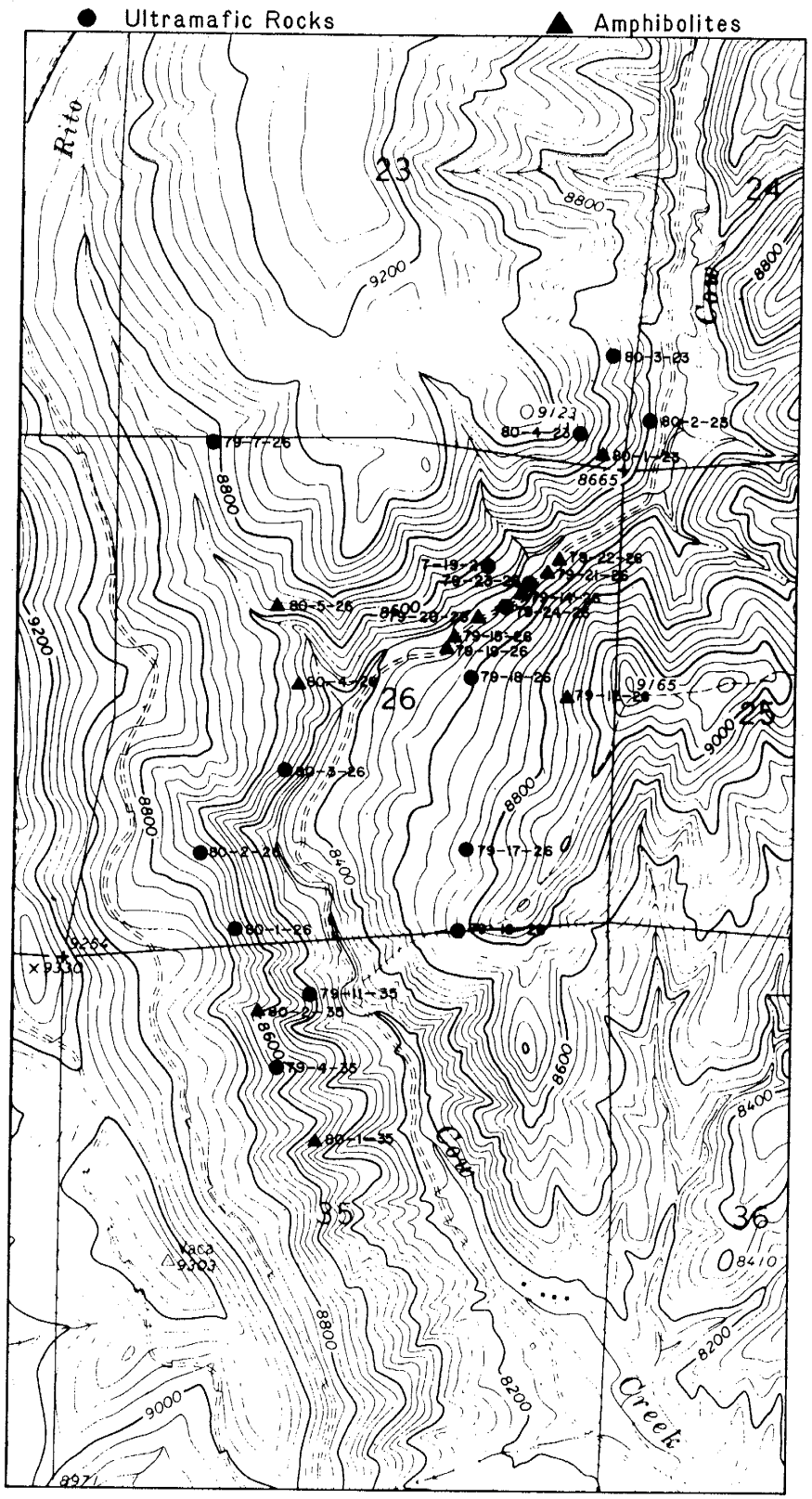

APPENDIX D

Sample Location Map

Area 2

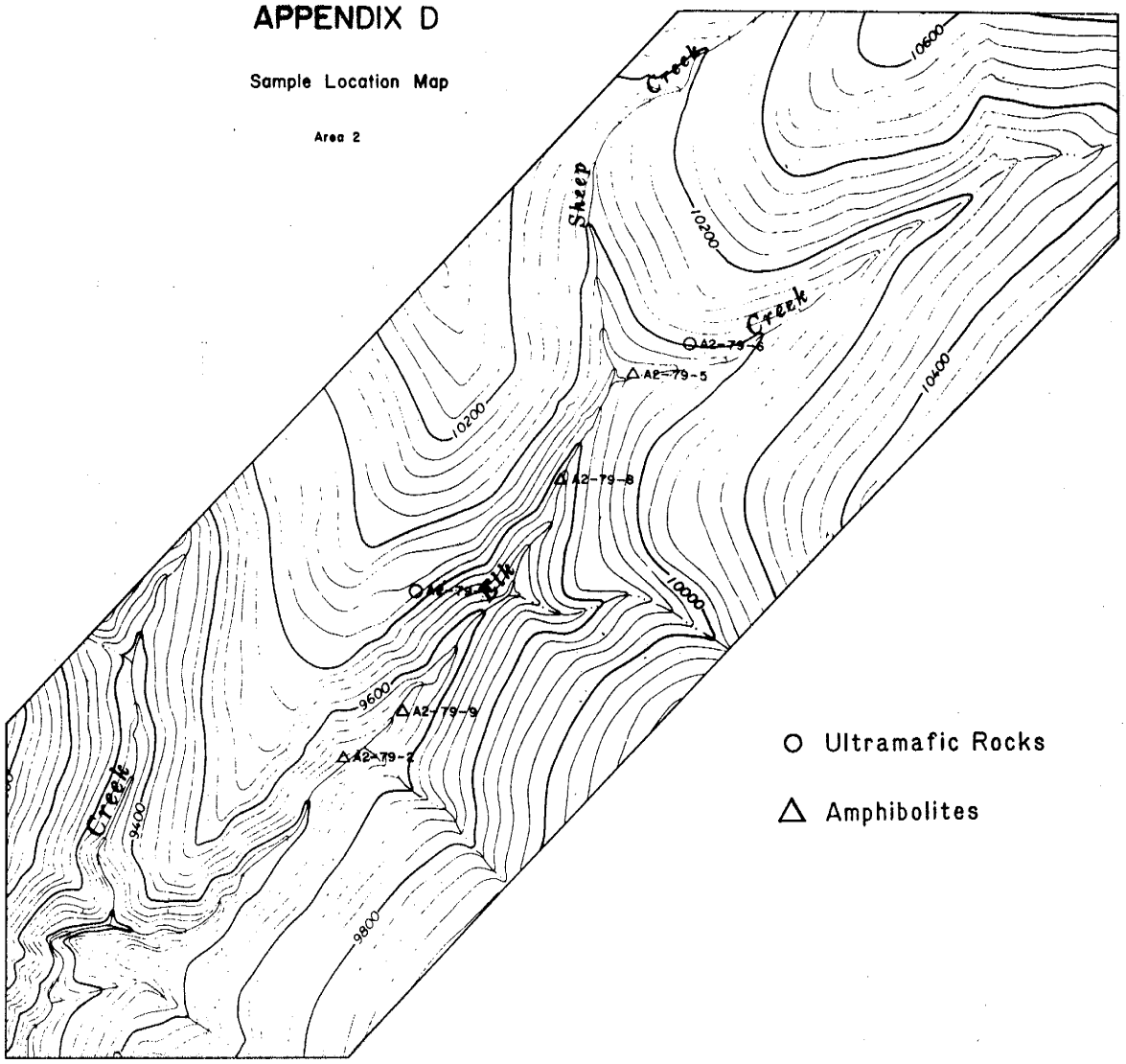

APPENDIX E

Chemical Compositions of Standards used in X-Ray Fluorescence Analyses

Standard	Peridotite PCC-1	Dunite DTS-1	Basalt BCR-1	Basalt JB-1	Diabase W-1	Andesite BR	Andesite AGV-1	Granite G-2	Granite GH
SiO_2	41.90	40.50	54.50	52.09	52.64	38.20	59.00	69.11	75.80
TiO_2	0.015	0.013	2.20	1.34	1.07	2.60	1.04	0.50	0.08
Al_2O_3	0.74	0.24	13.61	14.53	15.00	10.20	17.25	15.40	12.50
Fe_2O_3	2.85	1.21	3.68	2.30	1.04	5.58	4.51	1.08	0.41
FeO	5.24	7.23	8.80	6.06	8.72	6.57	2.05	1.45	0.84
Total iron expressed as Fe_2O_3	8.35	8.64	13.40	9.04	11.09	12.88	6.76	2.65	1.34
MgO	43.18	49.80	3.46	7.70	6.62	13.28	1.53	6.76	0.03
CaO	0.51	0.15	6.92	9.21	10.96	13.80	4.90	1.94	0.69
Na_2O	0.006	0.007	3.27	2.79	2.15	3.05	4.26	4.07	3.85
K_2O	0.004	0.0012	1.70	1.42	0.64	1.04	2.89	4.51	4.76
$H_2O^{(+,-)}$	5.20	0.52	1.57	1.98	0.69	2.80	0.97	0.66	0.52
CO_2	0.12	0.08	0.03	0.19	0.06	0.86	0.06	0.08	0.14
Loss on Ignition	NR	NR	NR	NR	NR	NR	NR	NR	NR
MnO	0.12	0.11	0.18	0.16	0.17	0.20	0.097	0.34	0.05
P_2O_5	0.002	0.002	0.36	0.26	0.14	1.04	0.49	0.14	0.01
Total	99.89	99.86	100.28	100.03	100.26	99.64	99.91	99.73	99.86
Cu	11.3	7	18.4	52	110	70	59.7	11.7	12
Ni	2339	2269	15.8	139	76	270	18.5	5.1	3
Co	112	113	38	39	47	150	14.1	5.5	1.5
Zn	36	45	120	83	86	160	84	85	80
Cr	2730	4000	17.6	417	114	420	12.2	7	6
S	<10	<10	392	50	123	-	<10	24	-

NR = Not Reported

This thesis is accepted on behalf of the faculty of the Institute by the following committee:

James M. Roberts
Adviser

David L. Norman

Kenneth R. Lemke

Oct. 9, 1980
Date